THE MOLECULAR ORGANIZATION AND FUNCTION OF PARANODAL SEPTATE JUNCTIONS

By
German P. Garcia-Fresco

A dissertation submitted to the faculty of the University of North Carolina at Chapel Hill in partial fulfillment of the requirements for the degree of Philosophical Doctor in the Curriculum of Neurobiology

Chapel Hill
2006

Approved by
Advisor: Manzoor Bhat
Committee Chair: Paul Manis
Reader: Eva Anton
Reader: Ken McCarthy
Reader: Franck Polleux
Reader Kinuko Suzuki

ABSTRACT

GERMAN P. GARCIA-FRESCO: The Molecular Organization and Function of Paranodal Septate Junctions
(Under the direction of Manzoor Bhat)

Close communication between axons and glial cells is required and necessary for maturation, organization and maintenance of the nervous system. The axon provides signals to promote differentiation, survival and proliferation of both oligodendrocytes and Schwann cells in the central and peripheral nervous systems respectively, while providing instructions to regulate myelin thickness. Conversely, glial cells provide reciprocal signals that regulate and control axonal mechanisms such as axonal thickness and transport. The combined efforts of glial and axonal signals result in a mature myelinated fiber that has a structural organization optimal for a maximum conduction velocity.

One characteristic feature of myelinated fibers is their ability to organize specialized domains with distinctive molecular and structural characteristics. The myelinated domains include the node of Ranvier, the paranodal junction, the juxtaparanodal junction and the internodal region. This domain organization is a result of the fine bi-directional communication between the axon and the overlying glial cell.

The paranodal axo-glial junction is a complex of proteins including: NCP1, Contactin (CN), Neurofascin 155 (NF155) and band 4.1B. NF155 is expressed by the overlying glial cell while the others are clustered on the axonal membrane. All proteins are necessary for the maintenance and establishment of the paranodal domain and provide a link to the axonal cytoskeleton.

We and others have previously characterized two knockout mice (*NCP1* and *CGT*) that display several signs of cerebellar deficits, including abnormal motor coordination, tremors at rest and ataxia. These knockouts share the same phenotypes one of which is their inability to form paranodal junctions properly. Interestingly NCP1 is an axonal protein and CGT is a glial protein suggesting a common mechanism of action by both cell types and the importance of axo-glial interactions in proper axonal development and organization.

The goal of this project is to further understand the role, molecular composition and organization of axo-glial junctions in vertebrate systems, in particular the paranodal junction of myelinated nerve fibers. We will use these two knockout mouse model systems to identify new key components that play a role in establishing a link between the axon and glial cells.

ACKNOWLEDGEMENTS

As it may seem a one man job, the doctoral dissertation comprises a magnitude of work that requires not only ones effort but that of others in the process. For this and for much more I am indebted to many people. I am most especially grateful to my parents, Stella Maris Fresco and Roberto Garcia, for making this journey and dream possible. Secondly I would like to express my gratitude to my siblings and close friends here and overseas for being there at all times, in good as well as bad. I also would like the opportunity to thank my co-workers and Dr. Jeff Dupree, for the extensive collaborations we endured together. Also, thanks to my committee members for their moral support, guidance and direction in completion of my work. Finally, I would like to thank my advisor, Manzoor Bhat, for his mentoring and support the past four years to ensure my success as a scientist.

TABLE OF CONTENTS

Page

CHAPTER I

INTRODUCTION

1 - A Historical Perspective

The nervous system did not emerge until the discovery of special techniques that allowed viewing entire nerve cells**.** There were distinct periods in the history of the nervous system that defined key structural components that lead to what we know today. These periods were marked by Ramon y Cajal and are known as the pre-Cajalian, the Cajalian, and the post Cajalian periods.

The pre-Cajalian period (1860-1885) was characterized by the different staining methods used by Golgi, Virchow, Dieters, Nissl and others (Lazzarini, 2004). In this period, nervous structures were identified using methods used today such as Nissl, hematoxylin and Golgi. The first successful method (1865) used was the microdissection of whole nerve cells from hardened specimens of brain and spinal cord which allowed Dieters to distinguish between the numerous branching processes that we now call dendrites and the single processes known as the axon. Towards the end of this period Golgi developed a method called "black reaction" which allowed investigators to see the whole nerve cell *in situ* for the first time.

When Cajal stepped into the neuroscience field (the Cajalian period 1885-1910) his initial attempts were using the Golgi technique. With this he was successful enough to

publish a detailed study on the nervous systems of birds (Cajal, 1888a). He particularly demonstrated differences in the nervous system of the avian cerebellum. That same year and again using the same technique he identified for the first time the presence of Nodes of Ranvier in fibers of the brains white matter (Cajal, 1888b) and later in the spinal cord and cerebellum (Cajal 1889). He was the first one to identify that axon collaterals bifurcate at sites of nodes of Ranvier. One of Cajal's marvelous insights was that neurons are topographically polarized so that its cell body and dendrites receive impulses from the axonal endings they are connected to and axons convey the information received away from the cell body towards its terminal arborization.

The post Cajalian period was an era in which one of cajal's disciple, Rio Hortega, challenged some of Cajal's theories and descriptions of the structures of the nervous system; not that Cajal was wrong but his techniques became limited. Rio Hortega innovated some of cajal's and Golgi's techniques and found for instance that most of the a-polar or a-dendritic cells described by Cajal indeed had processes. Rio Hortega and Cajal engaged in an intense dispute that ended in the dismissal of Ortega from Cajal's laboratory, which lead him to start his own laboratory and eventually his own journal.

One of Hortegas main discoveries was that of microglia and the fact that they are of mesodermic nature respectively. Cajal's view on microglia was not in agreement but later on in the early 1920's he published an article describing the same microglial cells in the cerebellum and acknowledging their existence as proclaimed by his former student (Cajal, 1920a, 1920b). In 1921 Ortega identified what he called oligodendroglia and their ectodermal origin (Rio Hortega 1921b). He found these cells by playing with fixation times and increasing the strength of the staining solution. He not only described its morphology but

also he reported that it was present in huge numbers in all regions of the central nervous system with strong predominance in the white matter areas. They were grouped along nerve fibers and rapidly increased in numbers about the time of birth coinciding with a period of active myelogenesis. He finally suggested that the membrane indicated by Cajal around the central fibers is in fact a derivative of these oligodendroglial cells that have functions similar to Schwann cells of peripheral nerve fibers.

In 1928 Rio Hortega came out with yet another publication on the structure of oligodendrocytes. He again, in the best Cajalian tradition developed another modification of the Golgi method obtaining excellent impregnations of oligodendroglia. In this report not only he shows illustrations, but for the first time ever in a publication he used photomicrographs to show the real staining. The most important finding in his article though was that oligodendrocytes acquire close relationships with nerve fibers forming delicate wrappings of laminar, fenestrated appearance, reinforced by rings and inter-annular trabecules. He then concluded that all of these structures are morphologically equivalent to those present in the cells and sheaths of Schwann in the peripheral nerves. Based on the presented evidence he also suggested that oligodendrocytes could potentially play a role in myelogenesis.

In the same year Ramon y Cajal stated in *Degeneration and Regeneration of the Nervous System* (Cajal, 1928) “Myelin is an organ which is adjunct of the axon, and as such, it is entirely foreign to Schwann cells”. This was obviously one of the few misinterpretations in Cajal’s light microscopic experiment observations. The misinterpretation of determining the source of myelin was merely technical, since it was impossible and even today to resolve the cellular boundaries of the axon and myelin at the light microscopic level. It was not until

the late 1950's that these fundamental questions regarding the structures of the myelinated axons could be addressed. As the methods of ultramicroscopy took place, myelin was able to be described accurately. In 1954 Dr. Geren was able to demonstrate unequivocally that myelin was a spiraled extension of the Schwann cell plasma membrane in the peripheral nervous system (PNS). Bunge and colleagues in 1962 then demonstrated the same findings but in oligodendrocytes of the central nervous system (CNS). Furthermore he demonstrated that oligodendrocytes were able to wrap more than one axon in contrast to one as observed by Schwann cells (Bunge et al., 1962). Eventually, other concepts emerged such as the notion of distinct domains in both CNS and PNS nerve fibers. The domain organization and structure of PNS and CNS fibers seem to play distinct roles in the fiber but are all interrelated and in relationship with the overlying glial cells. The development of the nerve fiber is in a close symbiotic relationship with the Schwann cell or oligodendrocyte it comes in contact with.

2 - Domains of a Myelinated Fiber

The main functions of the myelinating cell are to: 1) insulate axons by means of the high lipid content of the lipid bilayer; 2) reduce the current flow across the axonal membrane thereby reducing its capacitance and increasing its transverse resistance which allows a fast saltatory conduction of action potentials; 3) regulate aspects of the formation and maintenance of the nerve fiber such as axon caliber and domain organization. As a result of the high level of communication between the glial cell and the axon, the myelinated nerve fibers acquire distinct features that allow them to maximize the conduction velocity of the

nerve impulse. One of these features is the generation of specific domains throughout the length of the axon. These domains have distinct molecular, structural and functional properties, and include the node of Ranvier, the paranodal junction, the Juxtaparanodal junction, the internodal region and the compact and non compact myelin (Figure 1).

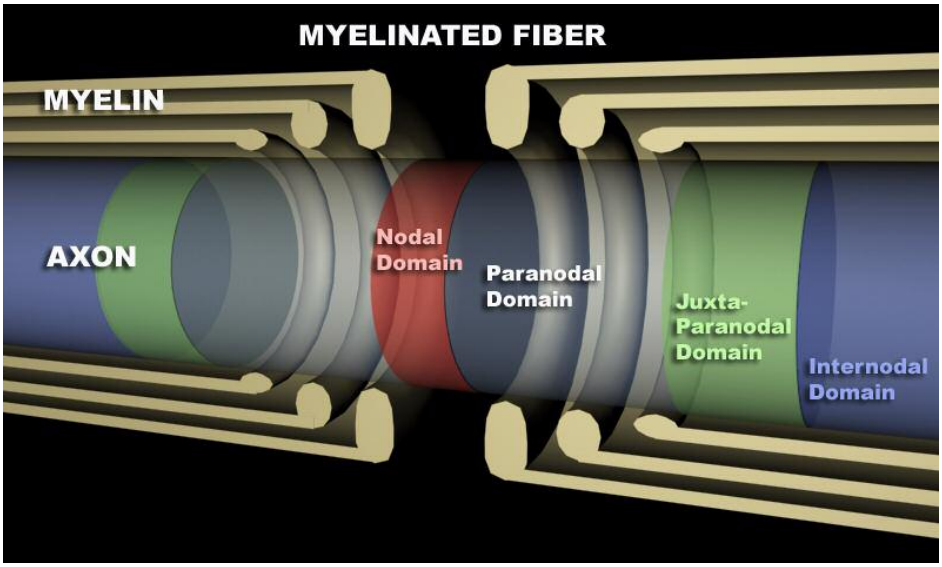

Figure 1 – Domain organization of a myelinated fiber

2a - The Node of Ranvier

The node of Ranvier has evolved into a highly efficient signal generator in the nervous system. Action potentials that propagate through a human peripheral nerve may pass through more than 1000 nodes in a single axon to reach their target. The nodes are short periodic interruptions of the myelin sheath spaced at intervals about 100 times the axonal diameter. CNS and PNS nodes are almost identical with slight structural differences between them. In the PNS, the entire myelin unit is covered by a basal lamina. The outer most layer of the Shwann cell covers the node by interdigitating microvilli projecting from the end of the

Schwann cell that closely appose the nodal axolema. By contrast, the CNS fibers do not contain a basal lamina and the nodes of Ranvier are contacted by perinodal astrocytes or synantocytes (except in small diameter fibers which are devoid of astrocytic processes (Ichimura and Elisman 1991; Bjatmar et al., 1994; Black and Waxman 1988; Butt et al., 2002).

Nodes of Ranvier are rich in Na^+ channels (>1200/μm^2) that are essential for the generation of the action potential during saltatory conduction (Waxman et al., 1980). Voltage gated Na^+ channels are multimeric complexes that consist of a pore forming α subunit and two auxiliary β subunits one disulfide linked and the other non-covalently associated (Caterrall 2000; Figure 2). So far 10 different α subunits have been identified which comprise a multigene family referred to by a common nomenclature following Nav1.X format (Goldin, et al 2000). Nodes of Ranvier in CNS and PNS are comprised primarily of Nav1.6 (Caldwell et al., 2000) and associate with the β1 subunit (Ratclife et al., 2001). Additionally Nav1.2 and 1.8 are found in many CNS nodes (Arroyo et al., 2002), whereas Nav1.9 is only found in PNS nodes (Fjell, et. al.,2000). During development, the α subunit undergoes an isoform transition in both the CNS and PNS. In early stages fibers express Nav1.2 which is later replaced by Nav1.6 in adults (Kaplan et al., 2001; Boiko et al., 2001). This physiological transition is not completely understood but it is suggested that it might allow neurons to adapt to high frequency firing (Goldin 2001).

Besides Na^+ channels, there are many other transmembrane proteins expressed in the nodal axolema: the cytoskeletal structural adaptor Ankryn-G (ank-G; Kordeli et al., 1995), cell adhesion molecules (CAMs) of the immunoglobulin (Ig) family Neurofascin 186 (NF186) and NrCAM (Davis et al., 1996), the actin binding spectrin βIV (Berghs et al.,

2000), and two new identified K^+ channels Kv3.1 and Kcnq2 (Devaux et al., 2003a-b). Other components at the nodal environ include the glycosyl phosphatidilinositol (GPI) –anchored adhesion molecule contactin (CN; Rios et al., 2000), that may associate with Nav1.2 and β1 subunit to enhance channel expression during development (Kazarinova-Noyes et al., 2001). In the CNS there are extracellular components at the nodes of Ranvier including tenascin R, which may stabilize the sodium channel complex by binding to CN, the β2 subunit of the Na^+ channel (Weber et al., 1999), and phosphacan, the secreted form of receptor protein tyrosine phosphatase β (RPTPbeta; Ratclife et al., 2000).

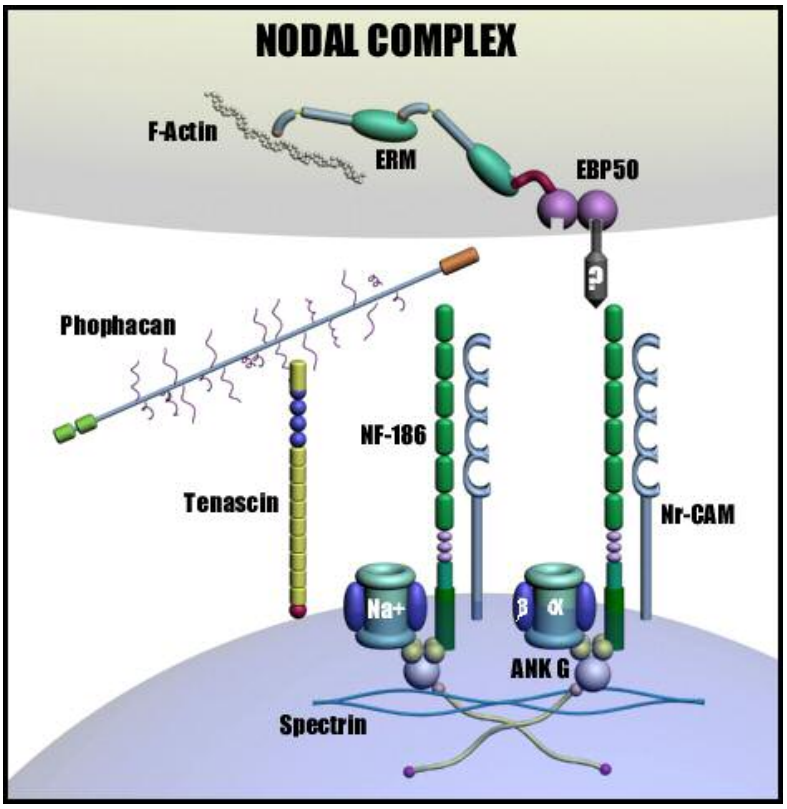

Figure 2 – Nodal complex of the myelinated peripheral nerve fiber. ANK – Ankryn; Na+ - Sodium channel; NF-186 – neurofascin 186.

Ank-G links integral membrane proteins to the spectrin cytoskeleton, it interacts with both α and β Na^+ channel subunits, NF186, Nrcam, and Kv3.1 (Garver et al., 1997; Malhotra et al., 2000; Lemaillet et al., 2003; Devaux et al., 2003a). The binding of Ank-G to the Na^+

channel β subunit is regulated by tyrosine phosphorylation (Malhotra et al., 2002) and is required for the recruitment of Ank-G to the nodal gap. Ank-G also binds spectrin βIV, an isoform that is enriched at the axon initial segments and the nodes of Ranvier. This binding anchors the whole nodal complex to the axonal cytoskeleton providing stability (Berghs et al., 2000).

As mentioned earlier the PNS nodes are contacted by Schwann cell microvilli. Ezrin, radixin, moesin as well as the ezrin binding protein EBP50 and Rho-A GTPase are localized at the microvilli (Gatto et al., 2003; Melendez-Vasquez et al., 2001; Scherer et al., 2001). These proteins form a complex that may link the microvilli with the nodal gap complex possibly via interactions with NF186.

In addition to the microvilli proteins there are other proteins present in the extracellular matrix (ECM) under the basal lamina, including proteoglycan versican, tenascin C and proteoglycan NG2 in the PNS and tenascin R, phosphacan and Bral1 in the CNS (Bretscher et al., 2001; Rieger et al., 1986; Martini et al., 1990; Martin et al., 2001; Saito et al., 1999; Weber et al., 1999; Ratclife et al., 2000). The function of most of these proteins is not yet clear, but based on the presence of acidic disaccharides; they could provide a negative environment that serves as an extracellular Na+ channel reservoir in the perinodal space (Oohashi et al., 2002).

2b - The Paranodal Junction

Paranodal junctions (PJs) are located between the nodes of Ranvier and the juxtaparanodal junctions (Figure 1). At this region the compact myelin forms cytoplasm filled loops (paranodal loops) that envelop the axons spirally. The interaction between the paranodal junctions and the glial cells is mediated by the paranodal complex (Figure 3) which, when represented by electron microscopy, appear as an array of dense bands (transverse bands) between the loops and the axon (Rosenbluth 1995). The development of axoglial junctions is somewhat a late event and it is directly linked to the myelination process (Tao-Cheng and Rosenbluth 1983). The first junctions occur closer to the node of the outer most paranodal loop, and continue inward towards the juxtaparanode as additional loops are formed and attached to the axon (Tao-Cheng and Rosenbluth 1983).

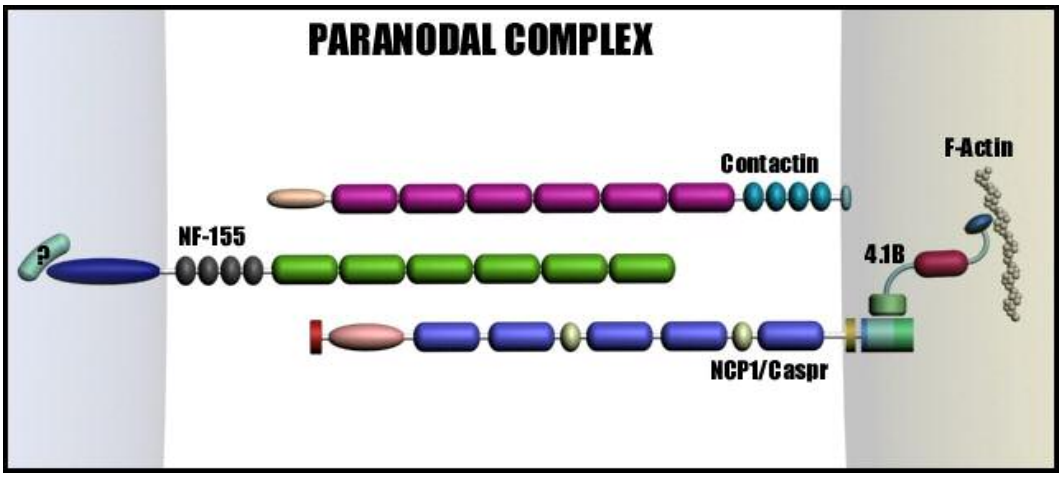

Figure 3 – Paranodal complex of the myelinated peripheral nerve fiber (adopteed from Bhat, 2003).

The paranodal junction contains a complex of cell adhesion and structural molecules including NCP1 and CN (Rios et al., 2000; Einheber et al., 1997; Menegoz et al., 1997) that

attach the complex to the axonal cytoskeleton. The NCP family belongs to a subgroup of neurexins and in humans is comprised of five genes (NCP1-5; Figure 4; Peles et al., 1997; Poliak et al., 1999; Spiegel et al., 2002). NCP1 is a type I transmembrane protein, it contains several domains involved in protein-protein interactions, including discoidin, a fibrogen-like domain, laminin G, and epidermal growth factor motifs. On its cytoplasmic tail NCP1 contains a domain shown to bind to paranodal protein 4.1B and an SH3 domain (Gollan et al., 2002; Poliak et al., 2001).

NCP1 protein interacts with CN in cis (Peles et al., 1997) and it is essential for the efficient transport of NCP1 out of the endoplasmic reticulum and it regulates the glycosylation of CN (Faivre-Sarrailh et al., 2003). Supporting these results, *CN* null mice showed an accumulation of NCP1 in neuronal cell bodies (Boyle et al., 2001). On the other hand, NCP1 is required for the proper localization of CN at paranodal junctions. Mice lacking NCP1 protein fail to concentrate CN at paranodes (Bhat et al., 2001). This then indicates that both NCP1 and CN are essential for the proper formation and maintenance of paranodal axoglial junctions since their absence results in the disappearance of the paranodal transverse bands as observed by electron microscopy (Boyle et al., 2001; Bhat et al., 2001).

A similar phenotype was also observed in other mutant mice: mice lacking UDP galactose ceramide galactosyltransferase (CGT) which do not synthesize galactocerebrosides (Galc) and sulfatides, and cerebroside sulfonotransferase (CST) null mice which only lack sulfatides (Bosio et al., 1996; Coetzee et al., 1998; Honke et al., 2002; Ishibashi et al., 2002). There is no direct evidence on the mechanism of complex disruption due to the absence of Galc and/or sulfatides. One possibility is that sulfatides might directly bind to the CN-NCP1 dimer.

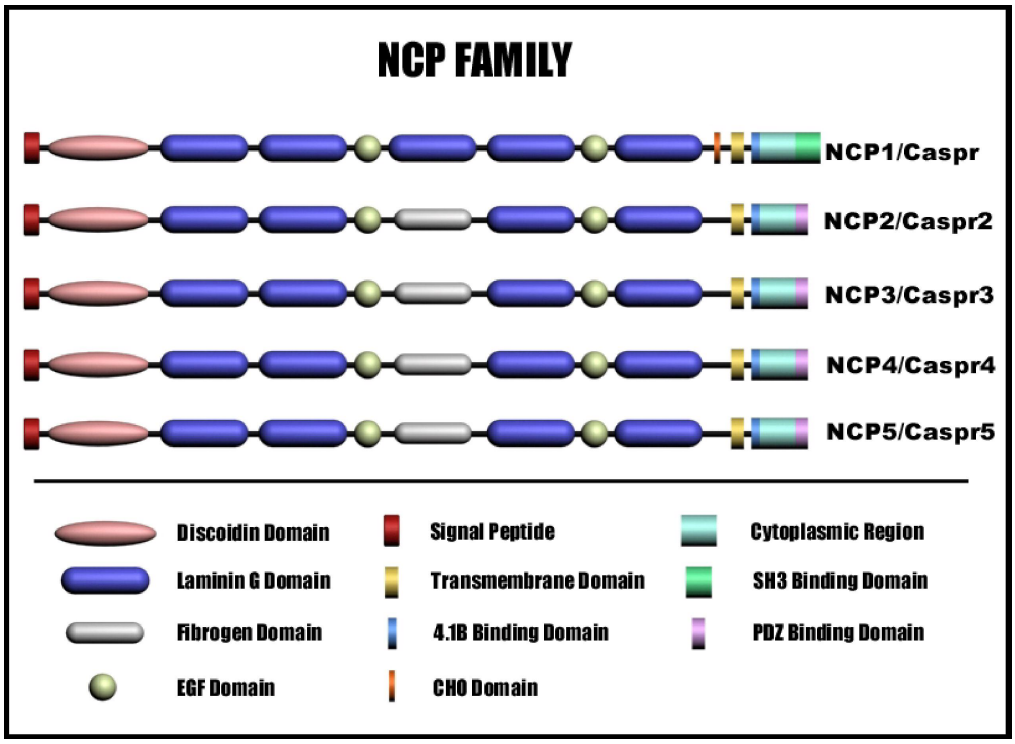

Figure 4 – NCP protein family.

As mentioned earlier, 4.1B binds to and colocalizes with both NCP1 and Caspr2 at the paranodes and juxtaparanodes respectively (Menegoz et al., 1997; Peles et al., 1997; Gollan et al., 2002; Poliak et al., 2001; Denisenko-Neherbass et al., 2003; Ohara et al., 2000; Parra et al., 2000). In addition, 4.1B contains an actin-spectrin binding motif that could potentially link the paranodal domain to the cytoskeleton, therefore immobilizing it (Gollan et al., 2002).

Mice lacking paranodal junctions show a disrupted localization of 4.1B at paranodes (Polliak et al., 2001; Gollan et al., 2002). On the glial side, an attractive candidate to mediate the interaction between glia and the axon in paranodal junctions is neurofascin 155 (NF155), a CAM molecule. Addition of soluble RPTPβ to co-cultured myelinated cells expressing both

NCP1 and CN perturbs the accumulation of NCP1, indicating that the localization of NCP1-CN at paranodes is also mediated by a glial ligand (Rios et al., 2000; Tait et al., 2000). In the absence of NCP1 and/or CN, NF155 does not localize to the paranodal junctions (Boyle et al., 2001; Bhat et al., 2001; Poliak et al., 2001; Marcus et al., 2002).

Paranodal junctions were initially believed to solely mediate the attachment between myelin and the axon, and in that way separate the electrical activity present at the node from the internodal region. It has now been proposed to serve as a fence that limits lateral diffusion of proteins in the axolema (Rosenbluth 1976; Bhat et al., 2001). The results presented in this proposal provide new insights of paranodal junction functions and new key molecular players, suggesting novel links to axonal neuropathies and neurodegenerative diseases.

2c - The Juxtaparanodal Junction

The juxtaparanodal junction lies just under the compact myelin beyond the innermost paranodal junction (Figure 1 and 5) and is enriched with two delayed rectifier potassium channels of the shaker family: Kv1.1, Kv1.2 and its β subunits Kvβ2 (Rhodes et al., 1997; Wang et al., 1993). These channels colocalize and create a complex with a member of the Caspr family, Caspr2 (Poliak et al., 1999). Additionally Caspr2 contains a PDZ binding motif in its carboxy terminal which might regulate the Caspr2- K^+ channel interaction with a yet unidentified PDZ domain protein. PSD95 contains three PDZ domains on its cytoplasmic tail. It has been shown that PSD-95 colocalizes and coimmunoprecipitates with Kvβ2 at the juxtaparanodes (Baba et al., 1999). However, it does not interact directly with Caspr2 (Poliak

et al., 1999), suggesting other proteins are involved in the complex. Indeed, mice deficient in PSD-95 still accumulate K+ channels at the juxtaparanodes (Rasband et al., 2002). Caspr2 also contains a FERM binding sequence that interacts with protein 4.1B, providing an anchor to the axon cytoskeleton maintaining the position of the juxtaparanodal complex along the axon (Denisenko-Nehrbass et al., 2003).

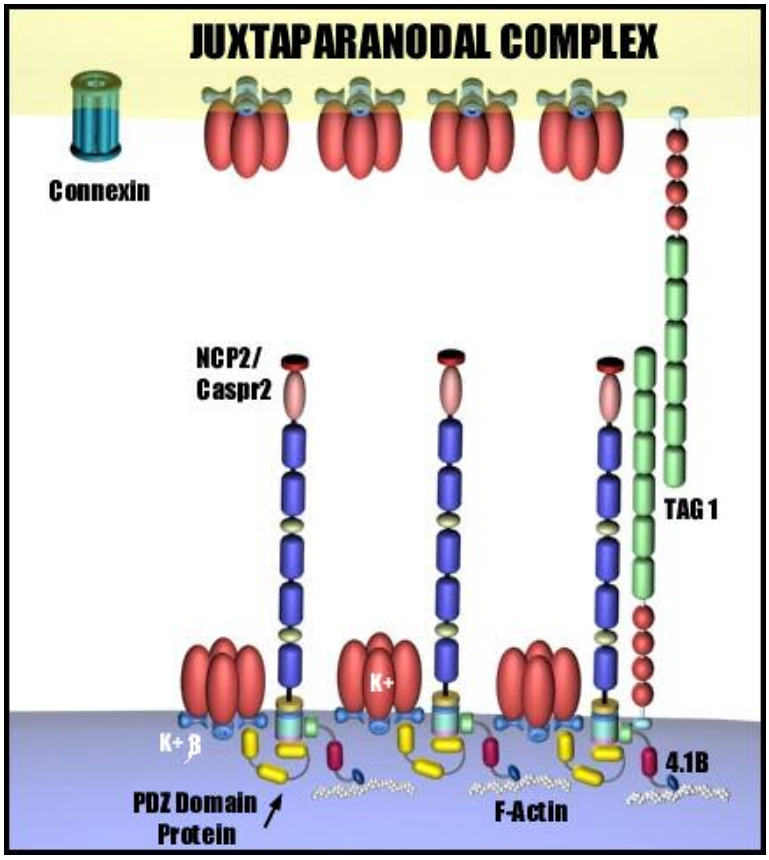

Figure 5 – Juxtaparanodal complex of the myelinated nerve fiber (adopted from Bhat, 2003).

Two other proteins found at the juxtaparanodal junction are transient axonal glycoprotein-1 (TAG1), a GPI motif containing protein related to contactin found on both axons and glia; and connexin 29 (Cnx29) found only along the glial membrane (Traka et al., 2002; Altevogt et al., 2002; Li et al., 2002). Two recent studies have shown that axonal

TAG1 interacts with Caspr2 in cis and also has a homophilic trans interaction with glial TAG1 (Figure 7; Traka et al., 2003; Poliak et al., 2003). The entire juxtaparanodal junction is dispersed in both *TAG1* and *Caspr2* null mutants, indicating the importance of these proteins in the formation or maintenance of the juxtaparanodal complex (Traka et al., 2003; Poliak et al., 2003).

Although the role of juxtaparanodal junction is not well defined, juxtaparanodal K^+ channels were proposed to prevent backfiring and hyper excitation (Zhou et al., 1999). However, despite the marked reduction of K^+ channel concentration at the juxtaparanodes in *Caspr2* and *TAG1* knockouts, there is no change in excitability of knockout nerve fibers (Traka et al., 2003; Poliak et al., 2003). Another proposed function of the juxtaparanodal junction is a role in the communication between the axon and the overlaying glial cell. One candidate for this function is Cnx29, which forms hemi channels that could provide a direct pathway for K^+ ions from the axon to the overlying glia (Altevogt et al., 2002).

The most extended site of interaction between axons and glia is the internodal region, which comprises 99% of the total length of the myelinated axon. There are no specialized junctions between the axonal membrane and the myelin observed throughout the internodal region. However, freeze fracture electron microscopy reveals that internodal axolema contains longitudinal lines (juxtamesaxonal lines) of intramembranous particles containing proteins found in paranodes and juxtaparanodes. These structures appear as if they are a continuation of these two structures (Miller and Da Silva 1977; Stolinski et al., 1985; Peles and Salzer 2000). Paranodal proteins NCP1 and CN are two paranodal proteins that are expressed throughout the internodal region as well as juxtaparanodal proteins Caspr2 and K^+ channels which are both expressed on both sides of the NCP1-CN dimer. These structures

then form a circumferential ring around the axon just below the inner aspect of the Schmidt-Lanterman incisures (a cytoplasmic channel connecting the adaxonal and abaxonal layers of the myelin sheath; Poliak et al., 2001; Arroyo et al., 1999). Concomitantly to the juxtamesaxonal line of the axonal surface, NF155, Cnx29 and TAG1 are localized in a complimentary distribution along the line but on the glial surface (the adaxonal surface), suggesting an adhesion complex keeping the glial cell closely apposed to the axon along the internodal region (Tait et al., 2000; Altevogt et al., 2002; Traka et al., 2002). One candidate glial protein that might also mediate the axoglial interaction is the myelin associated glycoprotein (MAG) which is expressed in the inner glial membrane along the internodal region (Trapp 1990). It has been shown that MAG interacts with sialylated glycoconjugates in the axonal surface (Kelm et al., 1994), and seems to be involved in signaling mechanisms (Garcia et al., 2003).

3 - The internodal region

In simple morphological terms, the myelin internode can be divided into two domains based on the compaction of myelin: compact and non-compact. Compact Myelin comprises about 99% of a myelinated nerve. It extends from node to node but does not include the paranodal junction nor the Schmidt-Lanterman incisures since those belong to non-compact myelin areas. It is noteworthy to mention though that Schmidt-Lanterman incisures are not a prominent feature of CNS internodes (Blackmore, 1969). Oligodendrocytes differ from Schwann cells as mentioned earlier in their ability to form multiple internodes in comparison to only one internode per cell in the case of Schwann cells. Oligodendrocytes have also de

ability to discern thick axons from thin axons. This then tells oligodendrocytes how many axons they can wrap at one time. They can wrap more thin axons at one time than they do thick axons (Fanarraga et. al, 1998). CNS internodes surrounding small diameter axons are shorter and thinner than those surrounding large diameter axons. This all suggests then that oligodendrocytes more or less have the ability to synthesize similar amounts of myelin whether it is multiple small internodes or few larger internodes.

Myelin is responsible to promote rapid and repetitive communication between neurons and it modulates the maturation and survival of axons. Neurons communicate with myelin by depolarizing the electrical potential of their axons, and they perform this task by exchanging Na^+ through Na^+ channels in an energy dependent manner. Unmyelinated axons generate action potentials along their surface at a speed that is proportional to the axonal radius. For an unmyelinated fiber to propagate rapid axonal communication it would require lots of energy and larger axons. Therefore a mechanism to overcome this was adapted throughout evolution that could propagate communication through thin axons in an efficient manner. Myelin-forming cells serve this function by producing a series of discontinuous insulation units called internodes along individual axons. The internodal region formed by myelin inhibits ion exchange during nerve conduction by having a low capacitance and a high resistance. The myelin then allows conductivities of up to 100m/sec in comparison to naked (unmyelinated) axons of velocities less than 1m/sec. This means that for a naked axon to achieve similar velocities as a myelinated nerve it would have to be about 100 times greater in size. This would present an enormous problem of space requirements to accommodate such quantities of large axons.

As I mentioned earlier most of the myelin present at internodes consists of compact myelin that appears as lamellar structures when visualized by transmission electron microscope (TEM; Figure 6A-B). Although compact myelin looks like a simple structure is not that simple to understand. It is best understood if it is considered a spiraled cellular process or sheet that contains two plasma membranes and no cytoplasm. Conventional TEM micrographs show an internal translucent core and two electron dense lines or leaflets at the extracellular and intracellular surface. In the compacted spiral, apposing extracellular leaflets (called intraperiod lines or intermediate lines) are separated by 2.0nm in the CNS and 2.5nm in the PNS. The cytoplasmic leaflets appear to be fussed and form the major dense lines (Alberts et al. 1994; Figure 6A-B).

There are slight differences between PNS and CNS. When both these structures are compared ultrastructurally, one is struck by the similar appearances of both the compact myelin and the axon. One needs to do morphometric comparisons in order to see a clear difference. CNS and PNS axons can be easily distinguished by one particular feature, and that is the presence of a basal lamina in the PNS fibers which is absent in the CNS nerves. At a more molecular level they differ by the distribution and ultrastructure of cytoplasmic channels at the outer margin of the internodes. The basal lamina which is a product of Schwann cells, contain laminin-2 and collagens II and IV (Carey *et al.,* 1983).

The main function of compact myelin is to insulate the underlying axon, for this reason this region of the myelin need not be biochemically or molecularly complex. The myelin membrane has a high content of lipids (about 75%), this imparts high buoyancy to homogenized myelin membranes upon sucrose gradient extractions and thus it is easy to separate them from other membrane samples where the lipid: protein composition is more

likely to be in a 1:1 ratio (Norton and Podulso, 1973). Because of this and for its abundance, myelin was the first membrane samples to be isolated biochemically and molecularly characterized. Several proteins are present in myelin which includes P0 protein, myelin basic proteins (MBP), and PMP-22 in the PNS myelin (Greenfield et al, 1973), and proteolipid protein (PLP) and MBP in the CNS (Lees and Brostoff, 1984; Figure 7). One of the breakthroughs in myelin biology started in the early 90's and is commonly being used today: the ability to generate gene knock-out mice.

One main interesting finding was that multilammellar myelin is still produced in the absence of *P0, PLP, MAG* and double mutants of *PLP/MBP* or even triple mutants PLP/MBP/MAG (Giese *et al*, 1992; Duncan *et al.*, 1987; Privat *et al.*, 1979; Montag *et al.*, 1994; Stoeffel *et al.*, 1997; and Uschkureit *et al.*, 2000). This suggests that spiral expansion of myelin sheaths do not depend on these proteins. It has been established though that MBP and PLP are required for the normal spacing of compact CNS myelin (Duncan *et al*., 1987). On the other hand, P0 is essential for the normal spacing of myelin in the PNS (Giese *et al*., 1992). In order to better understand the role and formation of compact myelin I have summarized the most outstanding features of the main molecular components (Figure 7).

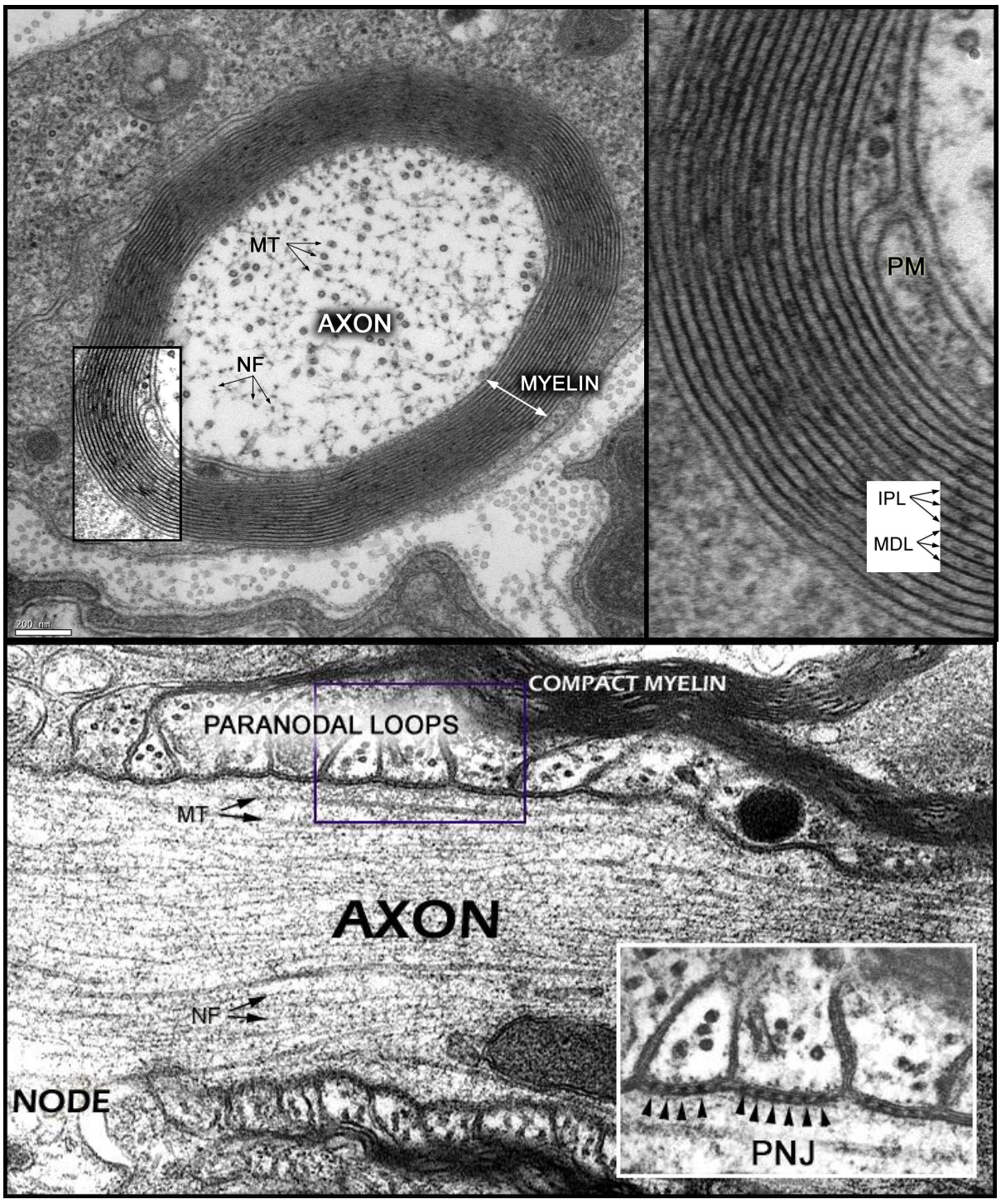

Figure 6 - Coronal (**A-B**) and Sagital (**C-D**) cerebellar sections of a myelinated nerve fiber. NF – neurofilament; MT – microtubule; IPL – intraperiod line; MDL – major dense line; PM – periaxonal mesaxon; PNJ – paranodal junctions. B and D are insets from A and C respectively.

Protein P0 contributes to approximately 65% of the total myelin proteins. It is a type I transmembrane glycoprotein with an apparent molecular weight of 30kD. It has a single extracellular immunoglobulin (Ig) like domain and a C-terminal (Lemke and Axel, 1985). It mediates homophilic plasma membrane adhesion and it also interacts in Cis via its extracellular domains with other P0 proteins forming tetramers from the opposite side of the membrane (Figure 7). The main function of this protein is to stabilize the intraperiod line by its homophilic interaction in the same and opposing side of the myelin membrane in PNS fibers. In P0 mice the spacing between extracellular leaflets is altered but overall the major dense line is similar to that of wild type (Diese *et al.,* 1992).

Myelin Basic Protein (MBP) is localized at the cytoplasmic surface of compact CNS and PNS myelin. The MBP are composed of several members that arise from alternative splicing and they are highly charged (Zeller *et al.,* 1984). These charges allow the MBP proteins to bind negatively charged lipids, especially phosphatidylserine residues. The *MBP* null mice were named the shiverer mice based on the constant shivering these mice express during adulthood. In these mutants the cytoplasmic leaflets of compact CNS myelin are not fused (Privat *et al.,* 1979). In contrast the major dense line in PNS of shiverer mice is not affected. Thus MBP maintains the major dense line of CNS but not of PNS.

Proteolipid Protein (PLP) is most abundant protein in the CNS myelin. It contains four transmembrane domains and has a molecular weight (MW) of 26kD. PLP knock outs result in the fusion of the extracellular leaflets of the compact CNS myelin (Duncan, *et al.,* 1987). PLP also contains a splice variant that is functionally distinct: DM20. This protein is expressed early in development in both PNS and CNS myelinating cells. Like PLP, DM20 is

essential for the formation of the myelin sheath and it is required to fill out the bulk of the intraperiod line in compact myelin.

Peripheral Myelin Protein 22 (PMP22) is found exclusively in PNS compact myelin (Snipes *et al.,* 1992). Like PLP it is also hydrophilic and it also contains four transmembrane domains and it has a MW of 22 kD. Knockouts of PMP22 do not have any apparent effect on compact myelin, but they do show severe hypomyelination early in development but it is compensated as the animals reach adulthood (Adlkofer *et al.,* 1995).

Myelin Associated Glycoprotein (MAG) is a type I transmembrane glycoprotein comprised of a single membrane domain, a C terminus and an extracellular N terminus with five immunoglobulin like domains. MAG contains two differential splice isoforms that are regulated developmentally, one with a MW of 72kD (Large or L-MAG) and one with a MW of 67 kD (Small or S-MAG; Salzer *et al.,* 1987). The differences in their domain lies in their cytoplasmic region, which often contain targeting or sorting signals. In CNS, MAG is enriched in the periaxonal membranes in CNS myelin as well as in the membrane (Trapp 1988) whereas in the PNS MAG is enriched also in mesaxons, Schmidt-Lanterman incisures, and the paranodal loops.

As mentioned earlier, the internodal myelin covers most of the axon's length. This region of the axon is highly rich in structural components such as, microtubules and neurofilaments (Figure 6 A-D). They provide the means of antero and retrograde transport to and from the cell body as well as the structural support of the axon.

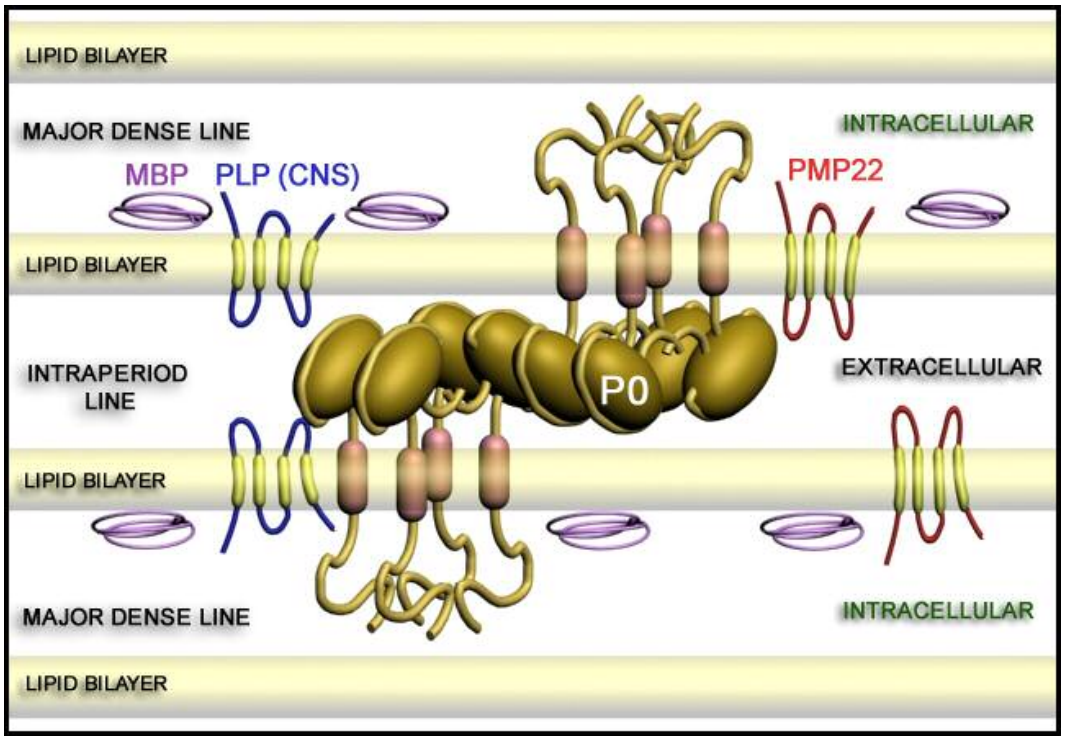

Figure 7 – Schematic representation of compact myelin. MBP – myelin basic protein; PLP – proteolipid protein; PMP22 – peripheral myelin protein 22; P0 – protein zero; CNS – central nervous system.

Microtubules are essentially tubes of tubulin, a globular polypeptide comprised of two forms: α and β tubulin. Each of these tubulins have a molecular weight of 50 kD. When tubulin is assembled into microtubules the dimers line up to form protofilaments in which the α-tubulin of one dimmer in the filament is joined to the β-tubulin of the next one in the chain. Normally 13 of these protofilaments become arranged parallel to each other and assemble to form the wall of the microtubule. Like actin filaments, microtubules also show the phenomenon of tread milling, a process that essentially consists of head-to-tail polymerization such that, as subunits are added to one end of the microtubule, other units are released from the other end. The ends in which microtubules subunits are added quickly are referred to as the plus end and the end where they are released is the minus end. The energy for this whole process is supplied by guanine triphosphate (GTP).

Neurofilaments are essential for axonal diameter (Hoffman et al., 1987). They are obligate heteropolymers composed of neurofilament light (NF-L) neurofilament medium (NF-M) and neurofilament heavy (NF-H). These are the most abundant structural components of large myelinated axons. They are synthesized in the cell body or soma and are then transported via slow axonal mechanisms to the axon. They are extremely long lived proteins and are involved in establishing and maintaining the three dimensional structure of the axoplasm.

Analysis of mutant mice confirmed indeed that neurofilaments are required for determining the axonal diameter of a mature axon. In these mice the loss of neurofilaments decreased remarkably the growth in axonal diameter (Elder et al., 1998; Jacomy et al., 1999; Zhu et al., 1997). It is noteworthy to mention that axonal diameter is not only affected by the loss of neurofilament subunits but also altered stoichiometry of the subunits as well. Increased expression of any single neurofilament subunit inhibits radial growth, whereas simultaneous overexpression of NF-L, M and H increases axonal diameter (Wong et al., 1995; Marszalek et al., 1996; Xu et al., 1996). It is widely known that neurofilaments form COOH-terminal phosphorylated cross-bridges which seem to span between adjacent neurofilaments and between neurofilaments and microtubules as well (Nakagawa et al., 1995; Rao et al., 2002). Radial growth in neurofilaments is associated with phosphorylation of the COOH-terminal tail domains of NF-M and H which contain a series of KSP repeats. These repeats are stoichimotrically phosphorylated in the internodal regions of the axons but are unphosphorylated in the unmyelinated regions such as the nodes of Ranvier or axons initial segments (Hsieh et al., 1994).

There are no specialized junctions between the axonal membrane and the myelin observed throughout the internodal region. However, freeze fracture electron microscopy reveals that internodal axolemma contains longitudinal lines (juxtamesaxonal lines) of intramembranous particles containing proteins found in paranodes and juxtaparanodes (see below). These structures appear as if they are a continuation of these two structures (Miller and Da Silva 1977; Stolinski et al., 1985; Peles and Salzer 2000). Paranodal proteins NCP1 and CN are expressed throughout the internodal region as well as the juxtaparanodal proteins Caspr2 and K^+ channels which are both expressed on both sides of the NCP1-CN dimer. These structures then form a circumferential ring around the axon just below the inner aspect of the Schmidt-Lanterman incisures (a cytoplasmic channel connecting the adaxonal and abaxonal layers of the myelin sheath; Poliak et al., 2001; Arroyo et al., 1999). Concomitantly to the juxtamesaxonal line of the axonal surface, NF155, Cnx29 and TAG1 are localized in a complimentary distribution along the line but on the glial surface (the adaxonal surface), suggesting an adhesion complex keeping the glial cell closely apposed to the axon along the internodal region (Tait et al., 2000; Altevogt et al., 2002; Traka et al., 2002). One candidate glial protein that might also mediate the axo-glial interaction is the myelin associated glycoprotein (MAG) which is expressed in the inner glial membrane along the internodal region (Trapp 1990). It has been shown that MAG interacts with sialylated glycoconjugates in the axonal surface (Kelm et al., 1994), and seems to be involved in signaling mechanisms (Garcia et al., 2003).

4 - Myelination

"The cell biological hallmark of myelination is membrane biosynthesis to produce a unique extension of the oligodendrocyte and Schwann cell plasma membrane that spirally wraps around the axons." (Lazzarini, 2004).

It is widely accepted that axons regulate the myelinating phenotype of oligodendrocytes and Schwann cells. Both the axon and the overlying glial cell engage in a bidirectional communication to ensure the proper development and maturation of a complete myelinated nerve. Both cell types are necessary and required for normal survival. There is little evidence as of what molecules are involved in this process, however electron microscopy has provided axonal parameters that indeed affect myelination as well as myelin pathology. Myelination is responsible for the increase of the axons maximum diameter (Windbank et al., 1985) as well as for the direction of Na+ channels to nodes of Ranvier and some associated proteins (Pedraza et al., 2001). This is a crucial event in the development of axonal fibers since axonal diameter has a direct effect on the conduction velocity (Arbuthnott et al., 1980).

Myelination results in the increase of phosphorylation states of neurofilament side arms (de Waegh et al., 1992; Hsieh et al., 1994; Sanchez et al., 1996). This increases the negative charge and lateral extension of the side arms which in turn increases neurofilament spacing and axonal caliber. In contrast to myelinated fibers, non myelinated fibers as well as non myelinated regions of the axon such as the nodes of Ranvier, have fewer neurofilaments and less neurofilament phosphorylation which results in less spacing of the filaments and smaller diameters (de Waegh et al., 1992; Hsieh et al., 1994). Many extrinsic factors also

affect axonal caliber such as mechanical compression of the nerve, alterations of conduction frequency, toxins, mutations that affect axonal cytoskeleton or molecules involved in the signaling pathways that lead to phosphorylation (Garcia et al., 2003) It is still uncertain how myelin recognizes properties of the axon to accommodate myelination to the axonal diameter. However oligodendrocytes use different axonal cues than Schwann cells to regulate myelin thickness (Elder et al., 2001). The ultimate dimensions of an axon are determined by a complex communication between both the axon and the myelinating cell. Although the axonal diameter is an intrinsic property of the axon it cannot be achieved without the process of myelination (Windbank et al., 1985).

As development of the myelinated nerve fiber takes place the different fiber domains are formed gradually. The nodal domain formed first followed by the transient formation of the juxtaparanodal domain which is displaced from the paranodal region as the paranodes begin their formation (Boiko et al., 2001; Vabnick et al., 1996; Vabnick et al., 1999; Figure 8). In both PNS and CNS, there is an initial clustering of the Na^+ channels at the edges of the myelinating cells. Ultimately two neighboring edges cluster to form a mature node (Rasband et al., 1999; Boiko et al., 2001; Ching et al., 1999). This suggests that Na^+ channel clustering is directed by the overlying glial cell. In support of this mechanism, the optic nerve has a myelinated and a non myelinated portion separated by the lamina cribosa. Na^+ channels are diffused in the nonmyelinated portion whereas the myelinated fragment contains Na^+ channel clusters (Boiko et al., 2001). Also, ablation of oligodendrocytes or Schwann cells abolishes Na^+ channel clustering as well (Vabnick et al., 1996; Mathis et al., 2001).

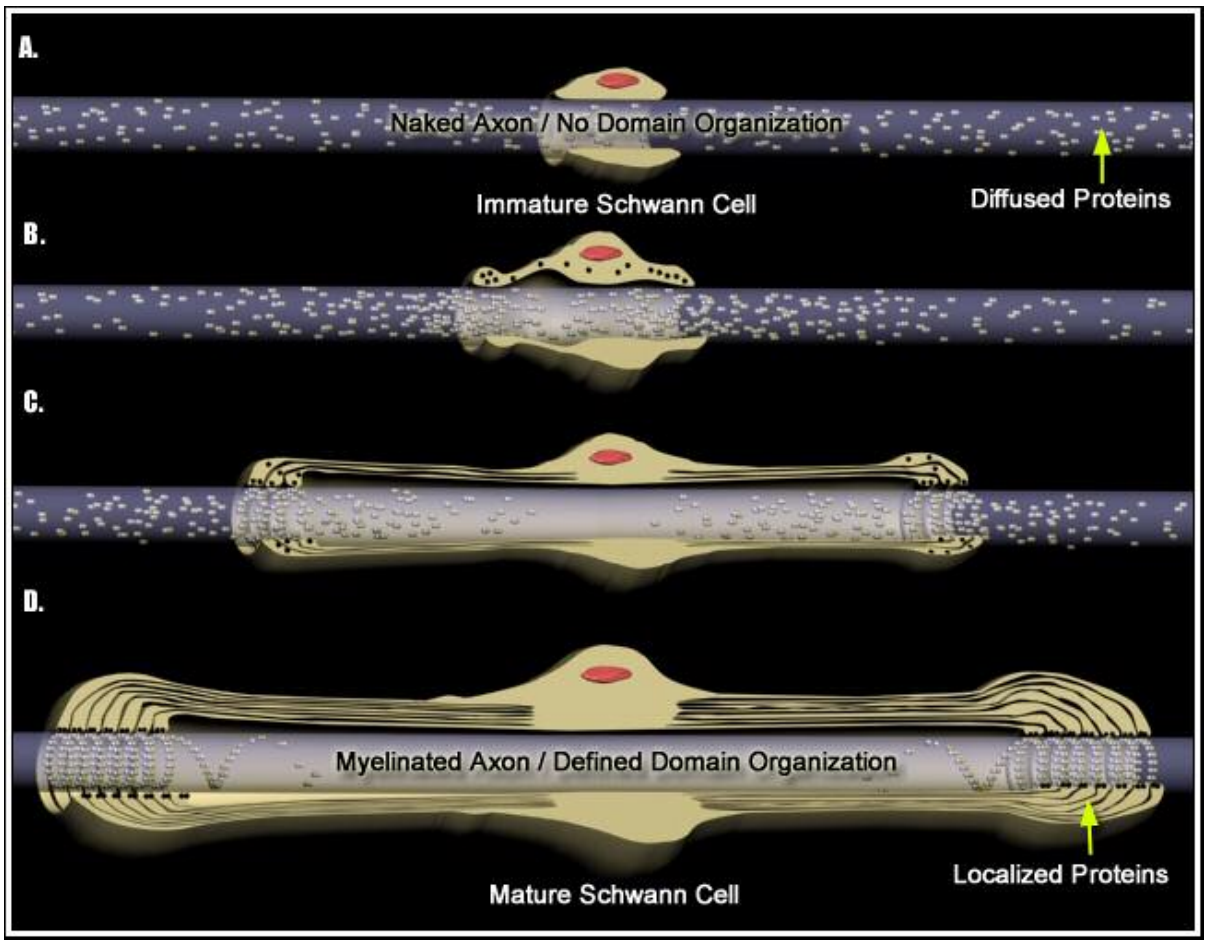

Figure 8 – developmental time points (A-D) schematic of a Schwann cell myelinating an axonal fiber and the establishment of a domain (adopted from Bhat, 2003).

During the process of myelination in the PNS, Nrcam and NF186 are detected at the nodes of Ranvier before Na^+ channel clusters. Subsequently Na^+ channel and Ank-G proteins cluster where NF186 and Nrcam are expressed (Lambert et al., 1997). In the CNS clustering of nodal proteins is formed in a different manner. Initially, Ank-G clusters at the nodes followed by the appearance of NF186 and Na^+ channels (Jenkins and Bennett 2002). After the clustering of the nodal components in the PNS, NF155 and the NCP1-CN dimmer begin their gradual accumulation at the paranodal junction followed by an accumulation of Caspr2 and K^+ channels at the juxtaparanodal junction (Boiko et al., 2001; Rios et al., 2000; Poliak

et al., 2001; Vabnick et al., 1999). Initially Caspr2, K^+ channels and TAG are first detected at the paranodes and subsequently relocate to the juxtaparanodal region as the paranodes become more compact (Poliak et al., 2001; Traka et al., 2003; Rasband et al., 1998). In paranodal mutants (*NCP1, CN, CGT* and *CST*), K^+ channel and Caspr2, fail to relocate to the juxtaparanode (Boyle et al., 2001; Bhat et al., 2001; Traka et al., 2003; Poliak et al., 2003; Ishibashi et al., 2002; Dupree et al., 1999; Poliak et al., 2001). In addition failure to express either Caspr2 or TAG1 results in a failure to concentrate K^+ channels to the juxtaparanodal domain (Traka et al., 2003; Poliak et al., 2003).

It is evident that distinct protein domains on axonal membranes are established via tight regulated communication between the axon and the opposing glial cell. This communication enables the proper sorting of proteins to their respective locations followed by clustering and anchoring of the respective complexes to the axonal membrane and cytoskeleton. Several distinct proposed molecular mechanisms by which the protein domains are formed have been proposed. One such mechanism proposed by Pedraza et al. (2001) suggests the existence of a sieve or molecular filter found at paranodes. They propose that such a sieve would selectively exclude large protein complexes such as the nodal complex and allow through only small proteins such as K^+ channels. This process would require an axoglial interaction without the need of the NCP1-CN complex, since in their absence the nodal proteins still clusters properly, which implies that the generation of paranodal transverse bands are not required for the efficient clustering of Na^+ channels. In fact the accumulation of NCP1 at paranodes and the nodal clustering of Na^+ channels happen before the formation of the transverse bands (Marcus et al., 2002). It is worthy of mentioning that

after Na^+ channels have clustered, the paranodal junctions play a role in maintaining the nodal complex in place.

Analysis of paranodal mutants showed that with time the Na^+ channel clusters broaden, indicating that once the nodal cluster is formed there is a necessity for the paranodal junctions to keep it compact (Ishibashi et al., 2002; Rios et al., 2003; Rosenbluth et al., 2003). A similar mechanism might be responsible for the proper clustering of the juxtaparanodal complex. Although in this case the molecular sieve might be a different one. In contrast to the clustering of the Na^+ channels at the nodes, the generation of the juxtaparanodal complex does require the paranodal axoglial junctions (Bhat et al., 2001; Dupree et al., 1999) thus indicating that it works as a molecular sieve. Finally there seems to be a molecular sieve at the nodal complex itself. Evidence for this comes from the fact that in paranodal mutants juxtaparanodal complex localizes to the paranodes (Bhat et al., 2001; Boyle et al., 2001), and it does not move into the nodal environment, suggesting that there might be a fencing mechanism limiting the entry of molecules to the nodal domain (Bhat et al., 2001; Dupree et al., 1999).

5 - Pathology and Deficiency of the Myelinated Fibers

Axonal loss is a major cause of neurological disability in inherited and/or acquired diseases of myelin which tends to occur as a late onset manifestation of dysmyelination. The early symptoms of patients are usually slow conduction velocities which is an indication of dysmyelination. As age prolongs conduction velocities remain constant but conduction block, an indication of axonal loss, correlates with disease onset and progression. These and other

observations have lead to the hypothesis that axons require glial-derived extrinsic trophic support for their survival (Lazzarini, 2004).

Late onset axonal pathology and degeneration has been described in mice deficient in PLP, MAG, P0, and complex gangliosides (Sheikh et al., 1999; Yin et al., 1998; Griffiths et al., 1998; and Giese et al., 1992) as well as other mice lacking paranodal proteins such as CN, and NCP1 (Bhat, et al., 2001; Boyle et al., 2001). The mechanism by how the loss of function of these proteins culminates in axonal pathology is still unclear, but axonal pathologies that precede axonal degeneration include axonal atrophy, axonal swellings, reduced axonal transport, and altered axonal cytoskeleton.

Protein dosage of compact myelin plays an important role in the normal generation of stable myelin, their stoichiometry is as important as the presence of these proteins. For instance three copies of the human gene *PMP22* cause Charcot Marrie Tooth disease type 1A and duplication of the *PLP* gene on the X chromosome causes inherited CNS hypomyelination disorder Pelizaeus Merzbacher disease. It is now clear that having altered copy numbers of either *PLP* or *PMP22* is major cause for inherited diseases of myelin.

There is increasing evidence suggesting that disturbances of the axonal domain organization and function are an important source of neurological disorders (see Poliak and Peles, 2003 for review). Disorders can arise from mislocalized channels, improper domain formation, defects of the axonal cytoarchitecture or from a miscommunication between the axon and the overlaying glial cell (Bhat et al., 2001; Boyle et al., 2001; Boiko et al., 2001; Boiko et al., 2003; Tait et al., 2000; Rasband et al., 1999a-b; Rasband et al., 2003; Lambert et al., 1997; Ishibashi et al., 2002; Ishibashi et al., 2003; Dupree et al., 1998, Dupree et al., 1999; Poliak et al., 2001; Poliak et al., 2003; Rosenbluth et al., 2003; Traka et al., 2002;

Gollan et al., 2002; Rios et al., 2003; Honke et al., 2003; Mathis et al., 2001; Vabnick and Shrager 1998). Although communication between neuron and glial cells is essential, loss of myelin does not have an immediate detrimental effect as observed in some demyelinating diseases (Mathis et al, 2001; Vabnick and Shrager 1998). One such disease has been described over one hundred years ago (1868) by Charcot: multiple sclerosis (MS). Although considered an autoimmune disease, MS is now beginning to fall into the field of axoglial neuropathies (Arroyo et al., 2002; Mathis et al., 2001; Wolswijk and Balesar 2003). Evidence for this came from studies of MS patient's myelinated fibers. MS axons have aberrant Na^+ channel isoform switching as seen in *NCP1* mutant mice and paranodal markers are lost earlier than nodal markers following demyelination (Rios et al., 2003; Kearney et al., 2002; Arroyo et al., 2002; Mathis et al., 2001; Wolswijk and Balesar 2003). These results suggest that paranodes can be a potential target for pathogenic mechanisms that lead to dispersion of the node and paranodal markers.

Another feature of MS nerve fibers is the abnormalities observed in the phosphorylation of neurofilaments (Trapp et al., 1998). Neurofilaments, the intermediate filaments of axons, are a major component of the axonal cytoskeleton. One of the main functions of neurofilaments is to control axonal caliber, which is crucial since the speed of conductivity of an impulse down the axon is proportional to the axonal caliber. Tempering with the neurofilament network has been shown to cause deficits in axonal transport and caliber of myelinated fibers, leading to axonal accumulations (axonal swellings) and degeneration (Griffiths et al., 1998; Popko 2003). Axonal swellings have been shown in a number of myelin deficient mice such as *CGT*, *CST*, *CN*, *Jimpy*, and *PLP* (Jenkins et al., 2002; Griffiths et al., 1998; Boyle et al., 2001; Dupree et al., 1998; Honke et al., 2002).

A direct connection between deficits in myelin and a downstream effect on the axonal cytoskeleton has not yet been made. We propose to establish such a link using two model systems namely *CGT* and *NCP1* knockout mice. *CGT* knockout mice have a deficiency in a glial enzyme that is responsible for the synthesis of galactolipids, whereas *NCP1* knockout mice are missing an axonal protein. Interestingly both knockout mice express the same phenotype, suggesting the existence of a common downstream mechanism, one coming from the overlying glial cell and the other from the axonal fiber. We suspect that the link is provided by NCP1 since this is the only protein from the paranodal complex that has extracellular as well as intracellular domains which can link both the glial cell and the axon cytoskeleton.

CHAPTER II

Axon-Glia Interactions and the Domain Organization of Myelinated Axons Requires Neurexin IV/Caspr/Paranodin

ABSTRACT

Myelinated fibers are organized into distinct domains that are necessary for saltatory conduction. These domains include the nodes of Ranvier and the flanking paranodal regions where glial cells closely appose and form specialized septate-like junctions with axons. These junctions contain a *Drosophila* Neurexin IV-related protein, Caspr/Paranodin (NCP1). Mice that lack NCP1 exhibit tremor, ataxia, and significant motor paresis. In the absence of NCP1, normal paranodal junctions fail to form, and the organization of the paranodal loops is disrupted. Contactin is undetectable in the paranodes, and K^+ channels are displaced from the juxtaparanodal into the paranodal domains. Loss of NCP1 also results in a severe decrease in peripheral nerve conduction velocity. These results show a critical role for NCP1 in the delineation of specific axonal domains and the axon-glia interactions required for normal saltatory conduction.

INTRODUCTION

The ability of myelinated axons to conduct action potentials by saltatory conduction depends on the distribution of numerous molecular components, notably voltage-gated ion channels, into distinct domains. These domains—the internode, the paranodal and juxtaparanodal regions, and the node of Ranvier—form as the result of specific interactions between axons and myelinating glial cells, e.g., Schwann cells in the PNS and oligodendrocytes in the CNS (Peles and Salzer, 2000). The molecular composition of these domains and the nature of the axon-glia interactions that are required for their formation are poorly understood.

Voltage-gated sodium (Na^+) channels are highly concentrated at the nodes of Ranvier, whereas delayed rectifier potassium (K^+) channels are localized to the juxtaparanodes. A series of cytoplasmic loops of the glial cells are interposed between these domains and flank the nodes of Ranvier. These glial loops spiral tightly around and form specialized septate-like junctions with the axon. In electron micrographs of longitudinal sections of myelinated axons, the paranodal junctions display periodic intercellular transverse bands. These junctions have several proposed functions: anchoring the paranodal loops to the axon, providing an ion diffusion barrier into the periaxonal space that prevents current loss, and serving as a physical barrier that maintains distinct axonal domains (Rosenbluth, 1995).

Support for the role of these junctions in domain organization has emerged from studies of *ceramide galactosyl transferase* (*CGT*) mutant mice (Bosio et al. 1998 and Coetzee et al. 1996). *CGT* mutant mice are unable to synthesize galactocerebroside and sulfatide, two abundant myelin glycolipids. These mice display a variety of paranodal and

nodal abnormalities, including absence of the transverse bands—the hallmark of the paranodal junctions (Dupree et al., 1999). Although the mechanisms underlying the paranodal defects in these mice are not understood (Dupree and Popko, 1999), the observation that K^+ channels are mislocalized in these mice (Dupree et al., 1999) suggested that the paranodal junctions play a key role in the delineation of channel domains.

The first molecular constituent of the paranodal junctions to be identified was the rat contactin-associated protein, Caspr (Einheber et al., 1997). This protein was independently identified and localized to these junctions and named Paranodin (Menegoz et al., 1997). Caspr/Paranodin exhibits significant homology in its ectodomain to Neurexins I, II, and III (Missler and Südhof, 1998) but is more similar to *Drosophila* Neurexin IV (NRX IV) (Baumgartner et al., 1996) and Caspr2 (Poliak et al., 1999). Hence, NRX IV and Caspr/Paranodin constitute a subfamily of Neurexin-like proteins referred to as NCPs (Bellen et al., 1998); we will refer to Caspr/Paranodin as NCP1. *Drosophila* NRX IV has been localized to pleated septate junctions of epithelial and glial cells. These junctions display a ladder-like electron-dense structure and are crucial to the integrity of the blood-nerve barrier in *Drosophila* (Baumgartner et al., 1996).

Biochemical studies have shown that NCP1 associates in *cis* with the GPI-anchored neural cell adhesion molecule contactin (Peles et al., 1997). Contactin is required for the surface expression of NCP1 (Faivre-Sarrailh et al., 2000) and both proteins form a high molecular weight complex in the paranodal junctions (Rios et al., 2000). The glial ligands for NCP1 or contactin in the paranodes have not been established. A potential candidate is the 155 kDa isoform of neurofascin, which is expressed by myelinating glia in the paranodal region (Davis et al. 1996; Collinson et al. 1998 and Tait et al. 2000). Based on the paranodal

abnormalities of the *CGT* mutant mice, galactocerebroside and sulfatide may also be considered potential glial ligands.

In this study, we address the role of mouse NCP1 in the formation and function of paranodal junctions. We show that loss of NCP1 in mice causes severe neurologic defects and aberrant organization, and axo-glial interactions in the paranodal region. In addition, the strict separation between Na^+ channels at the node and K^+ channels at the juxtaparanode is abolished and nerve conduction velocity is substantially reduced in the absence of NCP1. Hence, NCP1 plays a key role in the formation of the paranodal junction.

RESULTS

1 - Cloning of the Mouse *NCP1* Gene and Generation of Null Mutants

Human Neurexin IV sequences were identified through database searches using the *Drosophila Neurexin IV* (*nrx IV)* sequence. One of the human ESTs was used to screen a mouse embryonic cDNA library and overlapping clones were isolated, sequenced, and compiled as a cDNA sequence of 4496 base pairs (accession number AF039833). This sequence contains an open reading frame (ORF) of 1385 amino acids (153 kDa) with 93% identity to rat Caspr/Paranodin (Menegoz et al. 1997 and Peles et al. 1997) and is named NCP1 (Bellen et al., 1998). NCP1 contains an amino-terminal discoidin domain, a laminin G domain, two Neurexin domains, and a PGY-enriched segment in the extracellular region. The cytoplasmic domain contains a band 4.1 binding motif and a proline-rich sequence with at least one consensus SH3 domain binding site. In contrast to *Drosophila* NRX IV and Caspr2,

NCP1 lacks a PDZ binding domain consensus sequence at its carboxyl terminus (Baumgartner et al. 1996; Poliak et al. 1999 and Bhat et al. 1999).

Using the *NCP1* cDNA as a probe, 30kb of genomic DNA was cloned and mapped Bhat et al. 2001; Figure 1A). Based on a partial intron-exon structure of the *NCP1* locus, a targeting construct was designed to delete the first 7 exons, or 327 N-terminal amino acids.

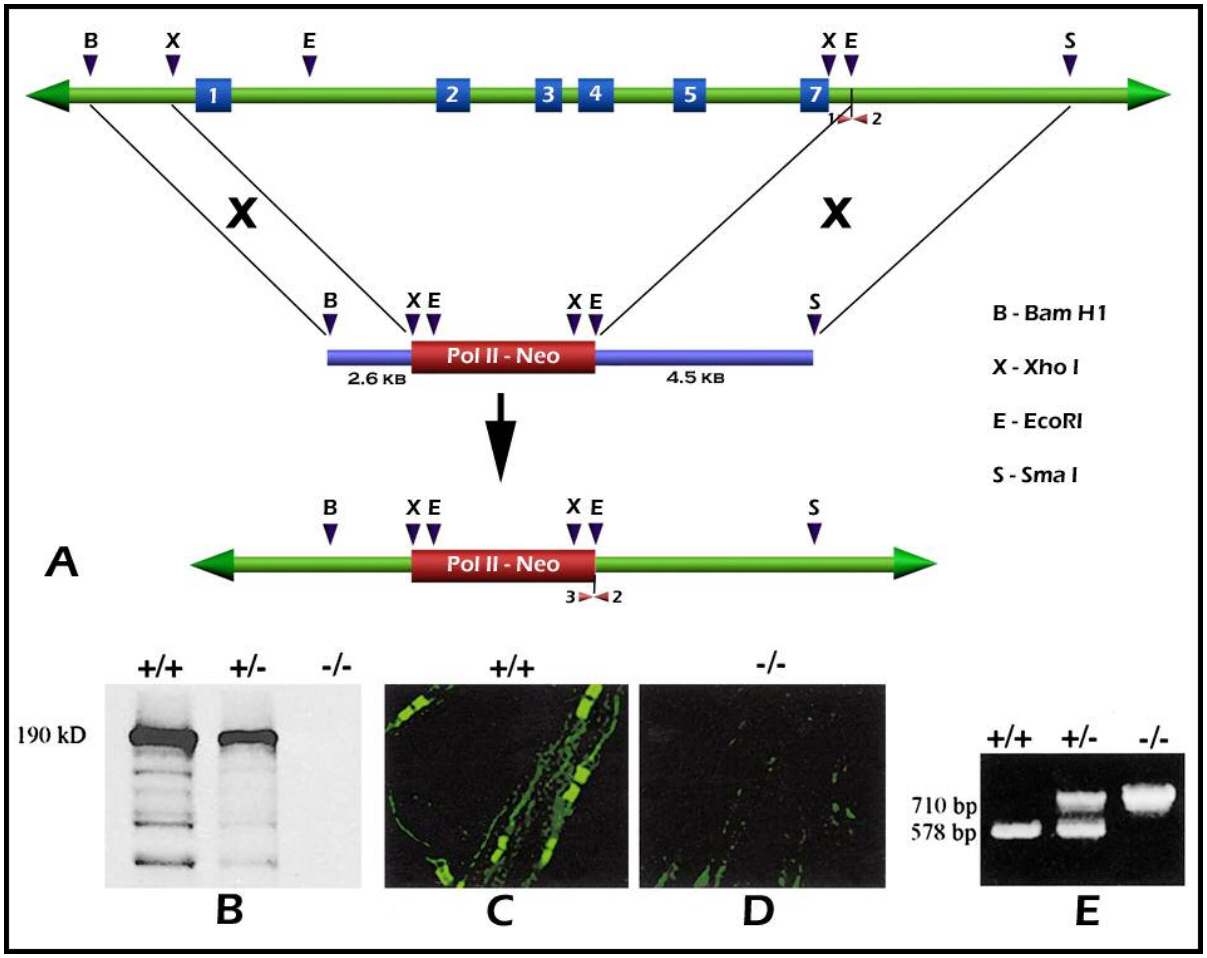

Figure 1 - (**A**) *NCP1* targeting vector. A restriction map of 30 kb genomic DNA containing the 5′ region of the *NCP1* gene and a partial intron-exon structure. The exons are represented as blue boxes. A targeting construct was designed with a *pol II-neo* resistance cassette flanked by genomic fragments that should delete the first 7 exons of the *NCP1* gene, including the 5′ regulatory sequences. This construct produced a targeted allele disrupting the *NCP1* gene. The numerical numbers 1–3 with small arrows indicate the PCR primers used for genotyping. (**B-D**) NCP1 expression. The protein lysates were prepared from brains of wild-type, heterozygous, and homozygous animals and processed for immunoblotting. The wild-type and heterozygous animals showed a predominant protein band migrating at 185–190 kDa that was not detected from homozygous animals demonstrating the loss of the NCP1 protein in *NCP1* mutant mice (B). Immunohistochemical analysis of sciatic nerves from heterozygous animals showed normal expression of NCP1 at the paranodal junctions (C), whereas the nerve fibers from homozygous animals did not reveal any immunostaining (D). The intensity of the green color in (D) was enhanced to reveal the

background of nerve fibers. (E) Genotyping by PCR used three primers. Two primers (1 and 2, see [A]) were directed against wild-type sequences to amplify a 578 bp fragment representing the wild-type allele, and one primer against the *neo* sequence (3, see [A]) with primer 2 to amplify a 710 bp fragment representing the mutant allele. The heterozygous animals amplify both fragments (as reported in Bhat *et al. 2001)*.

The targeting construct contained a *pol II-neo* resistance cassette flanked by a 2.6 kb BamHI-XhoI fragment (5′ homology) and a 4.5 kb EcoRI-SmaI (3′ homology) (Figure 1A). Upon recombination, this construct deletes the first 7 exons of *NCP1* and the putative regulatory sequences. The linearized targeting vector was electroporated into ES cells, and clones carrying the targeted allele were isolated (data not shown).

The clones were injected into mouse blastocysts, and a chimeric male was obtained that transmitted the targeted allele to its progeny. Heterozygous and homozygous mice were confirmed by genomic Southern analysis (data not shown) and PCR amplification (Figure 1E). Mice homozygous for the mutant allele are born at the expected Mendelian frequency from heterozygous intercrosses. The following data indicate that the *NCP1* mutation is a null mutation. First, the NCP1 protein was not detected in whole brain and sciatic nerve homogenates from homozygous mutant mice by Western blot analysis using two independent anti-sera generated to the C-terminal domain of NCP1; the same antisera revealed the 185–190 kDa NCP1 protein in wild-type tissues (Figure 1B). Second, the NCP1 protein could not be detected by immunohistochemical analysis of mutant sciatic nerves (Figure 1D) or in the CNS (see below), whereas wild-type or heterozygous littermates showed strong expression in the paranodal regions (Figure 1C). Taken together these data show that we have generated a complete loss-of-function of *NCP1.*

2 - *NCP1* Mutant Mice Display Sever Neurological Defects

The *NCP1* mutant mice are indistinguishable from their wild-type littermates until approximately postnatal day 10 (P10). Starting at P11, the mice become identifiable by their smaller stature and progressive neurologic defects that reach maximal severity in the third postnatal week (Figures 2A and 2B). The defects include hypomotility, a tremor that is accentuated with movement and a wide-based gait suggestive of a cerebellar defect. These mice cannot maintain their balance on a stationary beam and are nearly immobile in open field tests (Figure 2C). They also exhibit generalized motor paresis that is worse in the lower extremities and are unable to support their weight against gravity, climb ropes, or hold onto the edge of the cage.

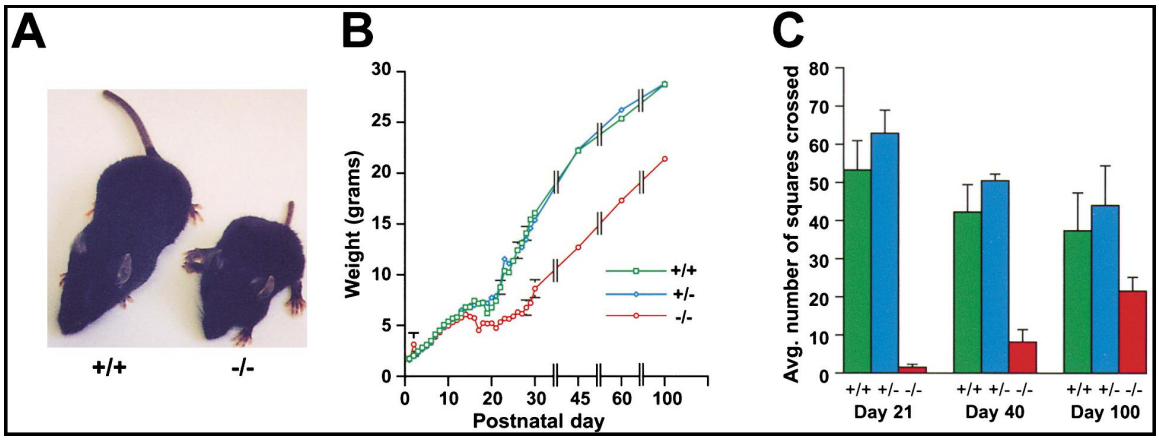

Figure 2 - Phenotype of *NCP1* Mutant Mice(**A**) Appearance of *NCP1* mutant mice. Wild-type (on left) and *NCP1* mutant (on right) littermates at day 35 are shown; the *NCP1* mutant mouse is approximately half the weight (8 g versus 17 g) of the wild-type mouse and also exhibits a characteristic wide base in the hind limbs.(**B**) Weight charts. The chart illustrates the weights of wild-type (+/+), heterozygous (+/–) and homozygous (–/–) male littermates. Wild-type and heterozygous mice were weaned at P19; homozygous mice were left with their mothers.(**C**) Motor activity in open field tests. The number of 5 cm × 5 cm squares crossed by each mouse was recorded over a one minute period at P21, P40, and P100. At all times examined, the *NCP1* mutant mice were hypomotile compared to their heterozygous and wild-type littermates although the activity improves at later developmental time points (as reported in Bhat *et al. 2001)*.

The mutant mice also exhibit occasional extensor spasms of the lower extremities and a hunchback appearance. Most of the mutant mice die at weaning (P21) or shortly thereafter (up to P33), possibly reflecting impaired feeding and maternal care. Removal of wild-type and heterozygous littermates from the cage significantly improves survival but does not alter the neurologic phenotype. These mice slowly increase in size and, in the case of males, approach the weight of their wild-type littermates (Figure 2B). The tremors, hypomotility, and weakness improve slightly (Figure 2C) but then worsen after about 5 months of age. At all ages, heterozygotes appear normal.

3 - Compact Myelin Formation in *NCP1* Mutant Mice

To determine whether the histological organization of the nervous system, including myelination, is affected in the *NCP1* mutant mice, we examined various regions of the CNS and PNS by light and electron microscopy (EM). Light microscopy did not demonstrate any obvious abnormalities in the histological organization or the extent of myelination.

To assess whether loss of NCP1 affected myelin composition, the levels of proteins expressed in compact myelin in the CNS were analyzed by Western blotting (Figure 3). Expression of two components of compact myelin, proteolipid protein (PLP), and myelin basic protein (MBP) was unchanged in heterozygous and homozygous

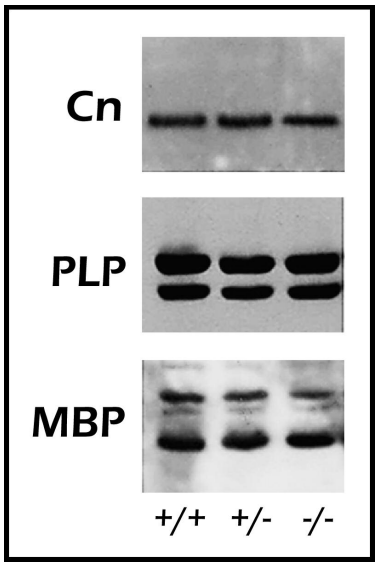

Figure 3 – Western blot analysis of myelin related proteins. Western blots of total brain extracts from wild-type (+/+), heterozygous (+/–), and *NCP1* mutants (–/–) were probed with antibodies to contactin (Cn), proteolipid protein (PLP), and myelin basic protein (MBP). No significant change in expression was observed (as reported in Bhat *et al. 2001).*

mutant mice. Expression of contactin, a protein that is complexed with NCP1 in the paranodal junctions (Rios et al., 2000), was also examined and found to be comparable to that of wild-type littermates (Figure 3B). Taken together with the histological analyses, these results indicate that loss of NCP1 does not affect compact myelin formation.

4 - NCP1 is Required for Formation of Paranodal Junctions

Since NCP1 is localized to paranodal junctions, we examined the ultrastructure of this region (Figure 4). As shown in Figure 4A, paranodal loops are arrayed sequentially and in close apposition to the axonal membrane in the CNS of wild-type mice. Between the loops and axon, periodic densities corresponding to the septate-like transverse bands are readily apparent (Figure 4C, black arrowheads). In contrast, in the CNS of animals lacking NCP1, the paranodal and nodal morphology is frequently grossly perturbed (Figures 4B-D). A consistent abnormality is the absence of the regular array of transverse bands between paranodal loops and the axon (Figures 4B and 4D). The most striking paranodal abnormality consists of "everted" loops, i.e., paranodal loops that face away from, instead of toward, the axonal membrane (labeled IL, Figure 4B.

Other striking abnormalities include occlusion of the node of Ranvier by paranodal loops from one myelin segment that override those from the opposite side, thereby creating a "pseudonode". In the example shown in Figure 4B (black arrows), paranodal loops from the myelin segment on the left (arrow 1) come to an almost contact from loops coming from the right (arrow 2), leaving little or no space for the node of Ranvier (asterisk). Additional defects included astrocytic processes that are interposed between the paranodal loops and the

axon and the presence of Schmidt-Lanterman-like incisures in the myelin sheaths of the spinal cord (data not shown); these incisures are normally rare in CNS myelin (Bhat et al. 2001).

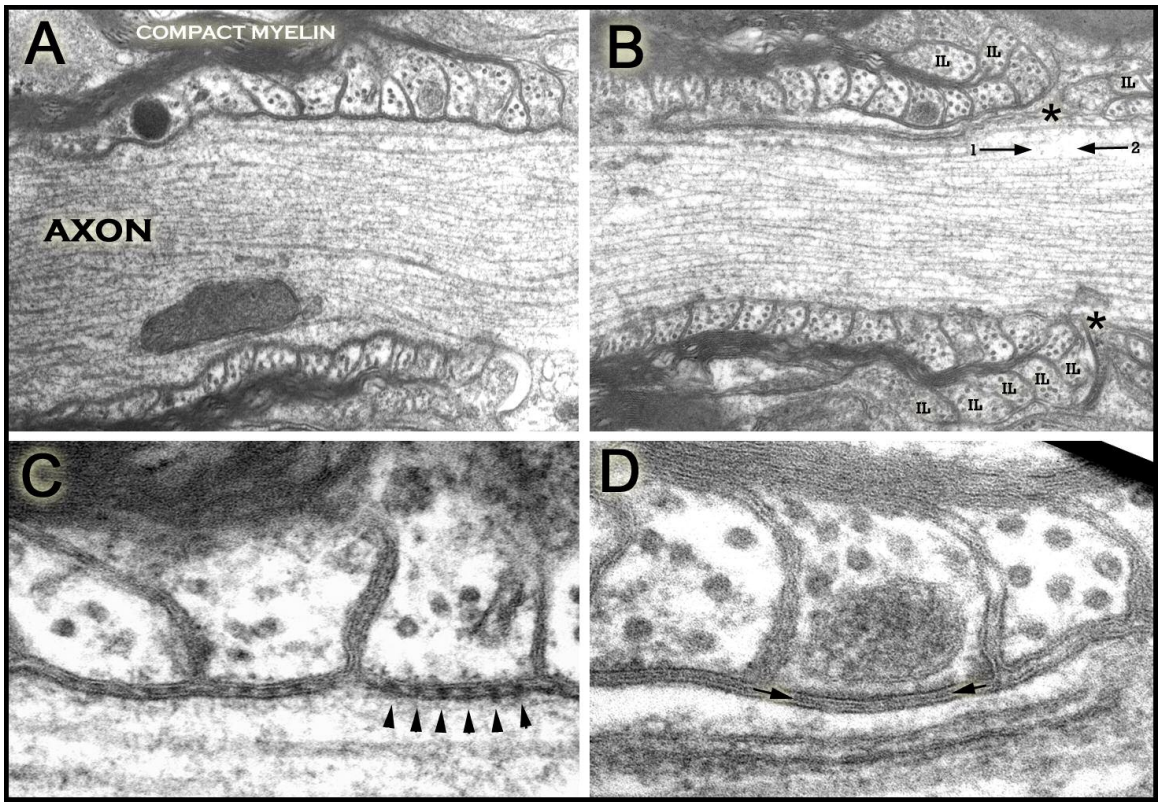

Figure 4 - Perturbation of the paranodal organization of *NCP1* mutant mice. Electron micrographs through the cerebellar paranodal region of wild-type (**A,C**) and *NCP1* mutant mice (**B,D**) are shown; (**A**) shows wild-type sagital section with paranodal loops tightly apposed to and indenting the axon, the characteristic transverse bands are also apparent (arrowheads in B). (**B**) Shows mutant sagital section with everted paranodal loops (IL); the node of Ranvier (*) is covered by paranodal junctions coming from opposite ends (Arrows 1 & 2). (**D**) Demonstrates closely apposed paranodal loops in the mutants that display electron dense intramembranous material (Black arrows) but lack transverse bands.

5 - Altered Distribution of Junctional Components in *NCP1* Mutant Mice

Our ultrastructural studies showed that the septate-like paranodal junctions are lacking in the absence of NCP1. We therefore examined the distribution of other proteins localized to this region. Contactin (CN) normally forms a *cis* complex with NCP1 (Peles et

al. 1997 and Rios et al. 2000) on the axon in the paranodes of both the PNS and CNS (Figures 5A and 5I); it is also present at nodes of Ranvier in the CNS (Figure 5G; Rios et al., 2000). In *NCP1* mutant mice, contactin is not detectable in either the nodes or the paranodes of sciatic nerve fibers (Figure 5B). In contrast, contactin expression remains robust in mutant optic nerves but its distribution is altered. In wild-type optic nerves, much of contactin is confined to paranodal regions and low levels of protein are present in the nodal region (Figure 5G). In mutant optic nerves, contactin localization is more diffuse and higher levels of this protein are observed in the nodes than in the paranodes (Figures 5H and 5J, arrowheads). These data indicate that NCP1 is required for the proper localization of contactin to the paranodal domain.

The failure to detect contactin in sciatic nerves may result from a diffuse distribution along the axon that is below the limits of detection or the loss of the protein altogether. To distinguish these possibilities, we performed Western blot analysis of the expression of contactin in peripheral nerves. We found that both the large and small molecular weight isoforms of contactin are present in wild-type sciatic nerves. These correspond to free (e.g., non-NCP1-associated) and NCP1-associated forms, respectively (Rios et al., 2000). However, only the higher molecular weight isoform is detectable in the mutant peripheral nerves (data not shown). These results suggest that loss of NCP1 does not affect the free isoform of contactin, which is likely to be predominately expressed by nonmyelinated axons in the peripheral nerve (Rios et al., 2000).

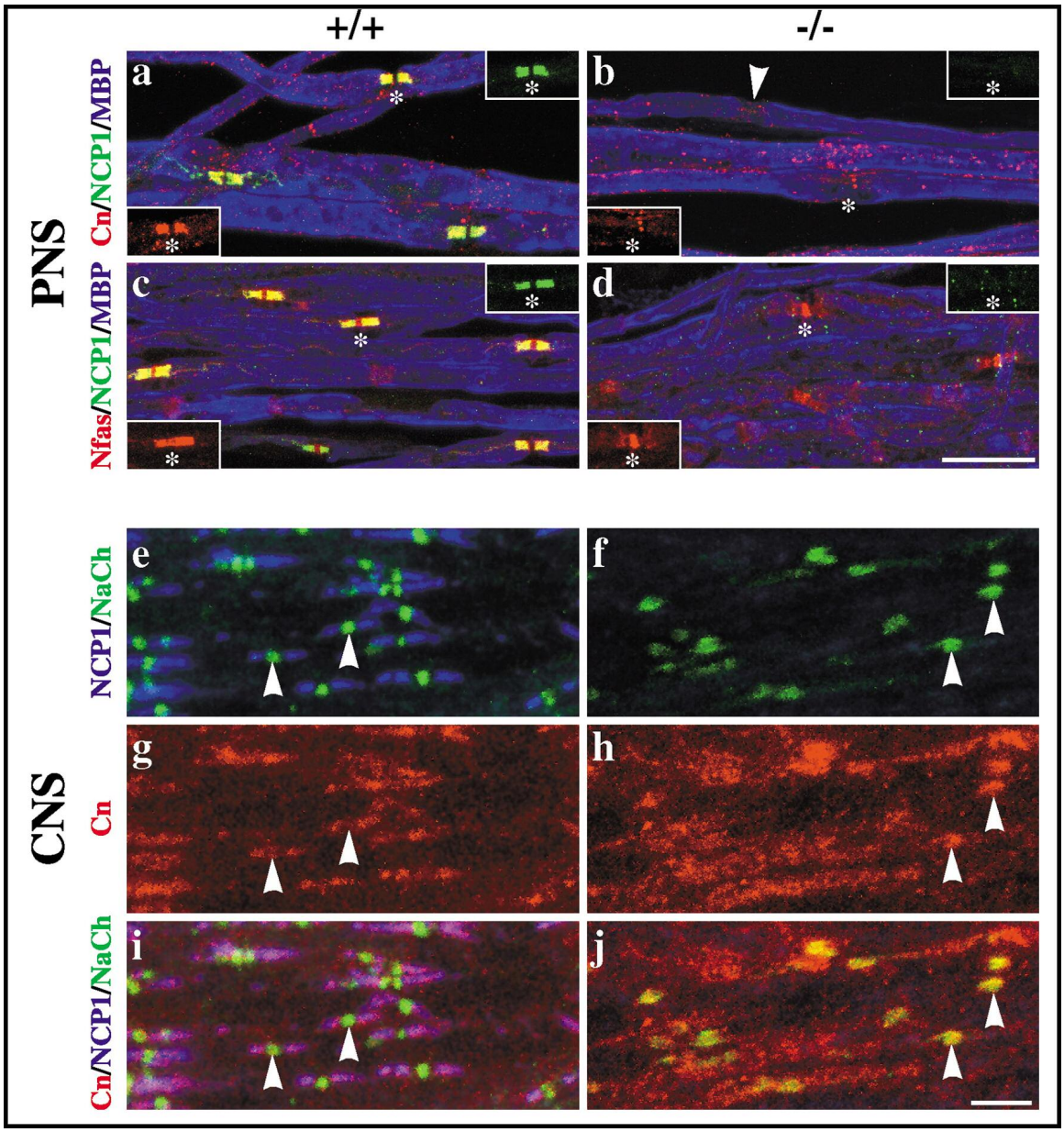

Figure 5. Expression of Paranodal Markers in Sciatic and Optic Nerves Teased sciatic nerves (PNS, **A–D**) and cryosections of optic nerves (CNS, **E–J**) from wild-type (+/+) and *NCP1* mutant (–/–) mice were stained for paranodal markers. Sciatic nerves were stained with NCP1 and MBP, and either contactin (Cn, **A** and **B**) or neurofascin (Nfas**, C** and **D**). The insets highlight a single node, indicated with an asterisk. In the wild-type nerves, NCP1 colocalizes with Cn in the paranodes; Nfas is present in both the node and paranodes. In the mutant nerve, NCP1 and Cn are not detectable in the paranodes and Nfas is largely present at the node. A second node is shown in (**B**) (white arrowhead). Bar, 20 µm.Optic nerves were stained for NCP1, Cn, and Na^+ channels (NaCh); several nodes are highlighted by the white arrowheads. In the wild-type nerves (**E, G,** and **I**), Na^+ channels at the nodes are flanked by NCP1 and Cn in the paranodal regions; Cn is also present at low levels at the node (**G**, arrowheads). In mutant nerves (**F, H,** and **J**), much of the Cn colocalizes with NaCh in the nodes (**J**, yellow in the merged images), whereas low levels are present in the paranodes. Bar, 5 µm (as reported in Bhat *et al. 2001)*.

Neurofascin is another protein localized to nodes and paranodes. Two neurofascin isoforms have been described: a 155 kDa isoform expressed by myelinating glia in paranodes (Davis et al. 1996 and Tait et al. 2000) and a 186 kDa axonal isoform localized to nodes of Ranvier. The 186 kDa isoform is thought to be part of a complex that contains ankyrin and Na^+ channels (Bennett and Lambert, 1999). To determine whether the distribution of neurofascin was affected in *NCP1* mutants, we stained peripheral nerves with a polyclonal antibody that recognizes both isoforms of neurofascin. In wild-type peripheral nerves, neurofascin is present in both nodes and paranodes (Figure 5C, red inset). In contrast, in the absence of NCP1, neurofascin is enriched in nodes but reduced in paranodes (Figure 5D, red inset). Taken together, these data demonstrate that absence of NCP1 is associated with a loss of paranodal components, indicating that it plays an important role in the molecular organization of these junctions.

6 - Ion Channel Distribution in the Absence of NCP1

A hallmark of myelinated axons is the localization of ion channels within discrete domains. Na^+ channels are concentrated at the nodes, whereas K^+ channels are largely restricted to the juxtaparanodes and to those regions of the internode that appose the noncompacted myelin membranes, e.g., the Schmidt-Lanterman incisures and the internal mesaxon (Peles and Salzer, 2000). To determine whether the defects at paranodal junctions in the mutant mice affect the distribution of these channels, we performed immunofluorescence staining of sciatic and optic nerves (Figure 6).

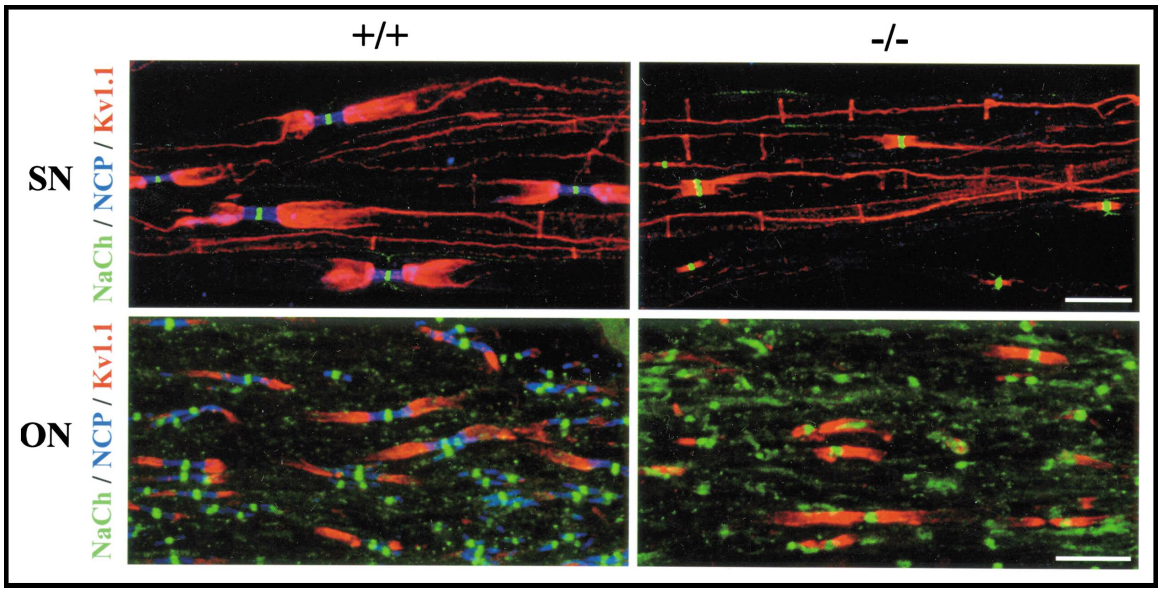

Figure 6. Voltage-Gated Channel Distribution Is Perturbed in *NCP1* Mutant Mice Teased sciatic nerves (SN) and cryosections of optic nerves (ON) from wild-type (+/+) and *NCP1* mutant (-/-) mice were stained with antibodies to ion channels. In the wild-type sciatic and optic nerves, the Na^+ channels (NaCh, green) and K^+ channels (Kv 1.1, red) are completely separated by NCP1 (NCP, blue) in the paranodes. In the mutant nerves, K^+ channels are aberrantly localized to the paranodes and overlap slightly with Na^+ channels (regions of overlap are yellow). In the PNS, there is also prominent K^+ channel staining in vertical stripes that appose Schmidt Lanterman incisures. Bars, 20 μm (SN); 10 μm (ON) (as reported in Bhat *et al. 2001).*

In wild-type and mutant mice, Na^+ channels (green) are largely confined to the nodes of Ranvier. The distribution of the Na^+ channels is wider and more diffuse at the nodes of mutant mice, particularly in the optic nerve (Figure 6, ON). In contrast, the distribution of the K^+ channels (red) differs markedly between wild-type and *NCP1* mutant mice. In wild-type nerves, K^+ channels are completely separated from the Na^+ channels by the paranodes. In the mutant mice, K^+ channels are mislocalized to the paranodal region, immediately adjacent to and, in some cases, slightly overlapping with Na^+ channels (areas of overlap appear as yellow in the merged images). K^+ channel staining remained robust in the internodal axolemma of mutant mice. Interestingly, there is an increase in the number of stripes of K^+ channels along the axon. These stripes are apposed to the Schmidt-Lanterman clefts as confirmed by double staining with myelin-associated glycoprotein (MAG) antibody, a marker of these incisures

(data not shown). Hence, these data indicate that paranodal junctions are required for the segregation of Na^+ and K^+ channels into distinct, nonoverlapping domains

DISCUSSION

The ultrastructure of the paranodal region was first described over four decades ago (Robertson 1957; Andres 1965 and Bargmann and Lindner 1964), but its molecular composition remained elusive until the identification of NCP1 as a major junctional component (Einheber et al. 1997 and Menegoz et al. 1997). Our data show that NCP1 is an essential component of the paranodal junctions. The *NCP1* mutant mice therefore provide a unique model to dissect the function of paranodal junctions in myelinated axons.

1 - Phenotypic Abnormalities of *NCP1* Mutant Mice

In the absence of NCP1, mice exhibit tremors, paresis, and ataxia. We believe that these neurologic defects reflect the function of NCP1 in the nervous system since we did not observe its expression in non-neuronal tissues (e.g., lung, heart, kidney, stomach, intestine, pancreas, and testes) by Western blotting analysis (data not shown). While we have focused our efforts on the paranodal junctions and the organization of myelinated fibers, NCP1 is also expressed by nonmyelinated axons and in the central gray matter (Einheber et al. 1997 and Menegoz et al. 1997). Therefore, the neurologic abnormalities may be due to paranodal and extrajunctional defects.

The neurologic defects of these mice resemble those of the contactin mutant mice (Berglund et al., 1999). As contactin is also localized to the paranodes (Rios et al., 2000) and is required for the cell surface expression of NCP1 (Faivre-Sarrailh et al., 2000), it will be of interest to determine the organization of the paranodal region in these mutant mice. Contactin mutant mice are ataxic and have striking defects in cerebellar development, reflecting its expression by several types of cerebellar neurons and its role in mediating neurite outgrowth and neuronal interactions (Faivre-Sarrailh and Rougon, 1997). NCP1 has been suggested to function as a co receptor for contactin and is highly expressed within the cerebellum (Peles et al., 1997; G.P.G.-F. and M.B., For review). Although the cerebellar development of *NCP1* mutant mice has not been examined, the ataxia, wide-based gait, and tremor of these mice may reflect defects of cerebellar development rather than abnormalities of the paranodal region per se. Contactin mutant mice are likely to exhibit more widespread defects than *NCP1* mutant mice in view of the extrajunctional expression of this protein at central nodes of Ranvier, by oligodendrocytes, and, potentially, specific neurons.

2 – Abnormal Axon-Glial Interaction at the Nodes and Paranodes of *NCP1* Mutant Mice

A major defect of the mutant mice is the absence of transverse bands, the hallmark of the paranodal junctions. These findings provide formal evidence that NCP1 is a key axonal component of these junctions, consistent with its striking localization to these junctions (Einheber et al. 1997 and Menegoz et al. 1997). In addition, the close apposition and indentation of the axon by the paranodal loops was frequently absent and, in the most severe

cases, the paranodal loops were detached from the axon (Figure 4D). These results indicate that NCP1 is required to stabilize the adhesion of these loops to the axon, either directly or in combination with other junctional components. Interestingly, the paranodal loops occasionally retain a close association with the axon and, in these cases, some intramembranous density is apparent by EM (see Figure 4D arrows). These findings suggest that other components of the junctions, yet to be identified, may be able to promote axon attachment in the absence of NCP1. Alternatively, Caspr2, which shares high homology to NCP1 in its ectodomain (Poliak et al., 1999) and which is mislocalized from the juxtaparanodes into the paranodal region of *NCP1* mutant mice (data not shown), may contribute to this adhesion.

In the CNS, the morphologic organization of the paranodal region is often grossly perturbed—most strikingly represented by the eversion of the glial loops (Figures 4B IL). Defective attachment of the paranodal loops to the axon in these mice seems likely to account for this anomalous morphologic organization. The myelin sheath is elaborated by circumferential growth of the inner turn of the glial cell membrane that spirals around the axon (Bunge et al., 1989). In the *NCP1* mutant mice, frequently only the paranodal loops of the innermost myelin turns remained attached to the axon, whereas the lateral loops of the outermost turns were often unattached, everted, and displaced medially. It is not known when the loops detach: potentially the inner turn of the myelin sheath may displace existing glial contacts with the axon as it spirals around the axon, or alternatively, the loops may detach after myelin sheaths have already formed. Other abnormalities, including loops from a single myelin sheath that appose each other and myelin segments that overlap, also suggest defective glial attachment. In PNS the paranodal abnormalities are not as abrupt (data not

shown). Potentially, the presence of a well-formed basal lamina and/or the Schwann cell microvilli which project to the node (Melendez-Vasquez et al., 2001), both of which are unique features of PNS myelin, may stabilize the paranodal loop organization sufficiently to prevent severe abnormalities. As the amount and organization of compact myelin was not affected in the mutant mice, radial growth of the myelin sheath does not require NCP1.

3 – *NCP1* Mutant Mice Are Deficient in Junctional Components

Based on immunofluorescence staining of peripheral nerves, two other components of the paranodal junctions, contactin and neurofascin, which are expressed by neurons and Schwann cells, respectively (Rios et al. 2000 and Tait et al. 2000), are undetectable or substantially reduced in the paranodal region. Initial immunoblotting studies of sciatic nerve extracts show that a lower molecular weight isoform of contactin that specifically associates with NCP1 (Rios et al., 2000) is undetectable and that the 155 kDa isoform of neurofascin is significantly reduced (data not shown). Thus, there is a global deficiency of the known paranodal components in the *NCP1* mutant mice. Whether the loss of these components reflects the failure of the paranodal loops to attach to axons properly in the absence of NCP1 or, alternatively, that these components are not properly targeted or are unstable in the absence of NCP1, is not yet known. However, loss of contactin and neurofascin is likely to further contribute to the defects of glial loop adhesion.

In the CNS, contactin is expressed at comparable levels in wild-type and *NCP1* mutant mice (Figure 3B) but its localization is perturbed. Specifically, staining of contactin in the paranodes is reduced whereas that in the nodes of Ranvier is increased and appears

diffuse (Figure 5). These findings suggest that in the absence of NCP1, contactin redistributes from the paranodes to the nodes and provide further evidence that NCP1 is required for the appropriate targeting of contactin to the paranodes (Rios et al., 2000). The normal expression levels of contactin seen by Western blotting may reflect a non-NCP1-interacting pool of this protein in oligodendrocytes (Einheber et al. 1997 and Koch et al. 1997) and at nodes of Ranvier in the CNS. These findings may also indicate that neuronal expression of contactin in extrajunctional sites is not dependent on NCP1.

4 – Paranodal Junctions and Domain Organization in Myelinated Axons

A striking finding of this study is that the delineation between channel domains requires NCP1 and the transverse bands. In their absence, the delayed rectifier K^+ channels are displaced into the paranodes adjacent to the node. The data also indicate that Na^+ and K^+ channels still cluster in the absence of these junctions. This is consistent with previous studies demonstrating that nodal clustering occurs prior to mature paranodal junction formation in the developing PNS (Melendez-Vasquez et al., 2001) and in the *CGT* mutant mice, which fail to form normal junctions (Dupree et al., 1999). It is of note that Na^+ and K^+ channel domains remain largely segregated, suggesting that even in the absence of the transverse bands, unique molecular interactions, possibly involving distinct scaffolding proteins (Peles and Salzer, 2000), maintain the separation of these channel domains. K^+ channels associate with the closely related Caspr2 protein (Poliak et al., 1999), which is also mislocalized to the paranodes (data not shown).

The paranodal defects of the *NCP1* mutant mice strikingly mirror those in the *CGT* mutant mice (Coetzee et al., 1996). Common features of both mutant mice include the absence of transverse bands, everted loops, and other paranodal abnormalities in the CNS, an increase in the number of Schmidt-Lanterman incisures in CNS myelin, and the relatively normal morphology of the paranodal region in the PNS. These common findings are reflected in the loss of the delineation between the channel domains and a reduction in the nerve conduction velocity and amplitude in the PNS (Dupree et al., 1998). Our results, therefore, indicate that the defects in the K^+ channel distribution in the *CGT* mutant mice are likely to be secondary to the loss of the paranodal junctions rather than a more generalized effect on myelin. There are, however, differences between the *CGT* and *NCP1* mutant mice. In particular, we did not observe the extensive myelin splitting or vacuolar degeneration in the *NCP1* mutant mice that has been reported for the *CGT* mutants (Coetzee et al., 1996). This degeneration had been suggested to result from increased permeability resulting from the loss of junctional integrity and entrance of fluid into the periaxonal space (Dupree et al., 1998). As such degeneration is limited in the *NCP1* mutant mice, the vacuolar degeneration may instead reflect abnormalities in the glycolipid composition of the *CGT* mutant mice. In addition, the K^+ channels in the *CGT* mutant mice exhibit a more diffuse distribution within the internodes rather than the discrete paranodal distribution characteristic of the *NCP1* mutant mice (see Figure 6). These latter results suggest that the glial interactions that regulate the distribution of K^+ channels may be more globally affected in the *CGT* mutant mice than in the *NCP1* mutant mice.

The striking homology between these mutants provides further support for a role of Gal C and/or sulfatides in the formation of the paranodal region. An interesting possibility is

that these glycolipids are themselves ligands for NCP1. Indeed, NCP1 is diffusely distributed throughout the internode in the *CGT* mutant mice, rather than confined to the paranodal region (Dupree et al., 1999). In addition, NCP1 contains a discoidin domain and laminin G domains that exhibit structural homology to lectins (Rudenko et al., 1999). Interestingly, laminin G domains bind several ligands including sulfatides (Talts et al., 1999). Alternatively, defects of these glycolipids may have generalized effects on the myelin sheath, including the composition or trafficking of glial junctional components.

5 – Conserved Function of the NCP Family During Evolution

Septate junctions form between the ensheathing glial cells that surround the nerve bundles in *Drosophila* and are essential for establishment of the blood-nerve barrier (Bellen et al., 1998). We have previously shown that the *Drosophila* NRX IV protein localizes to and is required for the formation of the ladder-like septae characteristic of these junctions (Baumgartner et al., 1996). In *nrx IV* mutants, these septae were absent, and another component of these junctions, Coracle, a band 4.1 homolog, was mislocalized (Baumgartner et al. 1996 and Ward et al. 1998). The current studies demonstrate that the septate and paranodal junctions appear to serve conserved functions in maintaining the axonal milieu required for action potential propagation. However, the topology and localization of the proteins is clearly different. In *Drosophila*, NRX IV is expressed by and localized between glial cells. In mice and other vertebrates, NCP1 is expressed by neurons and localized between the axon and glial cells. Hence, even though there is functional conservation, significant changes in expression occurred during evolution.

In summary, we have demonstrated that NCP1 has a key role in the formation of the paranodal junctions and, thereby, in the delineation of the axonal domains of myelinated axons. Future studies focused on the identification of other components of these junctions, including the glial ligands for NCP1 and the cytoskeletal protein(s) with which it interacts, should clarify how these junctions assemble and the mechanisms by which they promote separation of distinct populations of voltage-gated ion channels.

EXPERIMENTAL PROCEDURES

1 – Antibodies

Sequences corresponding to the cytoplasmic region of *NCP1* were cloned into an expression vector, pET-28a(+) (Novagen). The recombinant protein was expressed in *E. coli* BL21(DE3), resolved by SDS-PAGE, and used to immunize guinea pigs as described in Bhat et al. (1996). Other antibodies used included rabbit polyclonal antibodies to contactin-Fc (Rios et al., 2000), to human contactin/F3 (J. Hemperly, Becton Dickinson), to neurofascin (P. Brophy, University of Edinburgh, Scotland), to PLP (D. Colman, Mount Sinai, New York), a chicken antibody to ankyrin$_G$ (S. Lambert, University of Massachusetts Medical Center), and mouse monoclonal antibodies to the α subunit of the voltage-gated Na^+ channel (J. Trimmer, SUNY, Stony Brook) and to MBP (SMI 94; Sternberger Monoclonals). The secondary antibodies conjugated to rhodamine, fluorescein, or Cy-5 were obtained from Jackson Laboratories.

2 – Preparation of Teased Sciatic Nerve and Optic Nerve Fibers

Sciatic nerves were removed from litter-matched wild-type and mutant mice and fixed in phosphate buffer saline (PBS) with 1% or 4% paraformaldehyde for 1.5 hr. The nerves were then stored in PBS at 4°C until teased. Using fine needles, the individual fibers of the sciatic nerve were teased while in ice-cold PBS. Teased sciatic nerve fibers (TSNs) were then mounted on glass slides and dried overnight at RT followed by treatment with acetone at −20°C for 20 min. The slides were washed with PBS several times before immunostaining; in some cases, slides were stored at −80°C until processed further. Optic nerves were dissected out and fixed in 1% paraformaldehyde in PBS for 1.5 hr. Nerves were stored in PBS, cryoprotected with 30% sucrose, and frozen in Tissue-Tek OCT with isopentane cooled in liquid nitrogen. The tissue was sectioned at 10 μm on a Leica CM1900 cryostat with a chamber temperature of −26°C and stage temperature of −28°C.

3 – Immunofluorescence and Western Blot Analysis

Fixed tissue samples (TSNs and optic nerve sections) were permeabilized with acetone at −20°C, washed with dPBS, and blocked for 1 hr at room temperature in a blocking solution consisting of dPBS, 5% BSA, 1% normal donkey serum, and 0.2% Triton X-100 (Sigma Chemical). Primary antibodies diluted in blocking solution were added and left overnight in a humidifying chamber at 4°C. After washing several times with dPBS plus 0.2% Triton X-100, the tissue was incubated with corresponding secondary antibodies at a dilution of 1:100 in blocking solution for 1 hr at RT. For labeling with anti-contactin, tissue

was incubated with anti-contactin alone overnight and stained with donkey anti-rabbit rhodamine, prior to incubation with anti-NCP1 and anti-sodium channel antibodies. The tissue was then washed several times with dPBS, washed once with water, and mounted in Citifluor (Ted Pella, Redding, CA). The tissue was examined by epifluorescence on a Zeiss LSM 510 confocal microscope.

Whole brain or sciatic nerve lysates were prepared in 25 mM Tris-HCl buffer, pH 7.4, containing 2% SDS, 95 mM NaCl, 10 mM EDTA, 0.2 mM sodium vanadate, 10 mM sodium pyrophosphate, 1 mM PMSF, 10 μg/ml aprotinin, and 20 μM leupeptin, boiled for 5 min, and centrifuged for 10 min. The lysates were quantitated and subjected to SDS gel electrophoresis, blotted onto nitrocellulose, probed with primary antibodies and developed using the SuperSignal chemiluminescent substrate (Pierce).

4 – Electron Microscopy

Wild-type and mutant littermates (P20) were anesthetized with pentobarbital and perfused through the heart with either 3% glutaraldehyde/2% paraformaldehyde in 0.1 M cacodylate buffer, pH 7.3 (fixative 1), or 4% paraformaldehyde/2.5% glutaraldehyde in 0.1 M phosphate buffer, pH 7.4 (fixative 2). Samples of cerebellum prepared with fixative 1 were rinsed and postfixed in osmic acid/ferricyanide in 0.1 M cacodylate buffer. They were rinsed, dehydrated in an ascending series of methanol solutions, and embedded in Araldite. One micron sections were stained with toluidine blue for light microscopy, and 0.1 μm sections were stained with potassium permanganate followed by uranyl acetate for ultrastructural examination. The Cerebelli prepared with fixative 2 were postfixed in the

same solution for an additional 18–24 hr at 4°C. Vibratome sections (40 μm) of the samples were processed, embedded in Epon 812, and sectioned for electron microscopy as previously described (Einheber et al., 1997). Thin sections were examined with Philips 300, CM10, or CM 12 electron microscopes at 60 kV.

5 – Phenotypic Analysis of Mice

Weights were obtained daily up to P30, with data collected from 19 homozygous males, 44 heterozygous males, 24 wild-type males, 20 homozygous females, 30 heterozygous females, and 20 wild-type females; later time points correspond to fewer numbers of animals. To measure the motor activity, an open field test was performed at P21, P40, and P100 as described (Thullier et al., 1999). Briefly, animals were placed one at a time in standing position in the same middle square in a rectangular area 55 cm long by 30 cm wide with walls 30 cm high; this testing area was divided into a grid of 66 equally sized squares. Ink foot printing and careful observation allowed the number of crossed squares to be recorded for each mouse over a 1 min period.

CHAPTER III

Disruption of Axo-glial Junctions in the Cerebellum Causes Degeneration of Purkinje Neuron Axons

ABSTRACT

Axo-glial junctions (AGJs) play a critical role in the organization and maintenance of molecular domains in myelinated axons. Here, we report that a disruption of AGJs in *Neurexin IV/Caspr/Paranodin* (*NCP1*) and *Ceramide galactosyltransferase* (*CGT*) mutant mice results in cytoskeletal disorganization which is accompanied by large axonal swellings in cerebellar Purkinje neurons. Ultrastructural analysis shows abundant accumulation of mitochondria and smooth endoplasmic reticulum (SER) at paranodal regions, indicating impairment in axonal transport. Biochemical experiments indicate that NCP1 associates with key cytoskeletal proteins, band 4.1B, actin and αIIspectrin (fodrin), to establish a molecular link between AGJs and axonal cytoskeleton that is indispensable for the organization and function of the paranodal domain. Our findings indicate that AGJ disruption leads to axonal cytoskeletal disorganization and axonal degeneration resulting in severe motor deficits raising the possibility that some forms of human ataxia may be linked to components of the AGJs.

INTRODUCTION

The anatomical organization of myelinated fibers into distinct domains is the basis for the saltatory mode of action potential propagation. These molecular domains-- internode, juxtaparanode, paranode, and node of Ranvier-- form as a result of yet unknown signaling mechanisms between the myelinating glial cells and neurons. In the paranodal region closely apposed axon-glial membranes form specialized cell junctions which resemble the ladder-like invertebrate septate junctions, and are referred to as paranodal septate junctions or paranodal axo-glial junctions (AGJs) (Bhat, 2003a; Pedraza et al., 2001; Popko, 2003; Salzer, 2003) The formation, maintenance and distribution of the paranodal AGJs involves a number of proteins such as UDP-galactose:ceramide galactosyltransferase (CGT), proteolipid protein (PLP), 2', 3'-cyclic nucleotide phosphodiesterase, myelin basic protein, and myelin associated glycoprotein (MAG). (Coetzee et al., 1996; Honke et al., 2002; Klugmann et al., 1997; Lappe-Siefke et al., 2003; Rosenbluth, 1981; Trapp et al., 1989). Recently, three major proteins have been identified that localize to the paranodal AGJs: NCP1 and a GPI-anchored neural cell adhesion molecule, Contactin (CN) on the axonal side and Neurofascin 155 kDa isoform (NF155) on the glial side (Bhat et al., 2001; Boyle et al., 2001; Charles et al., 2002; Menegoz et al., 1997). NCP1 and CN are the only known axonal proteins that participate in the formation and/or organization of the paranodal AGJs. Mutations in *NCP1* and *CONT* result in the loss of paranodal AGJs and a failure to segregate Na_+ and K_+ channels at the nodes and juxtaparanodes respectively (Bhat et al., 2001; Boyle et al., 2001). Similar phenotypes were observed at the paranodal regions in *CGT* mutants (Dupree et al., 1999). *CGT* encodes an enzyme that is essential for the production of galactocerebroside and

sulfatide (Coetzee et al., 1996; Dupree et al., 1999). The mechanisms that underlie the paranodal defects in *CGT* mutant mice are not well understood (Dupree and Popko, 1999). Biochemical studies established that NCP1 associates in cis with CONT (Peles et al., 1997). CN on the other hand is required for proper surface expression of NCP1 (Faivre-Sarrailh et al., 2000) and both proteins form a high molecular weight complex in the paranodal junctions (Rios et al., 2000). Recently, the *Drosophila* homologs of NCP1 and CN have been shown to interact and colocalizes at the epithelial and glial septate junctions (Faivre-Sarrailh et al., 2004). To date NCP1 is the only identified axonal AGJ protein that contains a cytoplasmic domain and may therefore participate in signaling and/or mediate interactions with the axonal cytoskeleton (Bhat, 2003b), however, definitive evidence to support these assumptions has not been presented. Here we report that genetic ablation of *NCP1* and *CGT* in mice results in severe ataxia and motor coordination defects. Ultrastructural analysis of the mutant Purkinje neurons showed axons undergoing degeneration and axons with cytoskeletal abnormalities and heavy local accumulation of mitochondria, SER and phosphorylated neurofilaments near the paranodal regions. Biochemical experiments demonstrate for the first time that NCP1 at the AGJs is linked to axonal cytoskeleton via a complex containing an actin spectrin binding protein, band 4.1B, actin and a neuronal spectrin, fodrin or ⟨II spectrin. Taken together, our studies establish a new parallel between phenotypes caused by deficits in AGJ formation and neurodegenerative diseases and provide new insights for studies involving axonal degeneration in myelinated neurons.

RESULTS

1 - Genomic Organization of the *NCP1* Gene, Generation of the *NCP1- lacZ* Knock-in Mice and *NCP1- lacZ* Expression

We first determined the genomic structure of the *NCP1* gene by comparing the mouse cDNA sequence of *NCP1* (Genebank Accession #AF039833) with the genomic database sequences. This analysis revealed that the *NCP1* gene spans a total of ~14 kilobases (kb) and is composed of 24 exons. Northern blot analysis revealed that the *NCP1* gene does not seem to undergo any detectable alternative splicing. Based on the intron-exon structure of the *NCP1* locus, a targeting construct was designed to insert a *lacZ-neo* cassette at an appropriate restriction site within the *NCP1* coding sequence to mimic the expression of *NCPI*, which could be detected by β-galactosidase staining. A *lacZ-pgk-neo* cassette was flanked by a 4.5 kb EcoRI-SmaI fragment (5'-homology) (Fig. 1A) and a 2 kb SmaI fragment (3'-homology). This design placed the *lacZ* gene in the coding sequence of *NCP1* which would result in the transcription of *lacZ* mRNA in a pattern similar to that of *NCP1*. To generate *NCP1- lacZ* knock in mice, standard procedures were used (Bhat et al., 2001). The linearized targeting vector was electroporated into ES cells and clones carrying the targeted allele were injected into mouse blastocysts and a chimeric male was obtained that transmitted the targeted allele to its progeny. Heterozygous and homozygous mice were confirmed by genomic PCR analysis (Fig. 1Ba). Mice homozygous for the *NCP1-lacZ* allele are born at the expected Mendelian frequency from heterozygous intercrosses although they are severely affected. These mice display an identical phenotype as that of the *NCP1* mutant mice generated previously (Bhat et al., 2001).

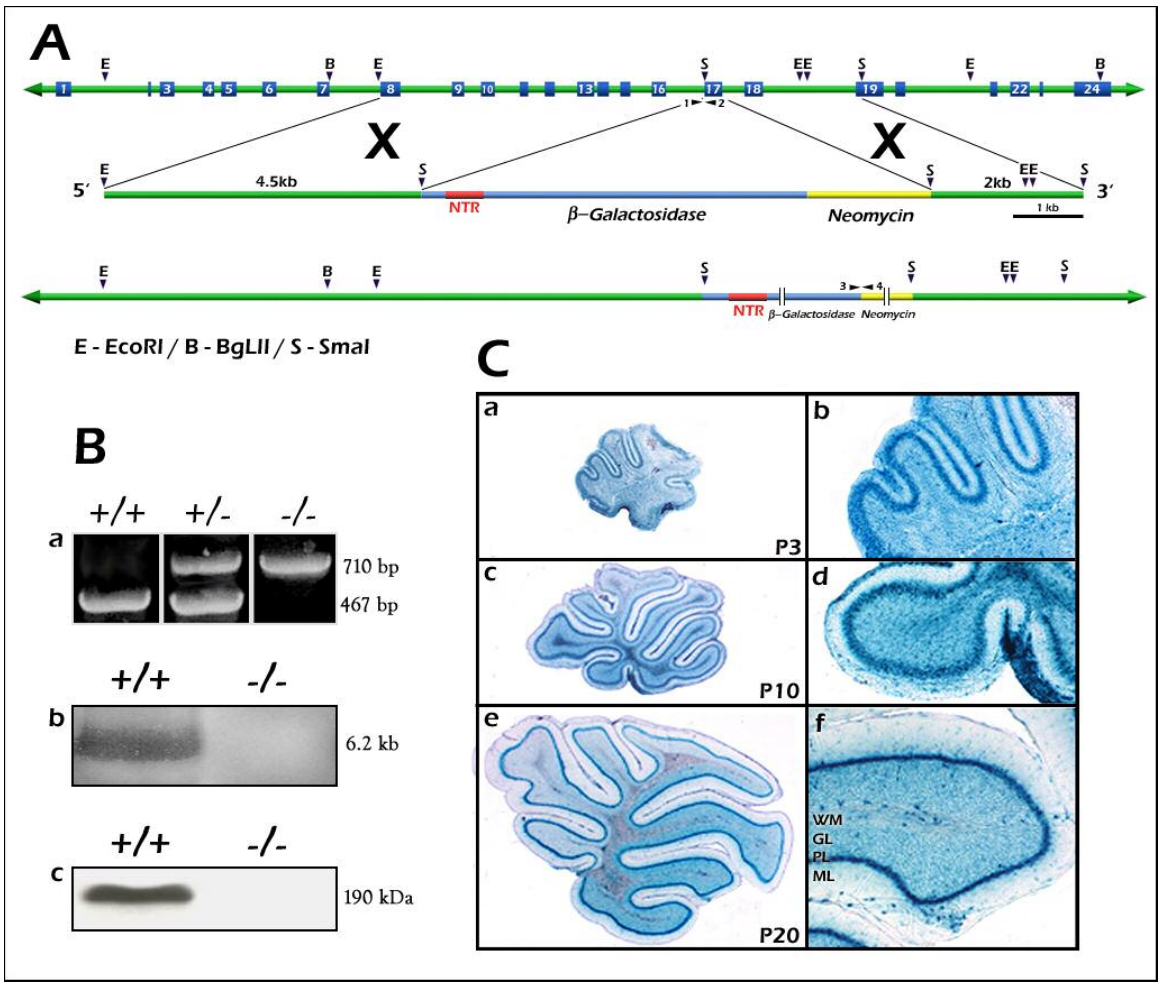

Figure 1. Generation of *NCP1-lacZ* Knock in Mutants. (**A**) *NCP1* genomic locus and *NCP1-lacZ* targeting vector. A restriction map of ~15 kb genomic DNA containing the entire *NCP1* gene. The exons are represented as blue boxes and some of the key restriction sites are indicated that were used to generate the *NCP1-lacZ* targeting vector. The *lacZ-neo* cassette was inserted between a SmaI site with a 4.5kb EcoRI-SmaI as the 5' homology region and a 2 kb SmaI-SmaI as the 3' homology region. Upon homologous recombination in the ES cells, the *NCP1-lacZ* targeting construct generated the *NCP1-lacZ* targeted allele. The *lacZ* transcript is expressed as a fusion transcript with NCP1 transcript, but is translated independent of *NCP1* translation as it contains a vertebrate translation initiation sequence (NTR). The numerical numbers 1, 2 and 3, 4 with small arrows indicate the PCR primers used for genotyping the wild type and *NCP1-lacZ* mutant alleles, respectively. (**B**) Genotyping. (Ba) Genotyping by PCR used two primers (1+2) amplifying a 467 bp fragment for the wild type (+/+) allele and two primers (3+4) amplifying a 710 bp fragment for the mutant (-/-) allele. The heterozygous (+/-) animals amplify both fragments. (Bb) Northern analysis. Poly A+ mRNA was prepared from wild type and *NCP1-LacZ* mice and processed for Northen blotting. A 3' cDNA fragment was used for hybridization which detected a 6.2 kb transcript in the wild type (+/+) mice. This transcript was not detected in the *NCP1-lacZ* (-/-) mutants indicating disruption of the *NCP1* gene. (Bc) NCP1 expression. The wild type (+/+) animals showed a predominant protein band migrating at 190 kDa which was not detected from homozygous (-/-) animals demonstrating the loss of the NCP1 protein in *NCP1-lacZ* mice. (**C**) β-Galactosidase expression. 30µm sagital sections of the cerebellum from P3 (Ca,b), P10 (Cc,d) and P20 (Ce,f) *NCP1-lacZ* animals were stained in X-gal solution. β-Gal activity is seen in the Purkinje neurons through all postnatal developmental stages. In addition, the β-gal activity is also present in the granular layer neurons. β-Gal activity is not seen in the molecular layer (Cf) at P20. Wild type animals did not reveal any β-gal activity (not shown). (ML, molecular layer; PL, Purkinje neuron layer; GL, inner granular layer; WM, white matter).

The following data indicate that the *NCP1-lacZ* mutation is a null mutation. First, the *NCP1* transcript is truncated as the coding sequence at exon 17 is disrupted. This was confirmed by Northern analysis using a cDNA probe that is downstream of the insertion site. No *NCP1* transcript was detected in the homozygous *NCP1-lacZ* mice as compared to the wild type (Fig. 1Bb). The NCP1 protein was not detected in whole brain and sciatic nerve homogenates from homozygous mutant mice by Western blot analysis using two independent anti-sera generated to the C-terminal domain of NCP1; the same antisera revealed the 190 kDa NCP1 proteins in wild type tissue (Fig. 1Bc). The severe motor coordination defects displayed by *NCP1* mice (Bhat et al., 2001) prompted us to analyze the expression of *NCP1-lac*Z in the cerebellum. To assess the expression pattern of the *NCP1-lac*Z, β-galactosidase (β-Gal) protein activity was localized in situ. The cerebella were dissected from *NCP1-lac*Z mice at P3, P10 and P20. As shown in Fig. 1Ca-c, β-Gal activity was seen in Purkinje cell layer and inner granular layer throughout postnatal development. β-Gal activity was strong in the Purkinje neurons and relatively low in the inner granular layer at all stages examined (Fig. 1C). Taken together, these data show that we have generated *NCP1-lacZ* mutant mice that lack the NCP1 protein and that β-Gal activity in situ can be used to monitor the spatiotemporal expression of the *NCP1* gene throughout development.

2 - Ataxia and Motor Deficits in AGJ Defective *NCP1* and *CGT*Mutants

Strong ß-Gal activity in the Purkinje cells indicates that NCP1 plays an important role in cerebellar function throughout the life span of the animal. This idea is further implied by the severe neurological phenotype that is prominent in both the *NCP1* and the *NCP1-lacZ*

mutant mice. For the current study, *NCP1* mutant mice were analyzed and wherever necessary, the phenotypes observed were confirmed in *NCP1-lacZ* mutant mice (data not shown). Starting at post-natal day 11 (P11), the mice display hypomotility, movement associated tremor, severely impaired control and coordination of movement and a wide based gait suggestive of cerebellar defect (Altman and Bayer, 1997; Palay and Chan Palay, 1974). As shown in Fig 2A, *NCP1* mutant mice lack control and coordination of movement, which is demonstrated by frequent falls during normal walking and by an impaired righting response.

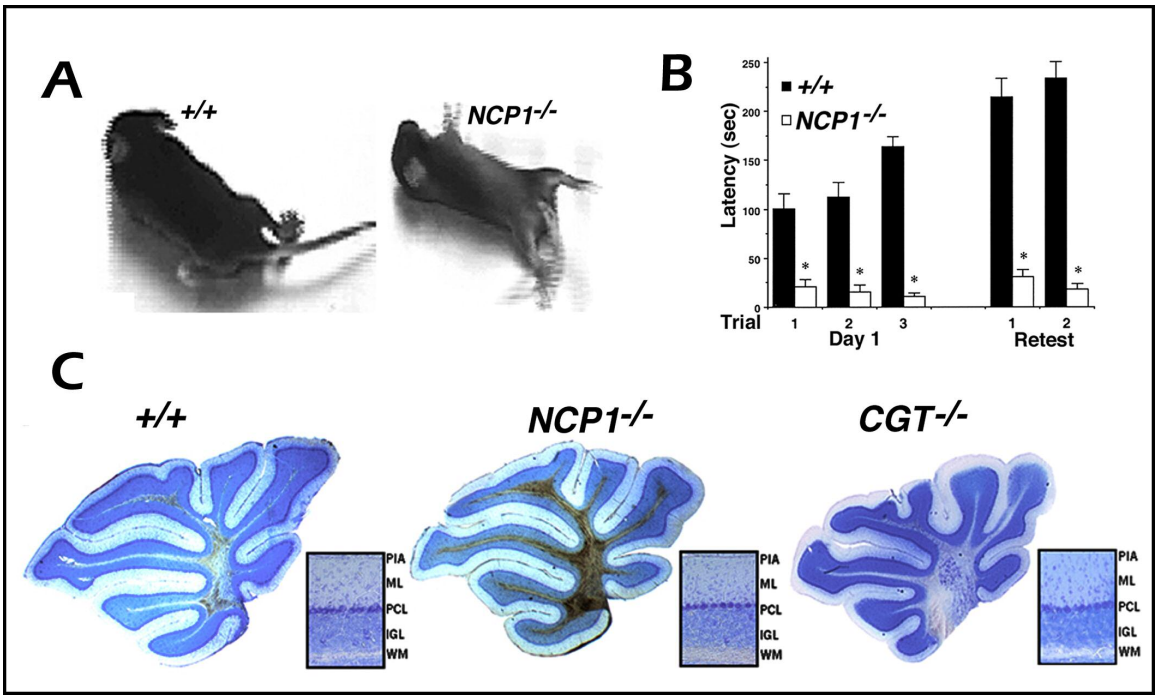

Figure. 2. Motor Coordination and Cerebellar Morphology in *NCP1* and *CGT* Mutants. (**A**) Visual appearance of a P20 *NCP1* mutant (-/-) and a wild type littermate (+/+). (**B**) Latencies of wild type (n=11) and *NCP1* mutant (n=7) mice to fall from an accelerating rotarod. *NCP1* mutants are unable to balance and walk forward on the rotating rod, and fall off quickly (* p<.05, post-hoc test following repeated measures ANOVA). (**C**) Overall cerebellar morphology in the wild type, *NCP1* and *CGT* mutants show no apparent differences. Insets in (C) shows magnified views of the cerebellar layers with no obvious defects in neuronal migration. (ML, molecular layer; PCL, Purkinje neuron layer; IGL, inner granular layer; WM, white matter).

Additionally, while wild type mice extend their hind limbs and digits in response to being suspended by their tail, *NCP1* mutants retract their hind feet and clench their digits

when similarly suspended. Furthermore, these mutants have an ataxic gait with a shuffling footprint pattern, a widened stance, and a lack of fore foot hind foot correspondence (data not shown). An accelerating rotarod was used to assess the ability of the surviving 3-month-old *NCP1* mice to coordinate movement (Fig.2B). Wild type littermate control mice demonstrated normal motor coordination and balance, and exhibited significant improvement in performance over successive training trials. In contrast, the *NCP1* mice were able to remain on the accelerating rod for only a few seconds, and their performance did not improve across successive training trials. Both cerebellar ataxia and peripheral deficits could contribute to these results. Measures of rearing and grip strength were similarly deficient in *NCP1* versus wild type controls (data not shown).

Although these neurological deficits are consistent with cerebellar dysfunction, the precise mechanism that accounts for this phenotype remains unclear. Our previous findings have shown that *NCP1* mutant mice display disrupted paranodal AGJs in the CNS (Bhat et al., 2001). Therefore based on our previous morphological observations combined with our current ß-Gal expression data, we postulate that the absence of NCP1, which results in the disruption of AGJs, is responsible for cerebellar dysfunction and the impaired motor coordination observed in the *NCP1* mutants. To test this hypothesis, we carried out a series of experiments exploiting the *NCP1* mutants that provide convincing evidence that cerebellar function is compromised in the absence of NCP1. Additionally, we have also analyzed the *CGT* mutant mice (Coetzee et al., 1996). The *CGT* null mice were chosen for this analysis since they also lack properly formed paranodal AGJs (Dupree et al., 1998). In addition, *CGT* mutants display a similar phenotype as the *NCP1* mutants with regard to hypomotility, movement associated tremor, severely impaired control and coordination of movement and a

wide-based gait. In contrast to the *NCP1* mice, the *CGT* mutants express normal levels of NCP1 but the distribution is altered and the genetic deficit in the *CGT* mice is in the glial cell whereas the genetic defect in the *NCP1* mutants is in the neuron.

Since previous studies of the *NCP1* and *CGT* mutants have not addressed cerebellar morphology, we first performed a detailed structural analysis of the cerebella of these mice. Using semi-thick sections (30μm) from P20 mice, we show that cerebellar morphology is not dramatically affected in *NCP1* and *CGT* mutants as compared to wild type animals (Fig. 2C). The *NCP1* and *CGT* mutants are generally smaller in size than their wild type littermates and have a smaller cerebellum. The cerebellar white matter tracts in the *NCP1* mutants labeled darker with toluidine blue staining compared to the wild type and *CGT* mice. It is not clear whether these differences reflect changes in the lipid composition of the myelinated axons or some other aspects of the white matter in the *NCP1* mutants. Moreover, the cerebellar layers in *NCP1* and *CGT* mutants were indistinguishable from their wild type littermates. These data indicate that mutations in *NCP1* and *CGT* do not affect gross cerebellar development and morphogenesis.

***3 - NCP1* and *CGT*Mutant Purkinje Neuron Axons Develop Large Swellings**

The expression of *NCP1* in the cerebellum, the behavioral deficits displayed by *NCP1* and *CGT* mutant mice, and the lack of appreciable morphological abnormalities in their cerebella, prompted us to analyze the cerebellar ultrastructure in more detail. A comparison of the β-gal activity and the NCP1 protein expression showed an identical expression pattern,

however, most of the β-gal activity (Fig. 1C) remains restricted to the neuronal cell bodies as it is not detected along the axons or dendrites (data not shown).

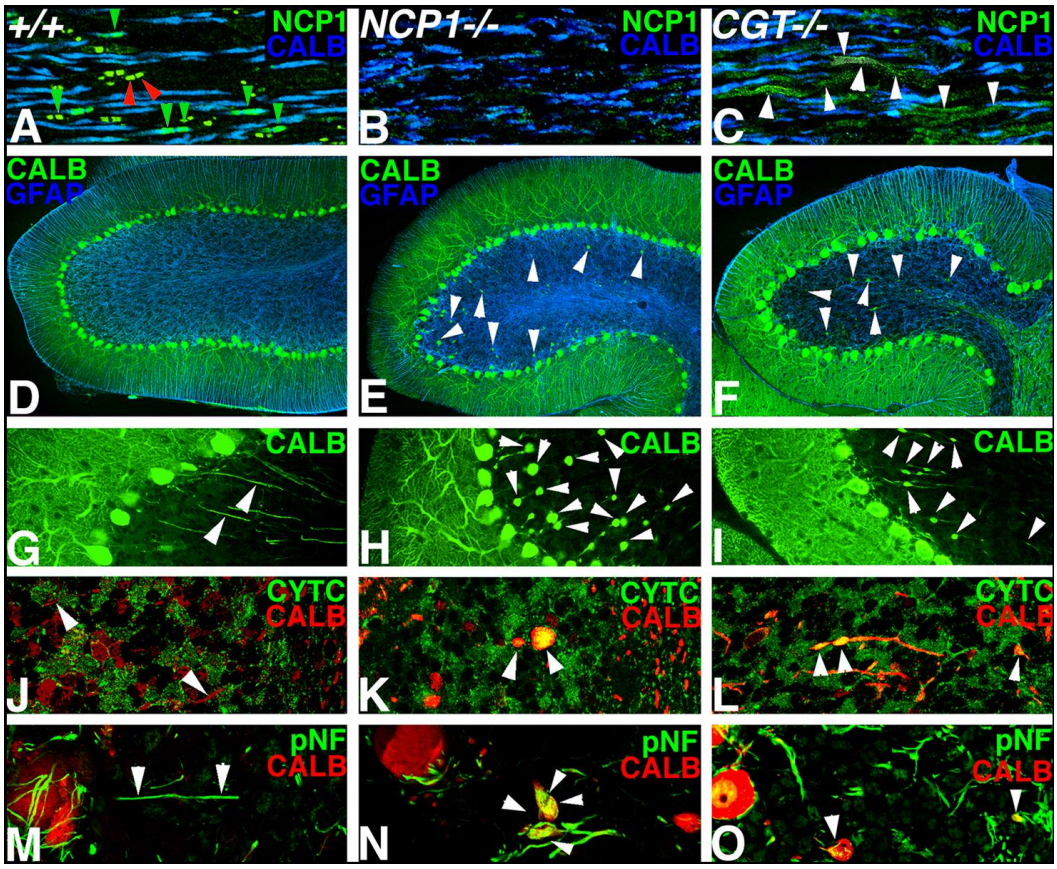

Figure 3 - Purkinje Neuron Axonal Swellings in *NCP1* and *CGT* Mutants**.** A portion of wild type (**A**), *NCP1* mutant (**B**) and *CGT* mutant (**C**) cerebellar white matter co-immunostained against NCP1 at paranodes (green, arrowheads) and calbindin (blue, axons). Red arrowheads point to paranodal regions of the non-Purkinje neuron axons. As expected, NCP1 is absent in (B). In *CGT* mutants, NCP1 does not show normal paranodal localization (arrowheads in C); instead the protein is diffused in the axon (compare with A). Cerebellar folia from wild type (**D**), *NCP1* mutant (**E**) and *CGT* mutant (**F**) co-immunostained against calbindin (green) and GFAP (blue). The cerebellar folial morphology in all three genotypes is indistinguishable, but signs of axonal swellings are clearly visible (arrowheads in E, F). At a higher magnification, wild type axons (**G**) show normal, axons with uniform caliber, whereas *NCP1* (**H**) and *CGT* mutant axons (**I**) show a beaded appearance with many axonal swellings (arrowheads). Immunostaining against the mitochondrial protein cytochrome c (green) shows accumulation of mitochondria in the swellings in *NCP1* (**K**, arrowheads) and *CG* mutants (**L**, arrowheads). Wild type axons did not show such cytochrome c accumulation in the axons (**J**, arrowhead). Immunostaining against phosphorylated neurofilaments (pNF, green) in wild type (**M**), *NCP1* (**N**) and *CGT* (**O**) mutants showed that the axonal swellings are enriched in pNF (arrowheads in N, O). Wild type axons did not show Pnf accumulation in the axons (M, arrowheads). Magnification bars: A-C, 100µm; D-F, 40 µm; G-1, 100µm; J-O, 200µm.

To determine precisely where NCP1 is localized in the cerebellum, wild type (Fig. 3A), *NCP1* (Fig. 3B) and *CGT* (Fig. 3C) mutant, tissues were immunostained with NCP1

antibodies to label paranodal regions and calbindin antibodies to label Purkinje neuron axons. The wild type Purkinje axons were NCP1-labeled in paranodal regions in the white matter (Fig. 3A green arrowheads). NCP1 also stains paranodal regions of myelinated axons not originating from the Purkinje neurons (e.g., mossy or climbing fibers, red arrowheads). The NCP1 staining was absent in the *NCP1* mice (Fig. 3B). Interestingly, in the Purkinje axons of *CGT* mice, NCP1 immunoreactivity was not localized to the paranodal regions but rather diffusely distributed in the axons (Fig. 3C, arrowheads) indicating that paranodal region formation was compromised in the *CGT* mice (Dupree et al., 1999).

To analyze the organization of the Purkinje neuron layer, astrocytic and Bergmann glial processes, the cerebella from wild type (Fig. 3D), *NCP1* (Fig. 3E) and *CGT* (Fig. 3F) mice were double stained with anti-calbindin (green) and anti-glial fibrillary acidic protein (GFAP, blue). Unexpectedly, from P10 onwards increasing numbers of focal axonal swellings were detected by calbindin immunoreactivity in both *NCP1* and *CGT* mutants in the Purkinje neuron axons. These swellings were observed in the myelinated regions distal to the axon initial segment (arrowheads in Fig. 3E, F). Such axonal swellings are not observed in the Purkinje axons of wild type littermates (Fig. 3D). At a higher resolution, Purkinje axons in *NCP1* (Fig. 3H) and *CGT* (Fig. 3I) mutant mice frequently display several consecutive swellings along the axons resembling beads on a string (arrowheads, compare with wild type in G). Some of these swellings reached 10-15 times the thickness of a normal myelinated axon. These data suggest that the loss of AGJs in both *NCP1* and *CGT* mutants results in large swellings in the Purkinje neuron axons.

Disruptions in axonal transport are known to lead to swellings containing aggregates of cellular organelles and proteins that are normally transported along the axons, for

example, mitochondria and neurofilaments. To determine if mitochondria were accumulating in these swellings, we immunostained cerebella from wild type (Fig. 3J), *NCP1* (Fig. 3K) and *CGT* (Fig. 3L) mutants with anti-cytochrome c antibodies, a marker for mitochondria. Cytochrome c immunoreactivity is enhanced in the swellings in NCP1 and CGT axons when compared to wild type axons (Fig. 3J-L, arrowheads). Similar axonal swellings have also been reported in PLP mutants, where the accumulation of mitochondria was attributed to impairment in fast axonal transport and associated with the accumulation of phosphorylated neurofilaments. We therefore determined the distribution of phosphorylated neurofilaments in *NCP1* and *CGT* mutant Purkinje axons.

As shown in Fig. 3M-O, (arrowheads), the axonal swellings in *NCP1* and *CGT* mutants also accumulate phosphorylated neurofilaments suggesting that axonal transport is impaired in *NCP1* and *CGT* mutant axons.

4 - Cytoskeletal Disorganization at the Paranodal Regions in *NCP1* and *CGT* Mutant Purkinje Axons

Since our immunocytochemical analysis revealed dramatic alterations in paranodal axolemma and in cytoskeletal organization, we decided to further analyze these abnormalities at the transmission electron microscopic (TEM) level. Axons from wild type mice display transverse septa, which link the paranodal myelin loops with axolemma (Fig. 4A, arrowheads). In both the *NCP1* and *CGT* mutant mice, paranodal transverse septa are absent (Fig. 4B, C, arrowheads).

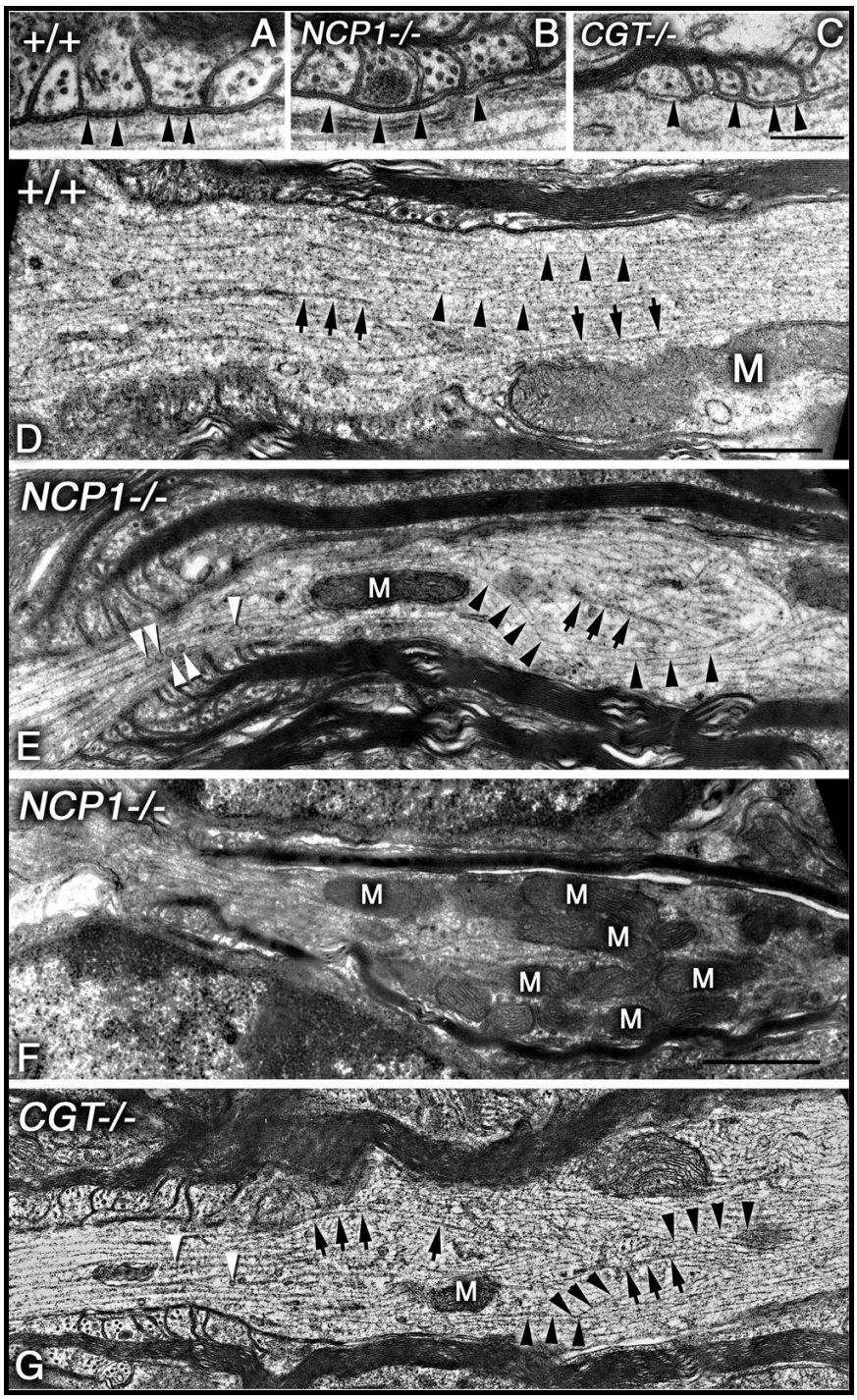

Figure 4 - Cytoskeletal Abnormalities in Purkinje Neuron Axons in *NCP1* and *CGT* Mutants. (**A**) Wild type myelinated axons show paranodal AGJs with clearly visible transverse septa (arrowheads). (**B**) In *NCP1* mutants paranodal AGJ formation is abnormal and transverse septa are not formed (arrowheads). (**C**) In *CGT* mutants AGJs fail to form and no transverse septa are visible (arrowheads). (**D**) Wild type axons display a highly ordered distribution of microtubules (arrows) and neurofilaments (arrowheads) in the paranodal region. (**E**) Paranodal region from *NCP1* mutants show axonal cytoskeletal proteins, neurofilaments and microtubules, losing their ordered distribution. The neurofilaments are demonstrating early signs of disorganization, which results in large axonal swellings. Several vesicles are visible along the microtubules (white arrowheads). (**F**) Another *NCP1* mutant axon showing abnormal accumulation of mitochondria (M) in the

paranodal/juxtaparanodal region. (**G**) Paranodal region of a *CGT* mutant axon also displays disorganization of both microtubules (arrows) and neurofilaments (arrowheads). Magnification bars: A-C = 0.25µm; D-G= 0.5µm.

Surprisingly, the *NCP1* and *CGT* mutant axons also display severely disorganized and misoriented microtubules (arrows) and neurofilaments (arrowheads) (Fig. 4E and G), the major constituents of the axonal cytoskeleton. This disorganization of the cytoskeleton contrasts to that of the wild type axons, which display parallel arrays of microtubules (arrows) and neurofilaments (arrowheads) (Fig. 4D). In addition to cytoskeletal abnormalities, mitochondria (M) accumulated proximal to the paranodal region (Fig. 4F). Taken together, the ultrastructural analyses indicate that AGJ disruption in *NCP1* and *CGT* mutant mice results in disorganized cytoskeleton and abnormal organelle accumulation specifically in the proximity of the paranodal junctional regions.

5 - Cytoskeletal Disorganization, Organelle Transport Defects and Axonal degeneration in *NCP1* and *CGT* Mutants

The combination of abnormal accumulation of mitochondria and phosphorylated neurofilaments and the cytoskeletal disorganization in mutant axons suggests that loss of *NCP1* and *CGT* leads to impaired axonal transport. This may result in a build up of various cellular organelles and axonal swellings. To fully characterize the ultrastructural defects of the mutant axons in the paranodal region, we performed further TEM analysis (Fig. 5). In *NCP1* (Fig. 5B) and *CGT* (Fig. 5C) mutant mice we find large intra-axonal accumulations of cytoskeletal proteins and organelles resulting in dramatically enlarged axon caliber as compared between wild type (A) and *NCP1* and *C*GT mutants (B and C, respectively). The intra-axonal swellings frequently form within or close to the paranodal region where axolemmal-cytoskeletal interactions have been lost (see arrows in A, B, C).

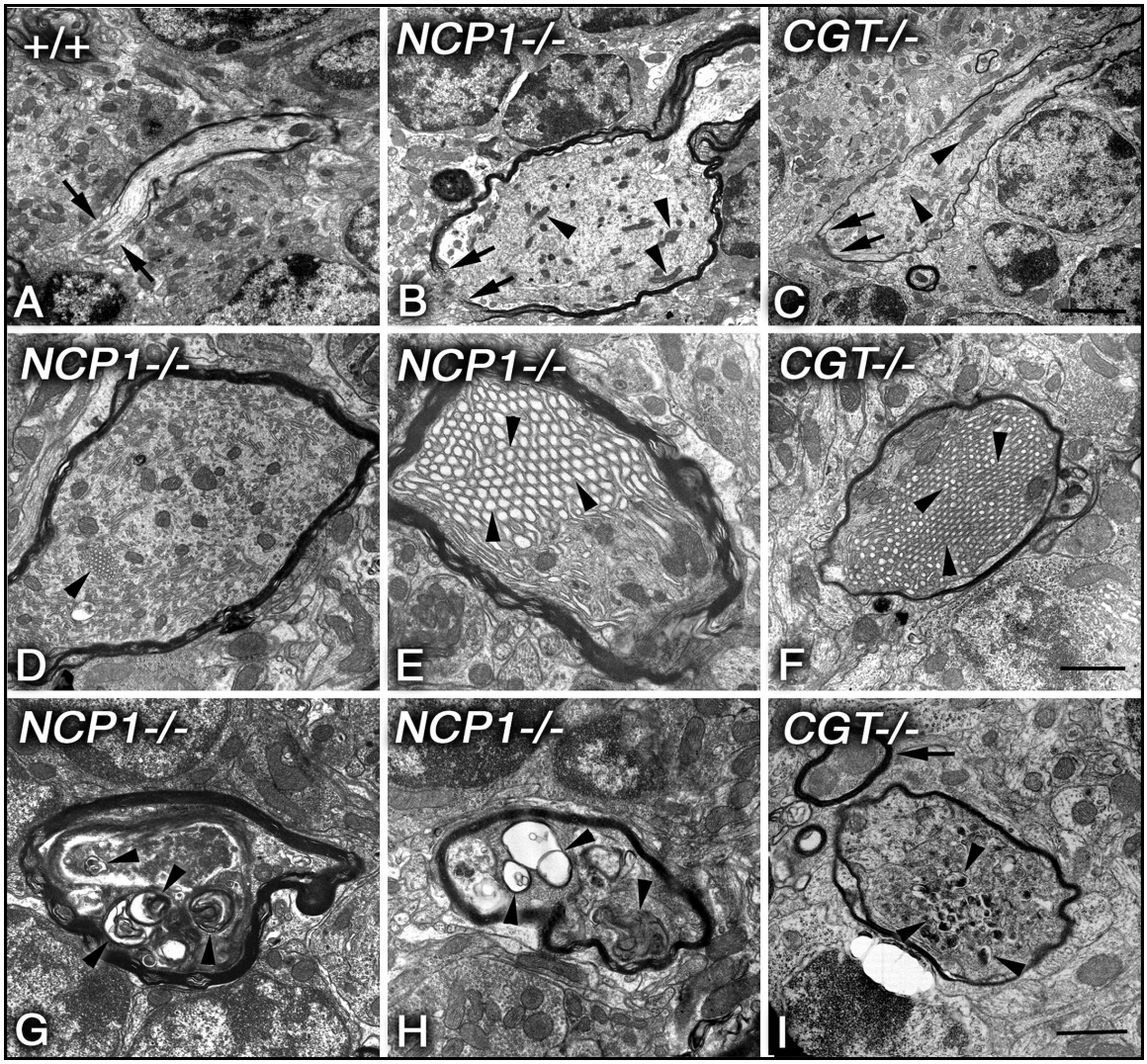

Figure 5 - Organelle Accumulation and Axonal Degeneration in *NCP1* and *CGT* Mutants. (**A**) A sagital section of a wild type axon through the paranodal region (arrows) showing normal axonal diameter and cytoskeletal organization. (**B**) An *NCP1* mutant axon shows a large swelling at the paranodal region (arrows). Note the accumulation of mitochondria (arrowheads) and cytoskeletal disorganization. (**C**) A *CGT* mutant axon also shows accumulation of mitochondria (arrowheads). Note the axon diameter disparity between wild type and mutants. (**D-E**) In *NCP1* mutant axons, the most abundant components of the swellings are mitochondria and SER. Accumulation of SER results in membrane lattices which fill most of the swellings (arrowheads). (**F**) The *CGT* mutant axonal swellings also develop SER membrane lattices as in *NCP1* mutants (arrowheads). (**G-H**) *NCP1* mutant axons in the process of degeneration showing vacuolation (arrowheads). (**I**) A *CGT* mutant axon in an early stage of degeneration displays electron dense bodies (arrowheads), which are a common feature associated with axonal decay and disorganized cytoskeleton. Arrow points to a normal myelinated axon. Magnification bars: A-F = 2 µm; G-I = 1µm.

In addition, the most frequent components of the axonal swellings are mitochondria (arrowheads in B, C) and smooth endoplasmic reticulum (SER) (*NCP1*, D, E; *CGT*, F, arrowheads). Accumulating SER is so extreme that it forms a lattice filling most of the

mutant axons (Fig. 5D, E, F, arrowheads). The accumulation of SER in cerebellar Purkinje cells has been proposed to correspond to a terminal stage of axonal degeneration (Palay and Chan-Palay, 1974). As postnatal development continues, the size of the axonal swelling increases and axonal degeneration becomes more prominent, as evidenced by vacuolation and fragmentation of the axonal cytoskeleton in both *NCP1* (Fig. 5G, H, arrowheads) and *CGT* (I, arrowheads). A normal diameter myelinated axon is seen next to a degenerating axon in the *CGT* mutants (I, black arrow). This axonal degeneration is consistent with impaired axonal transport resulting from cytoskeletal disorganization and organelle accumulation (Griffiths et al., 1998; Rhyu et al., 1999; Rosenfeld and Freidrich, 1983).

6 - A Molecular Link Between Paranodal AGJs and Axonal Cytoskeleton

The paranodal regions flank the nodes of Ranvier in myelinated axons. It is at the paranodes that the axolemma and the lateral loops of the myelin sheath maintain their closest apposition to establish the paranodal AGJs (Bhat, 2003a; Pedraza et al., 2001; Popko, 2003; Salzer, 2003)The cytoskeletal disorganization seen in the *NCP1* mutants suggests that NCP1 might play a critical role in linking paranodal AGJs with the axonal cytoskeletal network. We therefore carried out immunoprecipitation experiments using anti-NCP1 antibodies on cerebellar lysates obtained from wild type, *NCP1* and *CGT* mutants. Consistent with previous studies, these experiments revealed the presence of CONT and a brain specific isoform of actin/spectrin binding protein, band 4.1B (Denisenko-Nehrbass et al., 2003). The band 4.1 proteins bind to erythrocyte glycophorin and filamentous (F) actin/spectrin to link the cortical membranes with the cytoskeleton (Workman and Low, 1998). Interestingly, we identified

two additional cytoskeletal proteins in our immunoprecipitates: actin and axon specific neuronal spectrin, fodrin or αII spectrin (240 kDa) (Fig. 6A, +/+ panel) (Hirokawa et al., 1983; Zagon et al., 1986). The presence of αII spectrin in NCP1 immunoprecipitates was detected by a fodrin antibody and further confirmed by αII spectrin specific antibodies (data not shown). Brain specific αII spectrin has been reported to localize to myelinated axons in the mouse cerebellum (Zagon et al., 1986), however, its precise localization to the paranodal regions has not been established (see below). As negative control, none of these proteins were immunoprecipitated from *NCP1* mutant lysates (Fig. 6A, *NCP1*$^{-/-}$ panel). Since NCP1 protein was diffusely distributed in *CGT* mutant axons, we analyzed the NCP1-immunoprecipitates from *CGT* mutants, which revealed the presence of the same proteins as in the wild type (Fig. 6A, *CGT*$^{-/-}$ panel). These data suggest that in the absence of AGJs in *CGT* mutant mice, the axonal proteins still form a biochemical complex, but are not properly targeted to paranodal junctions. Thus, the biochemical experiments indicate a molecular link between NCP1 at the paranodal AGJs and 4.1B/actin/ αII spectrin of axonal cytoskeleton.

To establish whether these proteins are present or enriched at the paranodal junctions, we examined the sub-cellular localization of these proteins by immunocytochemistry. As shown in Fig. 6B, NCP1 (arrowheads) and CN localize to the paranodes, while 4.1B localizes to both paranodes and juxtaparanodes in the wild type cerebellum (Fig. 6B, left column). Interestingly, fodrin/ αII spectrin, which is expressed throughout the axon, is highly enriched at the paranodal junctions, in agreement with our biochemical observations. Immunostaining using anti-actin antibodies, which is expressed both by glia and axons, showed a modest enrichment around the paranodal area in the wild type axons (Fig. 6B, left column). The paranodal localization of these proteins was also analyzed in *NCP1* and *CGT* mice (Fig. 6B,

middle and right columns, respectively). All the proteins are diffusely present in the axons and are not enriched at the paranodes except for NCP1, which is absent in *NCP1* mutants.

The immunostaining data from *CGT* mutants raise an interesting possibility that the mere presence of NCP1 in the axons is not sufficient to establish or stabilize paranodal AGJs, rather it is the proper localization of NCP1 at the paranodes that is critical for the normal organization of the axonal cytoskeleton in the paranodal region. These results further highlight the fact that glial contribution is equally important for the organization of the paranodal domains. To demonstrate that NCP1 colocalizes with fodrin/ αII spectrin and actin at the paranodal junctions, we carried out double immunostaining. As shown in Fig. 6C, E (arrowheads), NCP1 and fodrin/ αII spectrin colocalize at the paranodes, indicating that fodrin/ αII spectrin is enriched at the paranodal junctions. Similarly, immunostaining with NCP1 and actin antibodies showed some regions of colocalization in the paranodal area (Fig. 6D, arrowheads), with expression of actin in the axons and the glial cells.

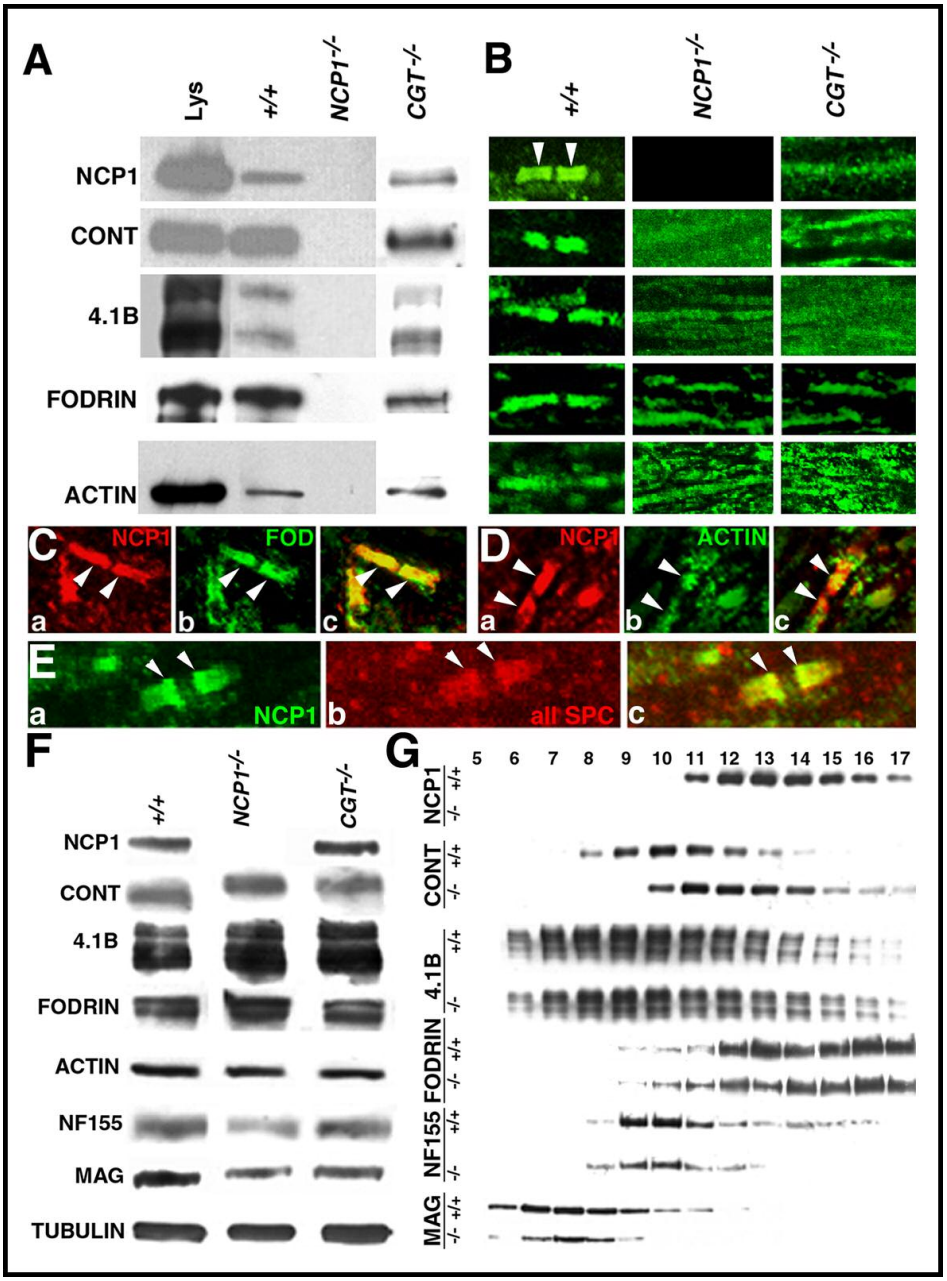

Figure 6 - AGJs at the Paranodes are Linked to Axonal Cytoskeleton. (**A**) NCP1-associated protein complex immunoprecipitated with anti-NCP1 antibodies from wild type (+/+), *NCP1* and *CGT* mutant cerebellar lysates (Lys). (**B**) Immunostaining of wild type Purkinje axons using NCP1, CONT, 4.1B, fodrin and actin antibodies. (**C**) Co-immunostaining of the wild type Purkinje axons with NCP1 (Ca) and fodrin (Cb) antibodies shows that fodrin colocalizes with NCP1 at the AGJs (Cc, arrowheads). (**D**) Co-immunostaining with NCP1 (Da) and actin (Db) antibodies shows areas of overlap at the paranodal regions (Dc, arrowheads). (**E**) Co-immunostaining of the wild type Purkinje axons with NCP1 (Ea) and αII spectrin specific antibodies (Eb) shows that αII spectrin colocalizes with NCP1 at the paranodes (Ec, arrowheads). (**F**) Analysis of the steady levels of relevant axonal and myelin proteins in wild type, *NCP1* and *CGT* mutants. (**G**) Sucrose density gradient centrifugation of the AGJ-associated proteins from wild type and *NCP1* mutant cerebellar lysates.

Taken together, the biochemical and immunohistochemical data indicate that NCP1/4.1B/actin/ αII spectrin form a biochemical complex which localizes to the paranodal junctions, and that loss of NCP1 or mistargeting of the NCP1/4.1B/actin/ αII spectrin complex (e.g., in *CGT* mutants) results in a similar phenotype. To determine whether the altered distribution of paranodal proteins in *NCP1* and *CGT* mutants is associated with reduced steady state protein levels, we analyzed the expression of these proteins in P20 wild type, *NCP1* and *CGT* mutant cerebella.

As shown in Fig. 6F, the levels of axonal cytoskeletal proteins 4.1B, fodrin/ αII spectrin and actin did not show any significant differences among genotypes. Interestingly, CONT, which interacts with NCP1 at paranodes, shows a higher apparent molecular weight in *NCP1* and *CGT* mutants when compared to wild type. The reason for this apparent size shift is presently not clear (Gollan et al., 2003). In contrast, glial proteins NF155 and MAG, which localize to the paranodal region on the myelin side, both showed reduced their levels in *NCP1* and *CGT* mutants, indicating that disruption of AGJs causes glial components of these junctions to be down-regulated or degraded. Most importantly, the short form of MAG (S-MAG), a hallmark of myelin maturation, seems to be specifically down regulated in both *NCP1* and *CGT* mice (arrowheads). Previous studies in *CGT* mice have reported altered expression of MAG isoforms (Coetzee et al., 1998). These observations raise the possibility that disruption of AGJs in *NCP1* and *CGT* mutants leads to changes in the levels of specific components of the paranodal junctions perhaps due to alteration in a signal transduction involving proper axon-glial interactions (Coetzee et al., 1998; Rios et al., 2003).

We hypothesized that loss of paranodal AGJs in *NCP1* mutants might reflect a disruption of protein complexes containing NCP1, and that such changes might be reflected

in buoyant density in sucrose gradients. As shown in Figure 6G, CONT complexes shift towards a higher density when compared to wild type. This shift in buoyant density suggests that CONT may be assembled into different protein complexes in *NCP1* mutants than in wild type. In contrast, band 4.1B and fodrin/ αII spectrin did not reveal any significant shift in their distribution. It is possible that any changes in the paranodal 4.1B and fodrin/ αII spectrin complexes have been masked by non-paranodal protein complexes, as these proteins are also expressed outside the paranodal region. Glial NF155 and MAG did not reveal any significant shift in their distribution, but again showed significantly reduced levels when compared to wild type (Fig. 6G). These sedimentation experiments suggest that loss of NCP1 affects the biochemical nature of the paranodal NCP1-associated protein complexes. Taken together, the biochemical experiments indicate that NCP1 links paranodal AGJs to axonal cytoskeleton through 4.1B and αII spectrin; and that loss (*NCP1* mutants) or mislocalization (*CGT* mutants) of NCP1 results in the disruption of AGJs and destabilization of the axonal cytoskeleton around the paranodal region. We propose that these events lead to axonal transport defects at and around the paranodal regions, causing a massive build up of mitochondria, SER and other transport cargo, which ultimately leads to degeneration of Purkinje neuron axons and severe motor deficits.

DISCUSSION

In the present study we have characterized two mouse mutants, *NCP1* and *CGT*, which both display severe ataxia and motor coordination defects. We show that disruption of paranodal AGJs leads to cytoskeletal disorganization and degeneration of Purkinje neuron axons in the cerebellum. We also provide molecular evidence that AGJs are linked to axonal

cytoskeleton. Our data show that AGJs are not only essential for the organization of the molecular domains in the myelinated axons (Bhat et al., 2001), but also for the stability of the nodal/paranodal axonal cytoskeleton to allow normal axonal transport. Our studies may be relevant to understanding the role of various components of AGJs in human demyelinating diseases, axonopathies, and ataxia.

1 - *NCP1* and *CGT* Mutant Mice Display Severe Motor Deficits

In the absence of *NCP1* and *CGT*, mice exhibit tremors, paresis, and severe ataxia. These neurologic defects reflect the function of *NCP1* and *CGT* in the nervous system and resemble neurologic defects displayed by *CN* mutant mice (Berglund et al., 1999). CN, a paranodal junction protein, interacts with NCP1 and is required for the cell surface expression of NCP1 (Boyle et al., 2001; Faivre-Sarrailh et al., 2000). *CN* mutant mice have striking defects in cerebellar development and CN is expressed by several types of cerebellar neurons and has been proposed to play a role in mediating neurite outgrowth and neuronal interactions (Faivre-Sarrailh and Rougon, 1997). In addition, *CN* mutants also display axonal swellings similar to *NCP1* and *CGT* mutants (Berglund et al., 1999). It is thus conceivable that these mutations impair a common mechanism in cerebellar function which leads to severe ataxia in addition to other neuronal defects.

Although the overall cerebellar development of *NCP1, CGT* and *CN* mutants is not severely affected, the ataxia, wide-based gait, and tremor of these mice reflect defects of cerebellar function stemming from abnormalities of the paranodal region. *CN* mutant mice are likely to exhibit more widespread defects than *NCP1* and *CGT* mutant mice in view of

the extrajunctional expression of this protein at central nodes of Ranvier, and also due to defects in the orientation of the granular neuron parallel fibers (Berglund et al., 1999). These defects seem specific to *CN* mutants as we did not observe any parallel fiber orientation defects in *NCP1* and *CGT* mutants (data not shown). These observations suggest that *CN* has additional functions which are independent of NCP1 and paranodal AGJs.

2 - Defective AGJs Lead to Cerebellar Dysfunction

The two mouse mutants studied in this work present defective AGJs caused by the ablation of either axonal (*NCP1*) or glial (*CGT*) proteins. It is generally accepted that defective motor coordination is an important sign of cerebellar dysfunction. We show here that *NCP1* mutants display severe motor impairment in a rotarod test, which has been successfully used as indicative of cerebellar lesions in mouse mutants (Pellegrino and Altman, 1979). The common phenotype of ataxia and deficits in motor coordination suggest that disruption of AGJs lead to impairment of cerebellar functions. Although, at low magnification, *NCP1* and *CGT* mutants show cerebellar morphology that is qualitatively indistinguishable from wild type littermates, our immunohistochemistry results at higher magnification revealed that all these mutants have swellings in Purkinje neuron axons in the cerebellum.

Axonal swellings have been observed in neuropathies induced by neurotoxic chemicals (Valentine et al., 1997), genetic ablation or expression of mutated genes in transgenic mice (Ferreirinha et al., 2004; Griffiths et al., 1998) and neurodegenerative diseases such as amyotrophic lateral sclerosis, Charcot-Marie-Tooth disease, Wallerian

degeneration, Alzheimer's disease and cerebrospinal ataxia (Brownlees et al., 2002; Collard et al., 1995; Stokin et al., 2005; Zoghbi and Orr, 2004). In all these situations the development of swellings has been proposed to indicate the early signs of axonal transport impairments. We found that the swellings in Purkinje axons of *NCP1* and *CGT* mice present aggregates of mitochondria, SER and neurofilaments. In cultured neurons, the physical constriction of the axonal transport in single axons leads to the development of axonal swellings that accumulate disorganized bundles of neurofilaments.

We detected a strong enrichment of phosphorylated neurofilaments in the axonal swellings in our mutants. Besides its significance as an indicator of disrupted axonal transport, these data may also be interpreted as defects in the intrinsic properties of the cytoskeleton of myelinated axons. The bundling of neurofilaments along myelinated axons shows a well defined architecture and, while the bundles of neurofilaments are spaced along the internodes, they are highly packed at the nodes of Ranvier. The phosphorylation of neurofilaments also modulates the interfilament spacing and it is thought to be part of the signaling for the myelin-dependent expansion of axonal caliber at the internodes (reviewed in Cleveland, 1996; Salzer, 2003). Although interactions between axon and glia are known to strongly regulate the axonal caliber, the mechanisms responsible for this regulation are not fully understood.

Our results raise the possibility that AGJs might participate in glial signaling to trigger stabilization and/or reorganization of axonal cytoskeleton at least in Purkinje neurons. This idea is strengthened by our TEM data showing that Purkinje axons in *NCP1* and *CGT* mutants present disorganized arrays of microtubules and neurofilaments. It is pertinent to highlight that the defects on axon-glial interactions of the mutants seems to be limited to the

paranodal AGJs and at present there is no evidence for obvious abnormal interactions along the internodes.. It has been previously shown that *NCP1* and *CGT* mice also have disrupted AGJs in the peripheral nerves (Bhat et al., 2001; Dupree et al., 1999). We did not observe axonal swellings in the sciatic nerves of *NCP1* and *CGT* mutant mice. These phenotypic differences suggest that there may be inherent differences in the cytoskeletal organization and or mechanisms of axonal transport. On the other hand peripheral nerves may take longer time to develop axonal swellings or have an inbuilt compensatory mechanism to prevent the formation of the axonal swellings. A better understanding of the differences in the molecular architecture of the peripheral and central paranodal/nodal regions may be required to resolve some of these differences. It would be interesting to analyze the peripheral nerves of much older mutants which may provide some clues whether they develop peripheral axon swellings.

3 - AGJs Stabilize Axonal Cytoskeleton at Nodal/Paranodal Regions

The molecular interactions between myelinating glial cells and axons are central in establishing highly specialized micro domains with specific protein components along the length of the axon (Bhat, 2003a; Pedraza et al., 2001; Popko, 2003; Salzer, 2003). Perturbations due to mutations in myelin or axonal components result in various types of neuropathies often identified as reductions in the speed of the propagation of action potentials. In addition, several myelin diseases cause axonal damage, leading to loss of axons and an irreversible functional impairment (Bjartmar et al., 2003; de Waegh et al., 1992; Martini, 2001). A link has been suggested between axonal degeneration, axonal swellings

and the organization of nodes of Ranvier. The ultrastructure of injured axons showed that axonal fragmentation occurred more often at the nodal/paranodal regions (Maxwell et al., 1993). After axonal injury, it was observed that damaged axons showed the presence of dilations of the nodes of Ranvier, which were named nodal blebs (Gennarelli et al., 1993). Similarly, the axonal swellings or nodal blebs we observed in *NCP1* and *CGT* mutants are characterized by cytoskeleton disorganization and accumulation of amorphous material. These different lines of evidence strongly suggest that axonal regions at the node and paranode may be more susceptible to cytoskeleton disorganization given the tight interactions with the overlaying myelin loops and presence of the AGJs. Thus, NCP1 is necessary for the formation of paranodal domain and for the proper organization of the cytoskeleton around the nodes of Ranvier. Most importantly, our data on the *CGT* mutants show that not only the absence of NCP1 in the axons but also its mislocalization lead to cytoskeletal disorganization and axonal swellings further highlighting the glial contribution and precise localization of NCP1 in the organization of the AGJs.

4 - NCP1 Recruits a Cytoskeleton-linked Paranodal Complex

Since NCP1 is the only AGJ protein known to project a cytoplasmic domain through the axolemma, it is possible that this protein establishes a link between AGJs and the axonal cytoskeleton. Through a series of biochemical and immunohistochemical experiments, we demonstrate that NCP1 forms a complex with actin and two actin-binding proteins: 4.1B and αII spectrin, which are members of families of proteins known to associate with actin and transmembrane proteins and to modulate the shape of cytoskeleton-linked membranes. Our

data from *CGT* mutants show that NCP1 retains the ability to recruit this complex despite its failure to organize the paranodal region in these animals. Taken together, the results presented in this work show that NCP1 recruits a protein complex at the axonal side of the paranodes, through which it links the AGJs to the axonal cytoskeleton. We have identified the core of this paranodal complex as actin, 4.1B and αII spectrin. It would be interesting to determine how and when αII spectrin gets enriched at the paranodes and whether similar mechanisms are involved in the nodal and paranodal domain organization (Poliak and Peles, 2003). We also show that NCP1 is able to recruit this complex even though it is unable to localize at the paranodes, i.e. in *CGT* mutants. However, the formation of a mislocalized complex does not prevent Purkinje axons from displaying disorganized cytoskeleton, developing axonal swellings or from undergoing axonal degeneration.

We have schematized a model (Fig. 7) in which AGJs might be stabilizing the cytoskeleton at the paranodal region. As previously proposed, in the wild type, NCP1 localizes at the paranodes, where its extracellular domain binds to CONT on the axonal side and the NCP1/CONT complex binds to NF155 on the glial side (Charles et al., 2002; Gollan et al., 2003). In addition, our data show that through the cytoplasmic domain, NCP1 forms a complex with 4.1B, actin and ⟨II spectrin and we speculate that this complex might be linked to microtubules in this region (Fig. 7A). We have previously shown that in the absence of NCP1, CONT does not localize to the paranodes, and in this study we show that the complex of 4.1B, actin and αII spectrin fails to link with the AGJs leading to disorganization of the microtubules near the paranodal region (Fig.7B). Furthermore, cortical actin filaments, microtubules and neurofilaments are interlinked by members of the plakin cytoskeletal linker family, which provides stability for axonal cytoskeleton at and outside the paranodal regions

(Garcia et al., 2003; Svitkina et al., 1996; Yang et al., 1996). Future studies aimed at determining the molecular mechanisms that link the actin/spectrin-AGJ complex to the microtubules and axonal cytoskeleton may provide new insights into how these interactions coordinate the organization of the paranodal domain in the myelinated axons.

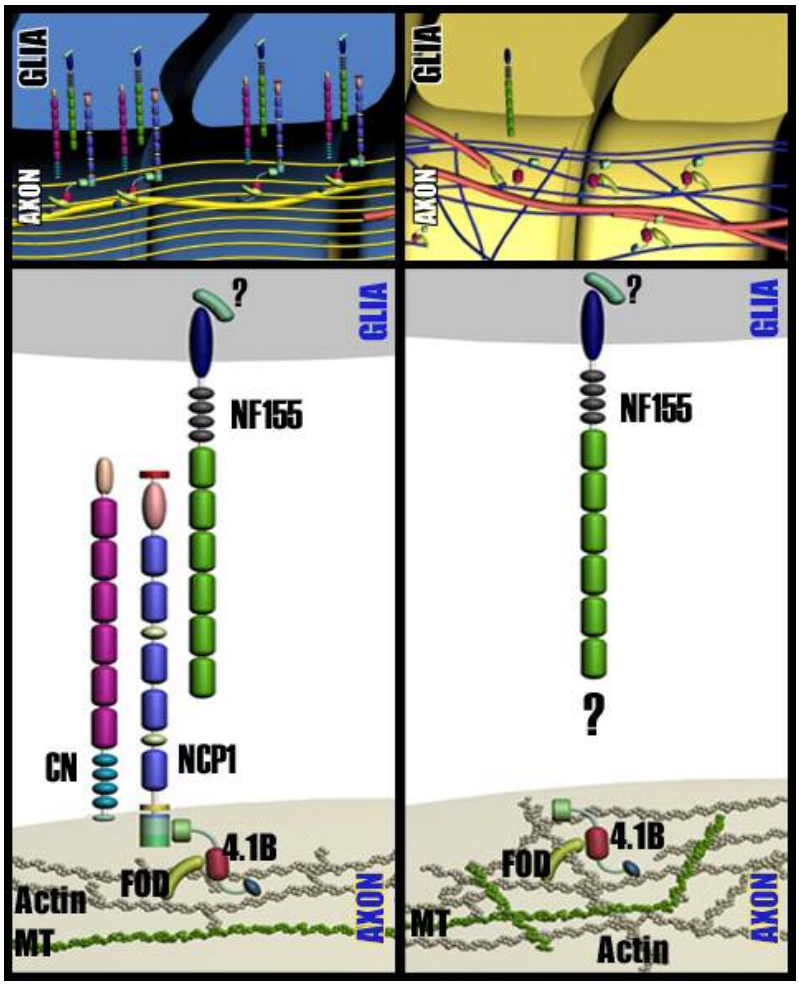

Figure 8 - A Schematic Model of the Paranodal AGJs and Axonal Cytoskeleton in Wild type and *NCP1* Mutants. (**A**) At the wild type paranodes, axonal NCP1/CONT interacts in trans with glial NF155 to establish AGJs. NCP1 links to the axonal cytoskeletal network through band 4.1B, actin and fodrin/ αII spectrin, which in turn are linked to microtubules and neurofilaments. These molecular interactions stabilize paranodal AGJs and the underlying axonal cytoskeleton. (**B**) In *NCP1* mutants, loss of NCP1 results in disruption of paranodal AGJs between myelin loops and axolemma and mislocalization of NF155. The axonal cytoskeleton fails to link with axolemma resulting in cytoskeletal disorganization at and around the paranodal region.

In summary, we provide evidence that AGJs are linked to the axonal cytoskeleton through NCP1, which recruits an actin-binding protein complex. The physiological relevance of this link is highlighted by the disorganization of the axonal cytoskeleton promoted by the absence of NCP1 or mislocalization of NCP1-associated protein complex in *NCP1* or *CGT* mutants, respectively. Furthermore, the loss of axons is a common feature in hereditary myelin disorders and neuropathies and the mechanisms of pathogenesis of axon loss in these disorders are not yet known. The current study raises an interesting possibility that the pathogenesis resulting from various myelin disorders may actually be linked to compromised AGJs leading to cytoskeletal disorganization, axonal neurodegeneration and severe motor deficits.

EXPERIMENTAL PROCEDURES

1 - *NCP1-lacZ* Targeting Vector and *NCP1-lacZ* Knock-in Mice

A mouse 129Sv/Ev genomic library in λFIX II (Stratagene) was screened and overlapping genomic DNA phage clones were isolated to establish a contiguous map of the *NCP1* locus. Based on the cDNA and genomic sequences in the mouse sequence data base exon-intron sequences were established and a targeting construct was designed with a 4.5 kb EcoRI-SmaI fragment as the 5' homology arm and a 2 kb SmaI-SmaI fragment served as a 3'homolgy arm flanked downstream by *thymidine kinase*, as a negative selection marker. A *lacZ-pgk-neo* cassette was inserted into exon 17 at SmaI site with *lacZ* serving as the gene for

β-galactosidase and *pgk-neo* for positive selection. The linearized targeting vector was electroporated into embryonic stem (ES) cells and standard cell culture and molecular biological procedures were used to confirm the targeting event in the *NCP1* locus. The targeted ES cells were used to obtain *NCP1-lacZ* homozygous mice using procedures described previously (Bhat et al., 2001).

2 - Staining for β-Galactosidase Activity

Mice at different postnatal ages were perfused with 4% paraformaldehyde and the cerebella were removed and cut into 30μm sections using a Leica Vibratome. Appropriate sections were rinsed several times in PBS and stained at 37$_{o}$C in dark for variable times with β-Gal staining solution [100 mM $K_3Fe(CN)_6$, 5 mM $K_4Fe(CN)_6$, 40 mg/ml 5-bromo-4-chloro-3-indolyl-β-D-galactopyranoside (X-gal) and 2 mM $MgCl_2$ in PBS]. The sections were briefly rinsed in PBS and photographed by a digital camera and processed by Adobe Photoshop.

3 - Rotarod Testing

Mice were tested on an accelerating rotarod (Ugo Basile, Comerio VA, Italy) to assess motor coordination. First session, animals were given three trials with 45 seconds between each trial. Two additional trials were given 48 hours later. Revolutions per minute (rpm) were set at an initial value of 3, with progressive increase to a maximum of 30 rpm

across 3 minutes (the max. trial length). Measures were taken for latency to fall from the top of the rotating barrel.

4 - Antibodies, Immunofluorescence and Western Blot Analysis

The primary antibodies used were anti- NCP1 guinea pig polyclonal antibodies (Bhat et al., 2001), rabbit anti-calbindin (Sigma), rabbit anti-GFAP (Chemicon), mouse anti-cytochrome C (M. Deshmukh, University of North Carolina), mouse anti-phosphorylated neurofilaments (Sternberger monoclonals), anti-CONT (J. Salzer, NYU, NY; S. Harroch, Pasteur Institute, France), anti-4.1B (ProteinExpress, Japan; P. Gascard, Lawrence Berkely Lab, CA), rabbit anti-fodrin (R. Cheney, University of North Carolina), rabbit anti- αII spectrin (S. Goodman, University of Texas, Dallas), mouse anti-actin (Chemicon) mouse anti-MAG (Chemicon), NF155 (M. Bhat, unpublished; A. Gow, Wayne State University), and mouse anti-β-tubulin (Chemicon). The secondary antibodies conjugated to rhodamine or fluorescein, were obtained from Jackson Laboratories. Immunofluorescence and Western blot analyses were carried as previously described (Bhat et al., 2001).

5 - Transmission Electron Microscopy

Wild type, *NCP1* and *CGT* mutant mice were deeply anesthetized and transcardially perfused with Millonig's buffer solution containing 4% paraformaldehyde and 2.5% glutaraldehyde (pH 7.3). Following the perfusion, the whole animal was post-fixed for 2 weeks at 4^{o}C in the same fixation solution. Following an overnight incubation in Millonig's

buffer, cerebellar tissue from each animal was postfixed for 1 hour in cacodylate buffered 1% osmium tetroxide. The tissue was then rinsed, dehydrated in increasing concentrations of cold ethanol, and infiltrated and embedded in PolyBed (Polysciences). One µm and 90 nanometer sections were cut and stained with toluidine blue or a combination of uranyl acetate and lead citrate, respectively. The one µm thick sections were analyzed with a Nikon Eclipse 800 and the thin sections were analyzed using a Zeiss EM 10CA. To produce digital images, EM negatives were scanned using a Microtek ScanMaker 5900. EM figures were assembled using Adobe Photoshop.

6 - Immunoprecipitation

Cerebella from wild type and mutants were dissected and homogenized in 10ml of ice cold buffer containing 50mM Tris-HCl (pH7.6), 3mM $MgCl_2$, 320mM sucrose and protease inhibitors using a glass homogenizer. The homogenates were centrifuged at 1000 x g for 15 minutes at 4^{o}C. The supernatants were centrifuged again at 100, 000 x g for 2 hours at 4^{o}C. The membrane pellets were extracted for 30 minutes on ice in buffer containing 50mM Tris-HCl (pH 7.6), 2% sucrose monolaurate, 0.1% sodium deoxycholate and protease inhibitors. The solubilized pellets were centrifuged again at 100, 000 x g for 2 hours at 4^{o}C. The supernatants were used for the immunoprecipitation. The Protein A beads (100µl) were pre-incubated with 8µl of NCP1 antibody for 3 hours and washed three times with phosphate buffered saline (PBS). The NCP1-Protein A beads were added to 1.5ml of the solubilized membrane fraction and incubated overnight at 4^{o}C. The beads were washed four times with 50mM Tris-HCl, (pH7.6) for 10 min each. The protein complexes bound to the beads were

eluted in 150 µl of 100mM glycine-HCl, pH 2.5. 20 µl of the samples from each genotype were separated on SDSPAGE for immunoblotting with respective antibodies.

7 - Sucrose Density Gradient Centrifugation

Cerebella were dissected and homogenized in 10mM Tris-HCl, pH 7.4 containing 100mM NaCl, 10mM EDTA, 1mM PMSF, 0.5% Triton X-100 with protease inhibitors followed by centrifugation at 100,000 x g for 20 min at 4^{o}C. After protein estimation, 2 milligram (mg) of total protein from each genotype was layered on a 10-45% continuous sucrose gradient followed by centrifugation at 100,000 x g for 20 hours at 4^{o}C. 250µL fractions were collected from the top and appropriate amounts were processed for immunoblotting as described above.

CHAPTER IV

Genetic Epistasis between NCP1 and CGT: Phenotypic Analysis of *NCP1/CGT* Double Mutants

ABSTRACT

Axo-glial junctions are essential for the organization of molecular domains in the myelinated fibers. They are dependent on a complex of proteins that are interlinked and act in conjunction to organize various molecular domains around the node of Ranvier. Two of these proteins, namely NCP1 and CGT are required directly and indirectly for axo-glial junction formation. Generation of *NCP1* as well as *CGT* mutant mice has been shown to have disrupted axo-glial junctions. Interestingly NCP1 is a protein that is expressed on the axonal membrane of axo-glial junctions, whereas CGT is an enzyme expressed on the overlying glial cell. For this study we generated *NCP1/CGT* double mutant mice. Immunohistological as well as ultrastructural analysis showed that double mutants lack axo-glial junctions and develop swellings in their Purkinje cell axons, which accumulate organelles, suggesting an impairment of axonal transport consistent with the phenotypes observed in both *NCP1* and *CGT* mutant mice. Our main goal in this study was to determine if the simultaneous removal

of these genes enhanced, suppressed or maintained the axonal degeneration phenotype. This would give clues to whether the phenotypes observed in single mutants follow a common pathway or are distinct events that could potentially utilize independent mechanisms.

INTRODUCTION

Myelinated axons contain regularly spaced unmyelinated gaps referred as Nodes of Ranvier and are critical for the proper function of the central and peripheral nervous system (Morell et al., 1994). The structure and function of this very specialized region is highly dependent on the interaction between the axon and the overlying Schwann cell or oligodendrocytes in the peripheral or central nervous system respectively. In addition paranodal junctions are formed adjacent to the node of Ranvier (Einherber et al., 1997). Structurally, these interactions establish the spacing of adjacent myelin segments and ultimately determine the position and length of the nodal gaps as well as the distribution of the underlying channel complexes.

Several mutations of key proteins have been shown to disrupt axo-glial interactions. These interactions are essential for the proper development, establishment and maintenance of myelinated fiber domains as well as their conductivities. The bi-directional signal between the neuron axons and the overlying glial cell must be under precise regulation for the survival of the cell. Proteins affecting axo-glial interactions therefore include proteins arising from the axonal membrane as well as proteins from the myelin sheath. Examples of these proteins include Contactin (CN), a glycosyl phosphatidylinositol (GPI) anchored protein that interacts in *cis* with NCP1. Mice deficient in CN display disruption of paranodal axo-glial junctions,

tremor and ataxia (Boyle, et al., 2001). A second key protein, NCP1 localizes to paranodal septate junctions (Bhat et al., 2001; Boyle et al. 2001; Peles et al. 1997). Genetic ablation of *NCP1* in mice showed that the mutant mice are viable with ataxia, motor deficits and have a dramatic reduction in nerve conduction velocity as was observed in the *CGT* mutants (Bhat et al., 2001). At the ultrastructural level, the mutant paranodes show aberrant organization of axo-glial interactions, loss of septate junctions and eversion of myelin loops away from the axonal surface (Bhat et al., 2001). In addition, the strict separation between Na^+ channels at the node and K^+ channels at the juxtaparanode is abolished (Bhat et al., 2001). These studies have demonstrated a critical role for NCP1 in the development and maintenance of paranodal axo-glial junctions.

Two of the major components of the myelin sheath are galactocerebroside (GalC) and sulfatide (sulfated form of Galc) (Morell et al., 1994). Their role in myelin is still unclear but previous studies have suggested that these lipids stabilize membranes. Membranes containing Galc or sulfatide are highly ordered and extremely thermostable when compared with membranes rich in phospholipids (Koynova and Caffrey, 1995), suggesting that lipids contribute to the remarkable stability of myelin and that they may play a role in cell-cell interactions (Coetzee et al., 1998).

Ceramide galactosyltransferase (CGT) is a 541 KDa microsomal enzyme that catalyzes the transfer of galactose from UDP-galactose to ceramide. These animals are unable to synthesize both Galc and their downstream byproduct sulfatide (Bosio et al., 1996; Coetzee et al., 1996), but are able to form myelin with an apparently normal ultrastructure. The CGT mutant mice exhibit a severe behavioral phenotype characterized by tremoring, ataxia and paralysis of their hind legs. Ultrastructural analysis has shown that the behavioral

phenotype observed is mainly due to a disruption of axo-glial junctions (Dupree et al., 1998). How the loss of CGT results in paranodal abnormalities is not clear. The idea that myelin galactolipids interact directly with the glial paranodal components, or may be required for their proper transport or localization, remains a strong possibility.

NCP1 and *CGT* mutant mice display severe ataxia and motor coordination defects commonly associated with cerebellar dysfunctions. In the current study we generated *NCP1/CGT* double mutant mice and our results clearly showed that these mutant mice lack axo-glial junctions, they develop swellings, accumulate organelles and have motor coordination problems all consistent with the phenotypes observed in both *NCP1* and *CGT* mutant mice. Our main goal in this study was to determine if the simultaneous removal of these genes enhanced, suppressed or maintained the axonal degeneration phenotype. This would give clues to whether the phenotypes observed in single mutants follow a common pathway or are distinct events that could potentially utilize independent mechanisms.

RESULTS

1 - Generation of *NCP1/CGT* double mutants

In order to determine if the observed phenotypes in *NCP1* and *CGT* mutant mice share a common pathway we generated *NCP1/CGT* double mutant mice using traditional Mendelian crossing strategies. The initial matings were between a heterozygous *CGT* with a heterozygous *NCP1* animal. The result of this cross generates several genotypes from which a double heterozygous *NCP1/CGT* was selected and paired with an animal of opposite sex

but same genotype. The mating of two double heterozygous mice (Figure 1) produced a progeny with sixteen probable genotypes. Four of these genotypes were double heterozygous which were used to maintain the stocks (Figure 1 – yellow squares). The double NCP1/CGT homozygous mutants were born at the expected Mendelian frequency of 1:16. This presents a potential problem due to the low frequency of double mutants born. In most cases the progeny of a double heterozygous cross did not produce any double homozygous mutant mice.

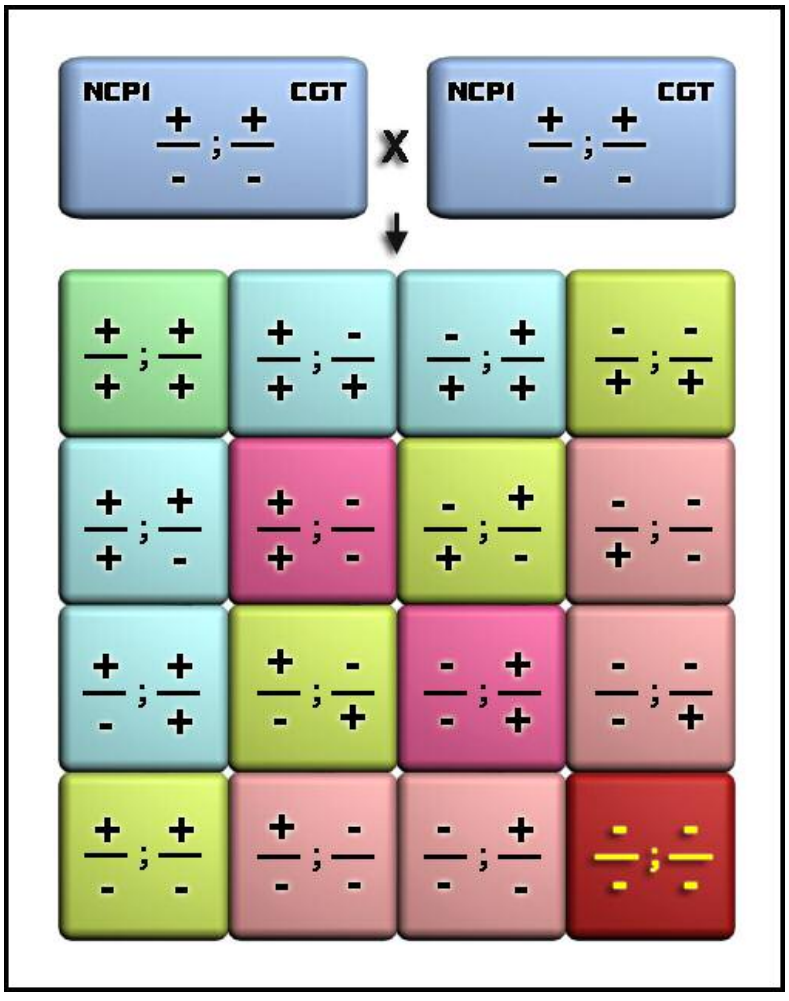

Figure 1 – **Punett square to generate the NCP1/CGT double mutant mice.** Genetic crosses between a male and a female double heterozygous for NCP1 and CGT (blue squares). The Mendelian ratio to obtain a double

homozygous mutant mouse is 1/16 (red square). Yellow squares denote the double heterozygous mice that are used to maintain the stocks.

These mice display an identical phenotype as that of the *NCP1* and *CGT* mutant mice generated previously (Bhat et al., 2001, Dupree et al., 1998) with no obvious behavioral difference that would stand out. The *NCP1/CGT* double mutation was confirmed with PCR using four sets of primers from which two were designed to detect the NCP1 null mutation (Bhat et al., 2001) and the other two for the CGT null mutation (Popko et al., 1998 – Figure 2).

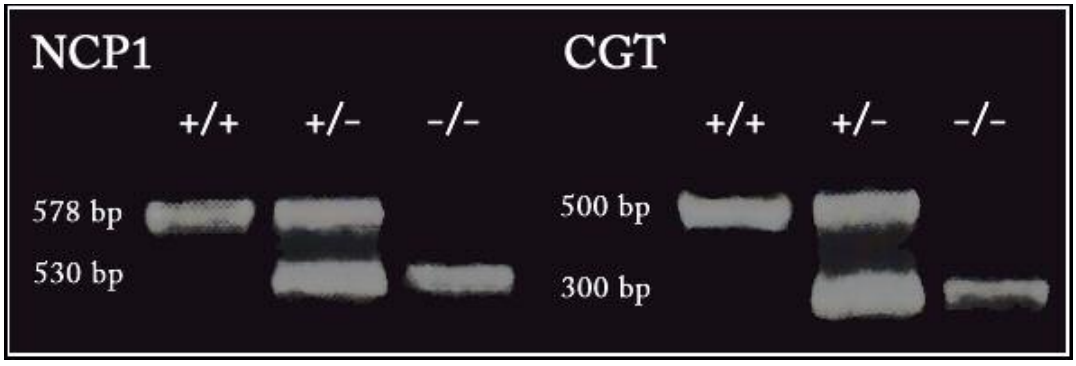

Figure 2 – **Genotyping by PCR.** PCR of NCP1 and CGT mice using two sets of primers against wild type sequences to amplify a 578bp and a 500 bp fragment respectively and one set against *neo* sequence to amplify a 530bp and a 300bp fragment respectively. The Heterozygous animals amplify both fragments.

2 - NCP1/CGT double Mutants develop axonal swellings in Purkinje neurons

Immunofluorescence analysis of wild-type, *NCP1, CGT* and *NCP1;CGT* double mutants using calbindin staining of the Purkinje neurons demonstrated large numbers of focal axonal swellings in all three mutant samples at postnatal day 20 (Figure 3 B-D). These swellings were not observed in the Purkinje axons of wild type littermates (Figure 3A). Interestingly, in many cases, Purkinje cell axons frequently display several

consecutive swellings on the axon resembling beads on a string (blue arrowheads), some of them reaching 10-15 times the thickness of a normal myelinated axon. These data suggest that the loss of AGJs in all three *NCP1, CGT* and *NCP1/CGT* double mutants results in the development of swellings in the Purkinje neuron axons.

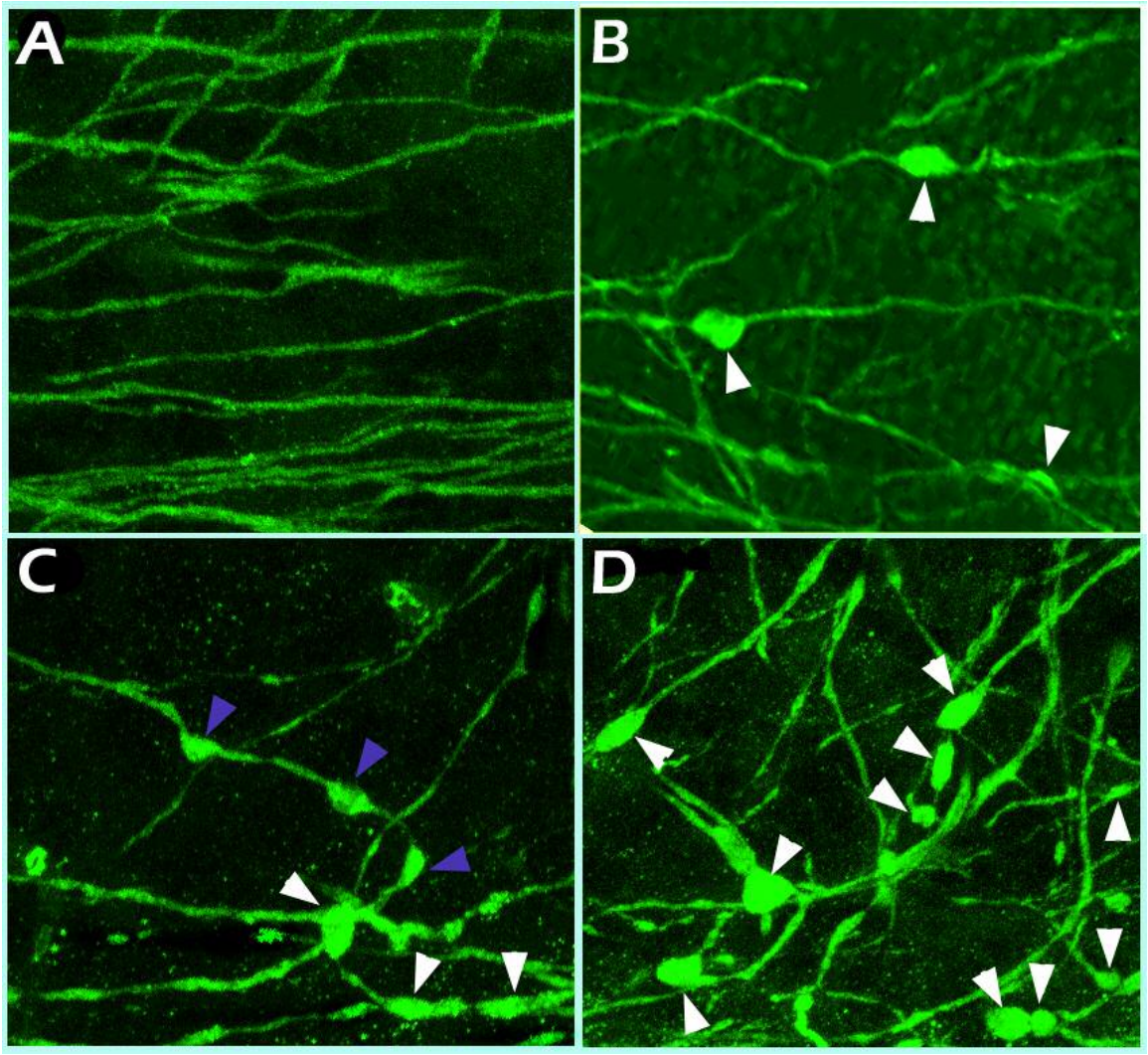

Figure 3 – ***NCP1/CGT* double mutants develop Purkinje neuron axonal swellings**. Immunohistochemical staining of wild-type (A), *NCP1* mutant (B), *CGT* mutant (C) and *NCP1/CGT* double mutant (D) Purkinje cell axons using calbindin antibody. White arrowheads denote individual axonal swellings while blue arrowheads denote axonal swellings in a tandem.

Previous data has shown that disruption of axonal transport has a direct link in the generation of axonal swellings, and that these swellings contain aggregates of cellular

organelles and proteins such as mitochondria and neuronal intermediate filaments that are usually transported along the axons in normal conditions. One such report was that of the PLP mutants in which accumulation of mitochondria and phosphorylated neurofilaments was attributed to the impairment of fast and slow axonal transport respectively (Griffiths et al. 1998).

To determine if neurofilaments were accumulating in these swellings, we immunostained cerebella from wild type, *NCP1, CGT* and *NCP1/CGT* double mutants with anti-phosphorylated medium neurofilament antibody. As shown in Figure 4A-D (arrowheads), the axonal swellings in all three mutants accumulate phosphorylated neurofilaments, suggesting that axonal transport is impaired in all three *NCP1*, *CGT* and *NCP1/CGT* double mutant axons.

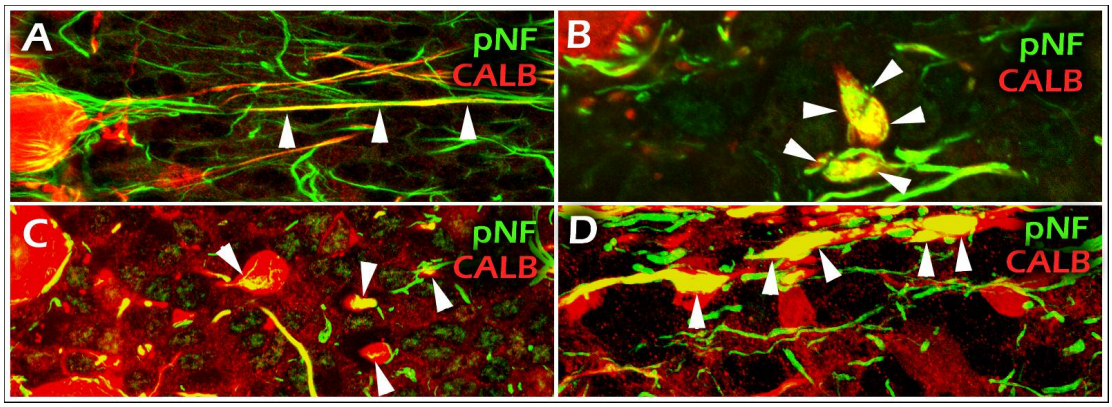

Figure 4 – ***NCP1/CGT* double mutants accumulate phosphorylated neurofilaments in their axonal swellings**. Immunohistochemical staining of wild-type (A), *NCP1* mutant (B), *CGT* mutant (C) and *NCP1/CGT* double mutant (D) Purkinje cell axons using calbindin (red), and phosphorylated medium weight neurofilament (pNF). Arrowheads denote overlapping staining between pNF and Calb.

3 - Increased Axonal Degeneration in *NCP1 CGT* Double Mutants

The similarity in the Purkinje neuron axonal phenotypes displayed by *NCP1* and *CGT* single mutants suggested that both genes are involved in paranode formation/stabilization. Therefore, we wanted to determine if the simultaneous removal of these genes enhanced the axonal degeneration phenotype.

A qualitative assessment of the cerebellar granular cell layer of the *NCP1/CGT* double mutants indicates a dramatic reduction in the total number of axons, and particularly of myelinated axons, when compared to wild type littermates (Fig. 5 A, B, arrowheads). Additionally as shown in Fig. 5C, wild type myelinated axons maintain a myelin sheath with normal thickness and morphology, whereas the *NCP1/CGT* double mutant axons display a thin myelin sheath, and in some cases there are completely unmyelinated axons (Figure 5 D-1,2,3). Presently, we have not determined whether the absence of myelin is the result of demyelination or if myelin formation is inhibited in these mice.

As presented in Chapter 3, where *NCP1* and *CGT* mutant mice showed prominent axonal swellings, *NCP1/CGT* double mutant mice also displayed these accumulations. In order to investigate the ultrastructure of these swellings we performed transmission electron microscopy (TEM) of longitudinal sections of the Purkinje axons. Consistent with previous work, our TEM data show that axons from wild type mice display normal axon thickness (Figure 6A,C arrows) whereas in the double mutant mice the axonal calibers reached up to ten times the normal axonal thickness (Figure 6C,D).

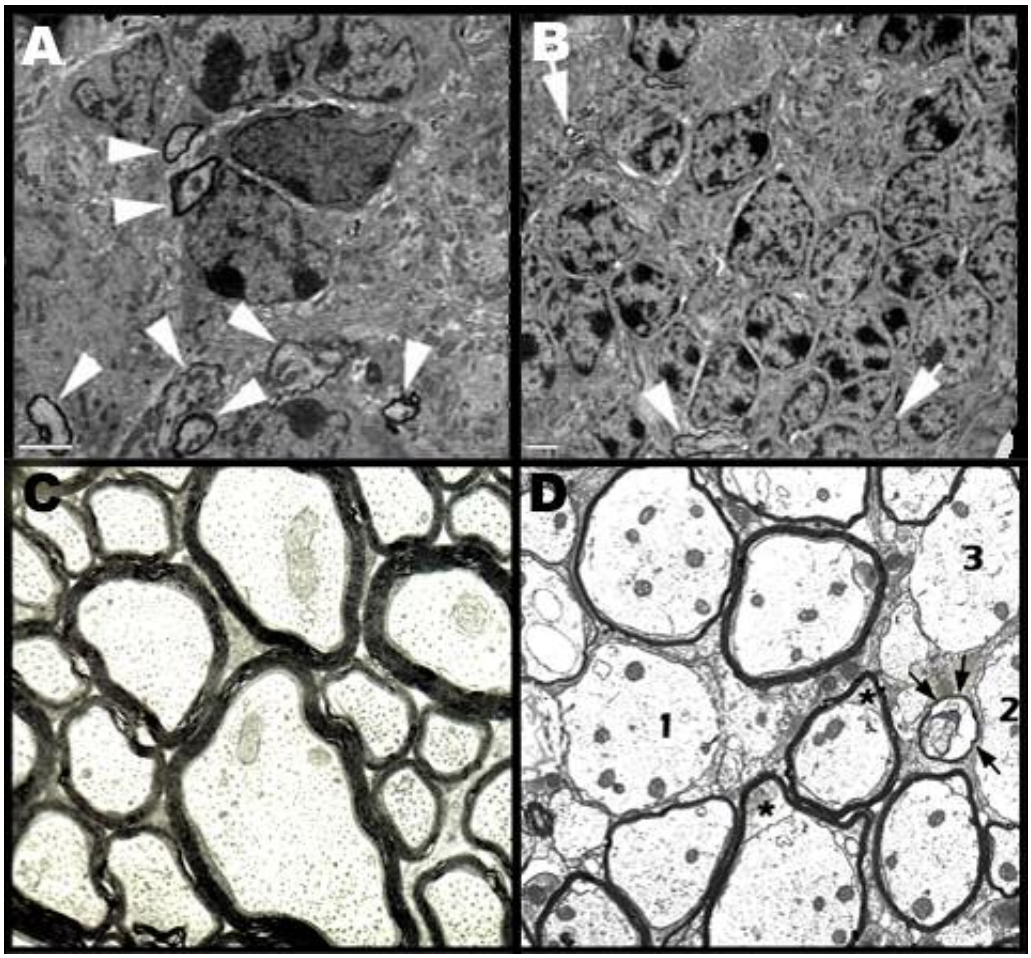

Figure 5 – **Myelination and axonal numbers is affected in *NCP1/CGT* double mutant mice**. Electron micrographs of transverse axons in wild-type (A,C) and *NCP1/CGT* double mutants (B,D) of cerebellar granule cell layer (A-B) and white matter tracts (C-D). Arrowheads denote axons. Arrows in D denote an axon undergoing demyelination.

We detected large axonal accumulations of organelles resulting in dramatically enlarged axon caliber as compared to wild type. In addition, the most frequent components of the axonal swellings are mitochondria and smooth endoplasmic reticulum (SER). The accumulation of SER is so extreme that it forms a lattice filling most of the mutant axon (Fig. 6D, asterisk). As postnatal development continues, the size of the axonal swelling increases and axonal degeneration becomes more prominent, as evidenced by vacuolation and fragmentation of the axonal cytoskeleton (Figure 6C). Taken together, the ultrastructural analyses indicate that AGJ disruption in *NCP1/CGT* double mutant mice results in

disorganized cytoskeleton and abnormal organelle accumulation and suggests that *NCP1* and *CGT* play important roles in the organization of the paranodal AGJs from the axonal and glial side, respectively. Additionally the absence of myelin may result from secondary effects on oligodendrocyte function or impaired axo-glial signal transduction and signs indicative of axonal degeneration including mitochondrial accumulation and prominent vacuolation (Fig. 6B,D).

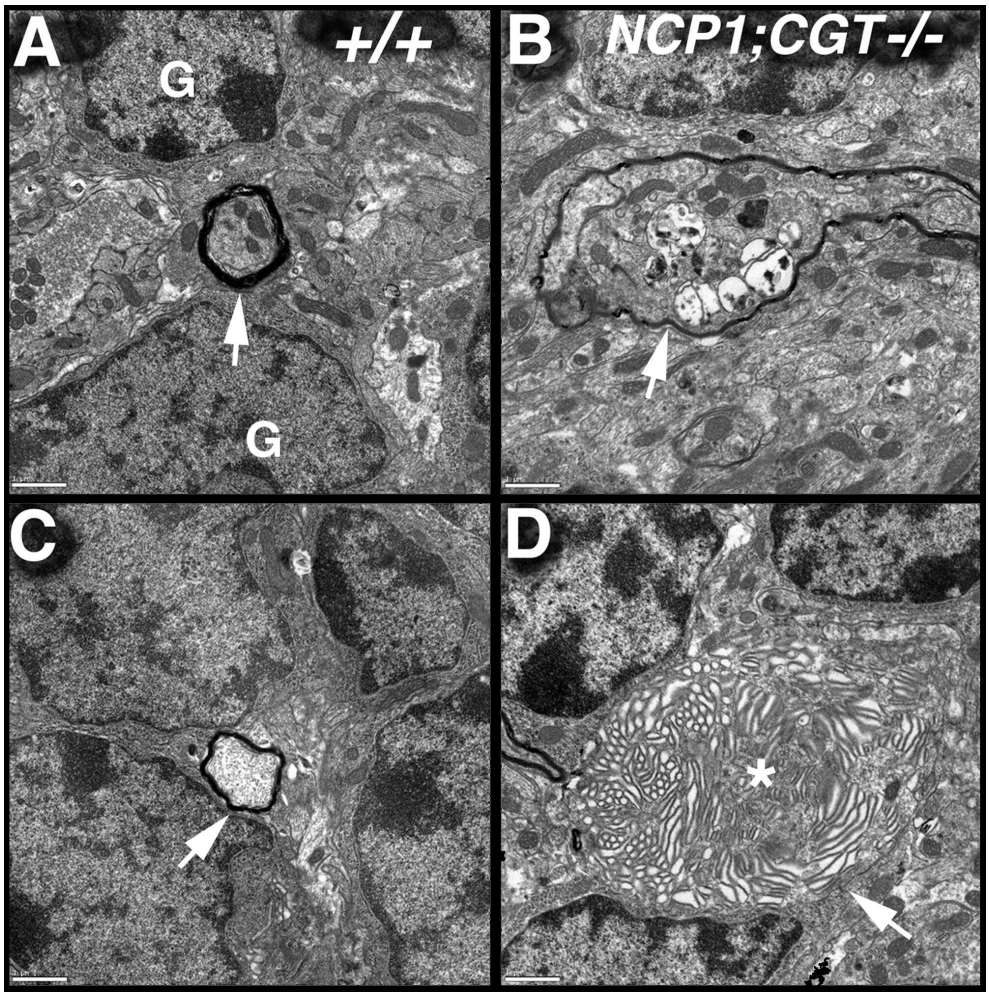

Figure 6. Axonal Pathology is Enhanced in *NCP1/CGT* Double Mutants (A) A P20 wild type axon from the granular layer and a swollen axon from the *NCP1/CGT* double mutant (B), also from the granular cell layer. Note the mutant axon has thin myelin (arrow) and prominently displays signs of degeneration including large vacuoles and electron dense bodies. (C) A wild type myelinated axon (arrow) revealing a normal complement of axonal content. Note the caliber of the wild type axon as compared to the unmyelinated, swollen axon in (D), which is very common in the *NCP1/CGT* double mutant mice. Magnification bars: A-D = 1µm; E, F = 2µm.

4 - AGJ disruption and cerebellar dysfunction

We have previously demonstrated that *NCP1* mutant mice display disrupted paranodal AGJs in the central nervous system (CNS) (Bhat et al., 2001). We therefore asked whether disruption of AGJs could be responsible for a cerebellar dysfunction that would lead to the impaired motor coordination observed in the *NCP1* mutants. To test this hypothesis we analyzed *NCP1* mice in parallel with *CGT* and the *CGT/NCP1* double mutant mice. *CGT* mice show disruptions of AGJs due to impairment of lipid biosynthesis in myelinating glia (Coetzee et al., 1996). One would expect that if cerebellar defects are caused by disruptions in AGJs, the phenotype should be reproduced in mutants with disrupted AGJs, regardless of whether the causal mutation takes place in the glia (*CGT*) or neurons (*NCP1*) or in both (NCP1/CGT). In fact, all three mutants display a similar phenotype with regard to hypomotility, movement associated tremor, severely impaired control and coordination of movement and a wide-based gait (Dupree et al. 1998; Bhat et al., 2001).

We first tested whether the cerebellar circuitry was disrupted in all mutants. The motor impairments and ataxia are readily detected in all three mutants as early as P15, suggesting that any circuitry defect responsible for this phenotype must take place before P15. The migration of granule cells and subsequent synaptogenesis take place in mouse cerebellum during the second week after birth and are complete by P21. We used transmission electron microscopy (TEM) to analyze the ultrastructure of the synaptic input of parallel fibers to Purkinje dendrites in the molecular layer of *NCP1, CGT* and *NCP1/CGT* double mutants at P20. The synapses in the molecular layer of the *NCP1, CGT* and *NCP1/CGT* double mutants (Figure 7B-D) presented all the key ultrastructural

components of asymmetric synapses observed in the wild type (Figure 7A). For example, the presynaptic terminal of parallel fibers contained numerous spherical vesicles, the postsynaptic dendritic spines of Purkinje neurons frequently contained SER, and the electron-dense band (active zone) between the terminal and the dendritic spine is asymmetric, consistent with the excitatory nature of the input (Figure 7A-D).

To further determine whether the mutations affect the synaptic density in the molecular layer, we quantified the number of synapses in the molecular layer of these mice (Fig. 7E). Our results show that the mutations did not significantly affect the number of synapses per μm^2 when compared to the wild type. We analyzed the deep cerebellar nuclei of cerebellar sections of P20 mutants and found that the Purkinje axons contact their appropriate postsynaptic targets in this region. Taken together, these results suggest that disruptions in the circuitry of Purkinje neurons in the cerebellum are not the underlying cause of the ataxia observed in *NCP1* and *CGT* mutants.

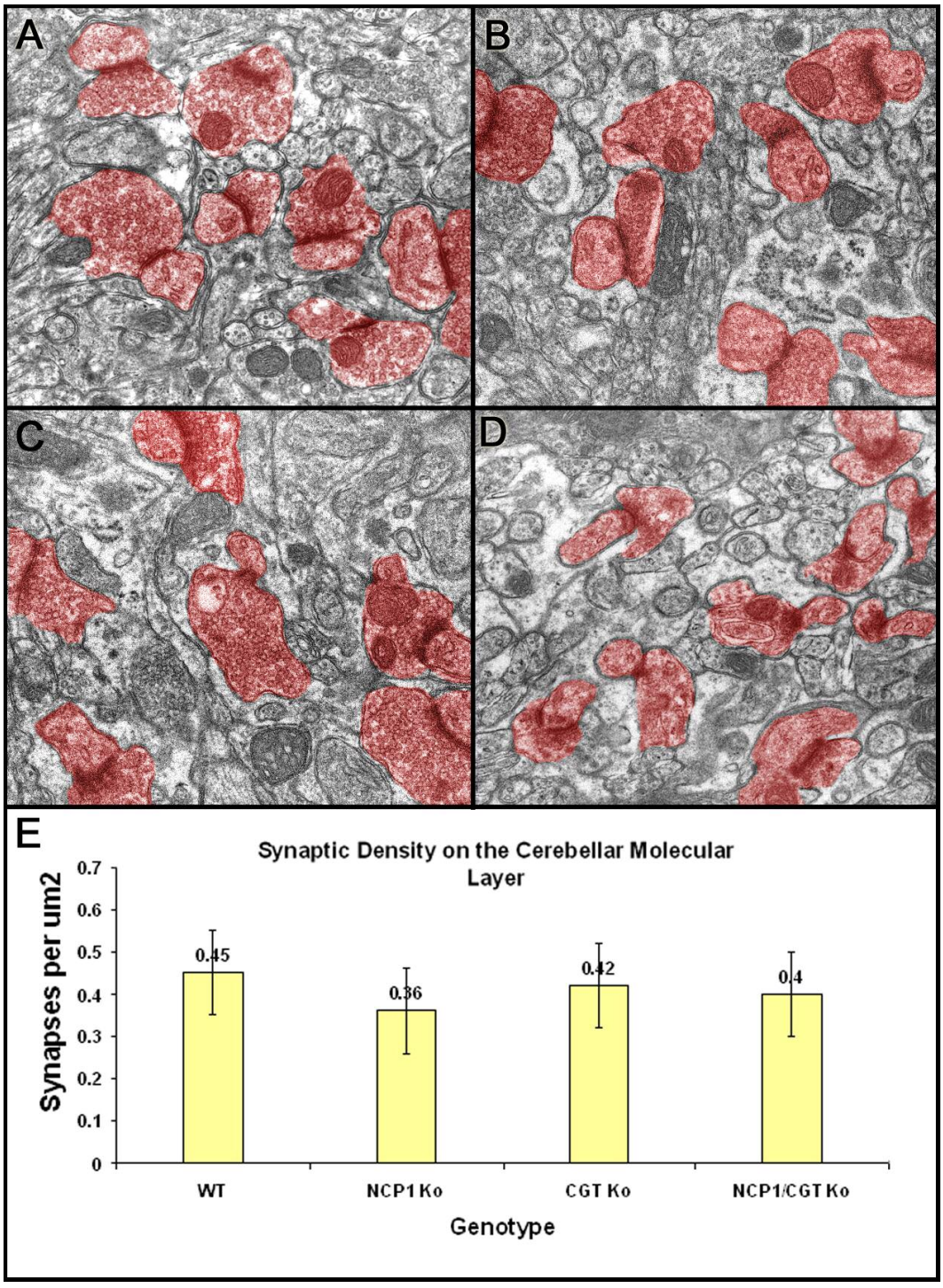

Figure 7 - *NCP1/CGT* double mutants do not display aberrant synaptic density in the molecular layer. Analysis of electron micrographs from the molecular layer of wild-type *(*A), *NCP1* (B), *CGT* (C) and *NCP1/CGT* double mutants (D) at P20 reveals synapses with all the key ultrastructural components (synapses are marked in red). (E) Synaptic density is not significantly affected in the molecular layer of *NCP1, CGT* and *NCP1/CGT* double mutant mice when compared to the wild type. Counting of synaptic density was based on the counting of 250-300 synapses corresponding to 10 images for each animal and at least 3 mice per genotype. Magnification bar: 0.5µm.

DISCUSSION

In this study we have analyzed three lines of mutant mice, *NCP1, CGT*, and *NCP1/CGT*. All these mice display severe ataxia and motor coordination defects. We show that disruption deletion of both *NCP1* and *CGT* genes leads to accumulation of axonal swellings and degeneration of Purkinje neuron axons in the cerebellum, consistent with the phenotype observed in *NCP1* and *CGT* mutant mice. We also provide additional evidence that deletion of both genes disrupts myelin formation. Our data suggests that deletion of both NCP1 and CGT does not suppress or enhance the phenotypes observed in individual *NCP1* and *CGT* mutants. Hence a common pathway that links both the glial cell and the underlying axon must exist and be responsible for the maintenance and development of axo-glial junctions.

1 - Two faces of AGJs: glial and neuronal

The three mouse lines studied in this work present defective AGJs caused by very different mutations. *CGT* mice present genetic defects in glial cells, whereas the genetic defect in the *NCP1* mutants is in the neurons. The double mutants *NCP1/CGT* present a genetic deficit coming from both ends, the glial as well as the axonal side. NCP1 is a key component of AGJs at the axonal side and the disruption of AGJs in *NCP1* mutants is due to the absence of this protein in the axons. In contrast to the *NCP1* mice, the *CGT* mutants express normal levels of NCP1 but the localization at the AGJs is disrupted. CGT does not

participate directly in AGJ formation but its activity is necessary for the segregation of lipid microdomains necessary for the clustering of NF155, the glial binding partner of the axonal paranodal complex (Charles et al., 2002; Schafer et al., 2004). Most importantly, one would not expect CGT mutation to affect NCP1 function that is not related to AGJ formation, as the absence of CGT is hypothesized to affect the clustering of the NF155-based glial complex which is the binding partner for the NCP1/CONT-based axonal complex in AGJs.

CGT mutant mice have been previously shown to have hypomyelinated as well as demyelinated axonal fibers in their spinal cords (Popko et al., 1998). Here we show that the *NCP1/CGT* double mutant mice contain demyelinated as well as hypomyelinated fibers as previously shown but are prominent in cerebellar Purkinje cell axons. On the other hand *NCP1* mutant mice do not show any demyelinating or hypomyelinating defects suggesting that the myelination defects observed are due to the lack of the CGT enzyme. Thus demyelination or hypomyelination do not share a common pathway with *NCP1* mutant mice since they are specific to the *CGT* mutants.

2 - Axonal swellings and axonal degeneration

Axonal swellings have been described for many years now. One of the earliest studies was done on the Quaking mice (Friedrich, 1974). These mice showed axonal enlargements that contained arrayed lattices later to be identified as smooth endoplasmatic reticulum (SER), they also had accumulated mitochondria and cell debris.

Since then many reports on axonal swellings have been published and have shown to be linked to neurodegenerative diseases such as amyotrophic lateral sclerosis, Charcot-Marie-Tooth disease, cerebrospinal ataxia, and others (Brownlees et al., 2002; Collard et al., 1995; Stokin et al., 2005; Zoghbi and Orr, 2004). In most cases but not all, axonal swellings have been linked to be a late sign of axonal transport impairment. It is still not known whether the transport motors themselves are a direct cause of the swellings, but we do know that a disorganized cytoskeleton does impair transport by disrupting neurofilaments and microtubular arrays, which are used as guides for motor proteins to carry their cargo (Garcia-Fresco et al., under review). These swellings have been shown to contain membranous organelles such as mitochondria and SER, which have been proposed to correspond to a terminal stage of axonal degeneration (Palay and Chan-Palay, 1974). Asides from mitochondria and SER we found that neurofilaments are highly enriched in axonal swellings. Neurofilaments are transported by what is known as slow axonal transport. *NCP1, CGT*, and *NCP1/CGT* double mutant mice have shown to accumulate large quantities of phosphorylated neurofilaments in the axonal swellings, which provide further evidence that axonal transport is impaired.

3 - AGJs and relevance to human diseases

Human diseases such as multiple sclerosis (MS) are broadly known to cause axonal degeneration and demyelination, but the mechanisms that lead to axonal degeneration remains largely unclear. Recently, Wolswijk and Balesar analyzed a number of human brains affected by MS and found that NCP1 is diffused along the axons of these samples (Wolswijk

and Balesar, 2003). The authors suggest that the aberrant location of NCP1 is an early sign of impending myelin loss in MS. Interestingly, this study also reports that NCP1 positive regions on some myelinated axons presented increased axonal caliber near the lesion edges (Wolswijk and Balesar, 2003). Although MS is a human disease, we show in this work that three different mouse models for AGJs disruption present axonal swellings close to the putative paranodal region and that the paranodal complex and/or its components are diffused in these axons.

4 - NCP1/CGT a Common Pathway

In the current study we raised the question whether simultaneous removal of *NCP1* and *CGT* genes enhanced, suppressed or maintained the axonal degeneration phenotype so that it would give us clues whether the phenotypes observed in their individual mutants follow a common pathway or they utilize distinct mechanisms. We have concluded that in all a common mechanism is present that leads to the ataxic events, the swellings and the disruption of axo-glial junctions. Despite the common phenotypes shared each individual gene mutation does have an effect of its own, for instance *CGT* mutants have been shown to have demyelinated as well as hypomyelinated fibers whereas *NCP1* mutant mice do not show any signs of demyelination (Popko et al., 1998; Bhat et al., 2001). Our *NCP1/CGT* double mutants however show a cerebellar demyelinating phenotype consistent with that of the *CGT* mutant mice, suggesting that a common signaling pathway that controls myelination is not shared by both proteins.

EXPERIMENTAL PROCEDURES

1 - Antibodies, Immunofluorescence and Western Blot Analysis

The primary antibodies used were rabbit anti-calbindin (Sigma C-2724) and mouse anti phosphorylated neurofilaments (Sternberger monoclonals SMI-31). The secondary antibodies conjugated to rhodamine or fluorescein, were obtained from Jackson Laboratories. Confocal images we were captured on a Zeiss Axioplan2 microscope with a BioRad Radiance 2000 scanning system.

2 - Transmission Electron Microscopy

Wild type, *NCP1*, *CGT* and *NCP1/CGT* double mutant mice were deeply anesthetized and transcardially perfused with Millonig's buffer solution containing 4% paraformaldehyde and 2.5% glutaraldehyde (pH 7.3). Following the perfusion, the whole animal was post-fixed for 2 weeks at 4^{o}C in the same fixation solution. Following an overnight incubation in Millonig's buffer, cerebellar tissue from each animal was postfixed for 1 hour in cacodylate buffered 1% osmium tetroxide. The tissue was then rinsed, dehydrated in increasing concentrations of cold ethanol, and infiltrated and embedded in PolyBed (Polysciences). One µm and 90 nanometer sections were cut and stained with toluidine blue or a combination of uranyl acetate and lead citrate, respectively. The one µm thick sections were analyzed with a Nikon Eclipse 800 and the thin sections were analyzed using a Zeiss EM 10CA. To produce

digital images, EM negatives were scanned using a Microtek ScanMaker 5900. EM figures were assembled using Adobe Photoshop.

3 - Synapse quantification

The quantitative analyses used electron micrographs taken from corresponding regions in the molecular layer of wild type, *CGT, NCP1* and *NCP1/CGT* mice at P20. We analyzed 10 images of each animal and a minimum of 3 mice per genotype (2 mice for the double mutants), summing a total of 250-300 synapses per genotype. Synapses between parallel fibers and Purkinje dendrites are excitatory and consequently asymmetric. We included a qualitative component in our analysis by counting only synapses that ultrastructurally qualified as asymmetric and displayed well-defined active zone, with a minimum extension of 150 nm. That might lead to sub estimation of the total number of synapses in the molecular layer in our quantification but it would detect gross defects in ultrastructural morphology of these synapses.

CHAPTER V

Gene Expression Profiling in NCP1 Mutant Cerebellum

ABSTRACT

Identification of mRNAs that have restricted expression patterns in the brain represents powerful tools with which to characterize and manipulate the nervous system. Here we utilized a strategy with microarray technology based on Affymetrix arrays, to identify mRNA transcripts in *NCP1* mutant mice that showed fold changes when compared to its wild-type counterpart. The gene expression profiles were compared between cerebella of 10 day old *NCP1* mutant and wild-type mice. Analysis of the total 22,244 genes was carried using three distinct methods and a total of 446 genes were found to be expressed differentially (up or down regulated). Among all the differentially expressed genes 15 genes represented a 50-100% fold increase or decrease in their levels of expression. 8 out of the 15 genes were consistent in all three methods used for analysis.

These studies suggest that NCP1 protein might be required not only for proper axo-glial junction formation and maintenance but also may directly or indirectly affect normal neuronal cell function.

INTRODUCTION

In recent years, DNA microarray technology has gained increasing popularity for gene expression studies (Greenberg 2001). Using these methods one can detect and quantify differential expression of thousands of genes simultaneously under almost identical experimental conditions. There are several different advantages of these studies one of them being that many molecular pathways can be investigated globally since most if not all the genes involved will be present in the analysis. This type of approach has initially been demonstrated in cancer research (Soriano et al 2000) and its use is growing in many different areas including those related to nervous function and disease (Jin et al. 2001; Raghavenrdra et al. 2002; Tang et al. 2002; Lu et al, 2003).

For our studies we used Affymetrix GeneChip microarrays to investigate the differential expression of genes in mutant mice lacking NCP1 protein. The model system we used was the mouse cerebellum for two main reasons: - *NCP1* mutant mice develop cerebellar ataxia thus it would be interesting to see what gene products suffer changes in their expression levels when compared to controls; this could give us clues to whether lack of NCP1 has only an effect in the generation of axo-glial junctions or it can also cause secondary effects that affect the overall cerebellar function.

The mammalian cerebellum is a system that has been used as a model to investigate many fundamental neurobiological processes ranging from development to information processing (Ito, 1984; Sotelo, 2004). It is a relatively large structure composed of highly ordered layers which makes it easy for study. Its development and cytoarchitecture are well characterized as well as neuronal cell markers so that it makes it easy to identify neuronal

cell types (Ziai et al, 2002; Nordquist et al,, 1988; Oberdick et al., 1988). Finally the cerebellum, more so than any other brain region, many spontaneous and induced mutations have been identified in mice that affect the structure and function of the cerebellum (Sidman et al., 1962; Sidman et al, 1970; Quackenbush, 2001; Mullen et al., 1976; Mariani et al., 1977; Landis et al., 1975). As some of these mutations lead to degeneration of specific neuronal populations, it provides an opportunity to identify differences between cell populations between normal mice and mice lacking a specific protein.

The cerebellum possesses eight types of neurons: Purkinje, granule, lugaro, stellate, basquet, Golgi, brush and candelabrum cell (Mariani et al., 1977; Mugnaini 1994; Ito 1984). By far the most relevant cell in the cerebellum is the Purkinje cell, which provide the sole output of the cerebellar cortex and are the pivotal element around which the cerebellar circuit is organized (Ito, 1987). The main connections of the Purkinje cells come from parallel fibers which are the axonal extensions of granule cells, the most abundant cell in the cerebellum. Purkinje neurons also receive extracellular inputs from climbing fibers as well as inhibitory imputs from stellate and basket cells. Purkinje cells are considered to be the primary site for information processing in the cerebellum and all that information is channeled out to the brain via the deep cerebellar nuclei (Ito, 1987). The information conveyed by the cerebellum is mainly responsible for motor coordination, motor tone and equilibrium (Ito, 1987). Thus any mutations affecting directly or indirectly Purkinje cells frequently result in tremors and ataxic behavior (Sidman, et al., 1970; Sidman, 1983).

These behavioral traits are useful then to identify genes that underlie the phenotypes observed. Recently we have generated a mutant mouse model in which the *NCP1* gene was removed (Bhat et al., 2001). The mice expressed a behavioral phenotype characterized by

tremors and ataxia by early adulthood. NCP1 is a transmembrane protein and is localized to paranodal junctions. It dimerizes with contactin protein and together they form a complex to keep the paranodal myelin loops attached to the axonal cytoskeleton. The behavioral deficit observed in NCP1 mutant mice affords the opportunity to identify gene products that are preferentially or selectively expressed in cerebellar cell populations.

Here we describe the use of Affymetrix microarray technology, combined with a bioinformatics analysis approach to identify new transcripts that are enriched in the cerebellum and might be up or down regulated when a wild-type mouse strain is compared to a mutant one.

RESULTS

For the Gene chips arrays we used Affymetrix Mouse Genome 430A 2.0 Arrays (Table A). These chips contain over 22,000 probe sets representing transcripts and variants from over 14,000 well characterized mouse genes that can be used to explore mechanisms behind biological and disease process. The sequences used in the design of these arrays were selected from GeneBank and refseq. Oligonucleotide probes complementary to each corresponding sequence are synthesized *in situ* on the array. There are eleven pairs of oligonucleotide probes that are used to measure the level of transcription of each sequence represented on the GeneChip array (www.Affymetrix.com).

Table A - GeneChip Mouse Genome 430A 2.0 Array Specifications

Number of probes set	>22.000
Feature Size	11µm
Oligonucleotide probe length	25-mer
Probe pair sequences	11
Control sequences included	GAPDH, β-Actin, Transferrin receptor, Pyruvate carboxylase
Detection sensitivity	1:100.000

1 - Gene Expression Profiling

Affymetrix has designed new algorithms for monitoring GeneChip expression data. These statistical algorithms, were designed to accommodate the typical distribution of data found in microarray experiments. The new statistical algorithms employ standard statistical techniques and are optimized to accommodate advancements in array and probe selection technology. They provide accurate, high-quality analysis for GeneChip array data.

The analysis process begins by obtaining data in the form of flat files that were generated by the scanning software used to analyze the Affymetrix chips. Raw data usually refers to the gene or spot intensity values in the scanned files. Once the software recognizes the raw data, it applies standard normalizations which are appropriate for our expression analysis. These normalizations then enable us to distinguish between real (biological) variations in gene expression levels and variations due to the measurement process. Normalizing also scales the data to allow us to compare relative gene expression levels. There are many different ways to normalize the data, and although Affymetrix chips are pre normalized they may not meet the standards of our software normalization requirements. One most common normalization method is called Per-chip normalization, which control for chip-wide variations in intensity. These variations may be due to inconsistent washing, inconsistent sample preparation, or other microarray imperfection. For our studies we performed per-chip normalizations normalizing to a median or percentile, which allows us to divide all of the measurements on each chip by a specified percentile value, which in our case was 50%.

We also normalized our data to a median, which accounts for the difference in detection efficiency between spots and it lets us compare relative change in gene expression levels. Finally we performed per-gene normalizations, just like per-chip normalization, each measurement was divided by the 50.0th percentile of all measurements in that sample. The per-gene normalizations were also normalized to a median using the same cutoff values (10) as those for per-chip normalizations.

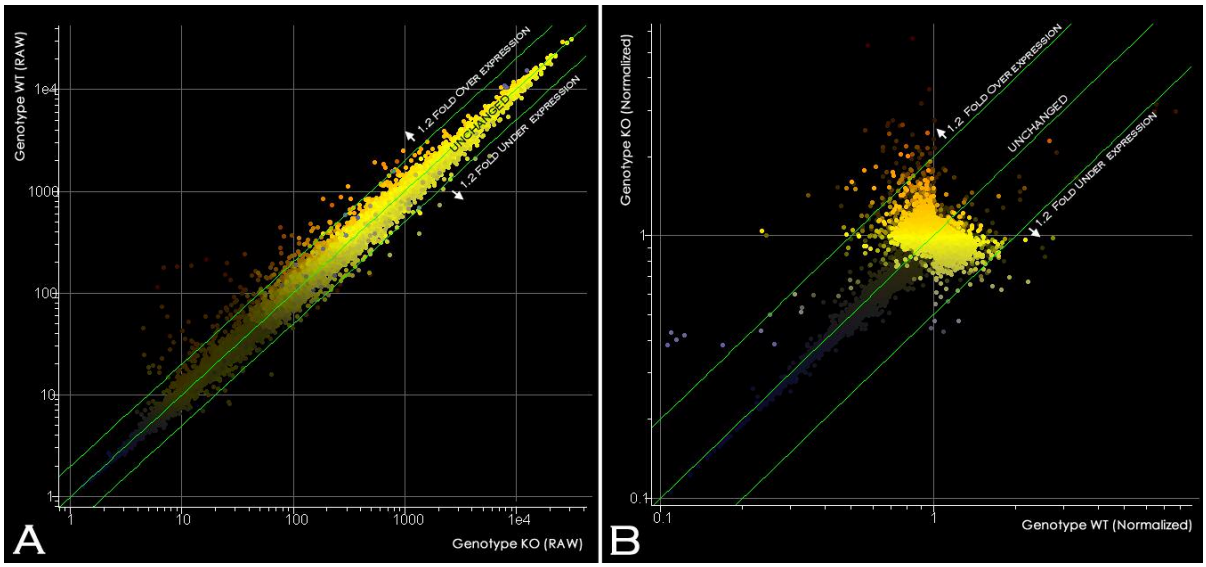

Figure 1 – Scatter plots of Raw and Normalized data of the 22.244 genes obtained after the initial gene spring analysis comparing wild-type and mutant gene chips.

Figure 1 show scatter plots of the raw data before normalization and after normalization of the 22.244 genes analyzed. Note the change in distribution of the spots after the data has been normalized. All viable spots concentrate in one area according to the parameters set by the normalization standards. The green lines represent fold changes of the gene values. The middle green line represents a neutral value, which represents no absolute fold change whereas the other two lines represent absolute fold changes above 1.2 or 20%, as established in the filtering parameters.

For our studies we used three analysis methods that use separate algorithms for the selection of significant gene fold-change values: GeneSpring, GC-RMA and GC-RMA-GEM. GeneSpring utilizes an algorithm known as MAS 5.0. The Signal algorithm implemented in MAS 5.0 is very robust against corrupted data and the results remain well-correlated even when as much as 20% of the data is corrupt. Naturally, additional noise never improves the quality of the data, and so does degrade the results, but robustness provides a safety net against corrupted data completely destroying the utility of an array. The second method, GC-RMA (Robust Microarray Analysis) depends on the Guanine-Cytosine content present on the array probes. This algorithm is usually chosen for its much improved performance in reporting low- and high-level expression over the other methods as well as its dynamic range for single probe sets. Finally, the third method GC-RMA-GEM utilizes the same algorithm as GC-RMA but it has added to it a Global Error Model (GEM), which performs chip estimations based on the variation between the chips. Although it is not extremely accurate it is a good system for a general estimation.

We used a total of 5 arrays. Two represented the wild-type cerebellum of p10 mice whereas the other three were used for p10 NCP1 mutant mice. A total of 22,244 genes were analyzed in our chips. All arrays were compared to each other using the three methods described above. From the 22,244 genes we obtained a total of 550 genes that were significant (Figure 2). We performed two filters for the selection of the genes: 1 – genes had to have an expression signal greater than 53 and less than 32,200 in all 5 chips. 2- Genes selected from the knock out samples that have normalized data values greater or less than those from the wild type samples by a factor of 1.2 fold. That is any gene that is up regulated or down regulated 20% from its wild-type control.

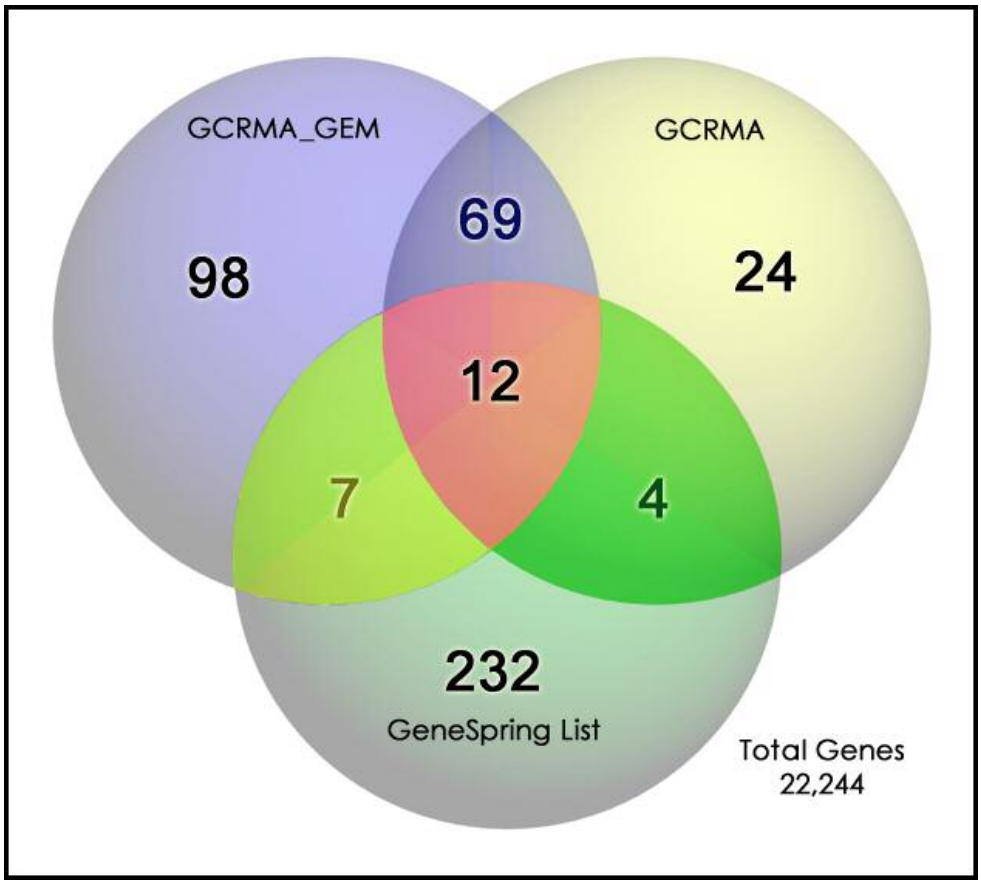

Figure 2 – Venn Diagram of the comparison of the three analysis methods used in this study.

From the 550 genes obtained by our filtering methods, 255 genes were from GeneSpring, 186 from GC-RMA-GEM and 109 from the GC-RMA algorithm (Figure 2). Only 12 genes were consistently up or down regulated in all three methods as shown in the figure in red where all three circles overlap. When comparing two methods at the same time, GeneSpring did not seem to be consistent with the other two methods. It only had 7 and 4 gene in common (Figure 2 – yellow and green) which represented a 2.74 and a 1.56% of genes, thus a very low overlap. When comparing the CG-RMA and GC-RMA-GEM methods, the overlapping genes represented a total of 63 and 37% respectively. Based on this we decided to use the GC-RMA gene list for our selection.

2 - NCP1 Mutant Mice Affect Indirectly Other Gene Functions

Table 2 lists the 109 genes obtained with the GC-RMA algorithm after filtering. 109 genes represent a large number of genes to work with. We decided to filter genes even further by only analyzing genes that were 50% up or down regulated. That is their fold change value had to be -1.5 < X > 1.5 where X represents fold change. As noted in table 2, genes that fell in that category are underlined in yellow. Table 2 also shows one underlined gene (ID: 1437180_at) in blue, which represents an unknown gene product normally referred to as RIKEN cDNA. A total of 15 genes were selected (table 3) and chosen for a more detailed analysis. Note that from those 15 genes 8 of them were present in all 3 analysis methods which had an absolute fold change greater than 50% (Figure 1- red ; Table 4). From the 15 genes obtained in the GC-RMA algorithm, 14 of them were down regulated and only one, UDP-Gal:betaGlcNAc beta 1,4- galactosyltransferase was up regulated.

GENE ID	GENE SYMBOL	GENE TITLE	FOLD CHANGE
1435035_at	Rg9mtd2	RNA (guanine-9-) methyltransferase domain containing 2	1.178879310
1424443_at	Tm6sf1	Transmembrane 6 superfamily member 1	-1.471095571
1421192_a_at	**Itsn1**	**Intersectin 1 (SH3 domain protein 1A)**	**-1.690156600**
1456057_x_at	1110006I15Rik	RIKEN cDNA 1110006I15 gene	-1.171907757
1428751_at	Pacrg	Park2 co-regulated	1.076680672
1450105_at		A disintegrin and metalloprotease domain 10	-1.260975610
1418295_s_at	Dgat1	Diacylglycerol O-acyltransferase 1	1.419908467
1430125_s_at	Pqlc1	PQ loop repeat containing 1	-1.141201264
1426326_at	Zfp91	Mus musculus Balb/c zinc finger protein PZF (Pzf) mRNA, complete cds.	-1.396273292
1439441_x_at	Lats2	Large tumor suppressor 2	-1.459887006
1427016_at	4932438A13Rik	RIKEN cDNA 4932438A13 gene	-1.172413793
1439380_x_at	Gtl2	BB093563 RIKEN full-length enriched	1.425925926
1415963_at	Hnrph2	Heterogeneous nuclear ribonucleoprotein H2	-1.443699732
1438759_x_at		AU046270 Mouse sixteen-cell-embryo cDNA Mus musculus	-1.256890849
1418629_a_at		KH domain containing, RNA binding	-1.098018770
1436834_x_at	Mdh1	Malate dehydrogenase 1, NAD (soluble)	-1.407676349
1437223_s_at	Xbp1	X-box binding protein 1	-1.180598555
1421025_at	Agpat1	1-acylglycerol-3-phosphate O-acyltransferase 1	1.075365579
1454807_a_at	Snx12	Sorting nexin 12	-1.110062893
1423599_a_at	Pdcl	unnamed protein product; phosducin-like (MGD|MGI:1914716	-1.305429864
1422697_s_at		Jumonji, AT rich interactive domain 2	-1.274099884
1416725_at	Tcf4	Transcription factor 4	-1.142640364
1437205_at		DNA segment, Chr 8, ERATO Doi 325, expressed	1.181923523
1436152_a_at	Hbxip	Hepatitis B virus x interacting protein	-1.361963190

GENE ID	GENE SYMBOL	GENE TITLE	FOLD CHANGE
1457588_at	Vlcp	Valosin containing protein	1.261388286
1417781_at	Lass4	Longevity assurance homolog 4 (S. cerevisiae)	1.356790123
1420950_at	Znrf1	Zinc and ring finger 1	1.218241042
1426795_at	Ptprs	protein tyrosine phosphatase, receptor type, S	1.253065775
1417963_at	Pltp	Phospholipid transfer protein	-1.310796074
1452359_at	AA536743	Expressed sequence AA536743	-1.243272336
1418772_at	BC016423	cDNA sequence BC016423	-1.390742734
1448941_at	**B4galt2**	**UDP-Gal:betaGlcNAc beta 1,4- galactosyltransferase, polypeptide 2**	**1.742566510**
1449111_a_at	Grb2	Growth factor receptor bound protein 2	-1.073921971
1432394_a_at	Aatf	apoptosis antagonizing transcription factor	-1.422037422
1419814_s_at	S100a1	S100 calcium binding protein A1	1.330891331
1416041_at	**Sgk**	**Serum/glucocorticoid regulated kinase**	**-1.645728643**
1438637_x_at	Sf3b2	Splicing factor 3b, subunit 2	-1.257328990
1424672_at	Dxml1	RIKEN cDNA C630007L23 gene (Dmx-like 1)	-1.456193353
1452207_at			-1.207674944
1437180_at	6530403A03Rik	RIKEN cDNA 6530403A03 gene	1.623298033
1448704_s_at	H47	Histocompatibility 47	-1.253863135
1433574_at	Cdc37l1	Cell division cycle 37 homolog (S. cerevisiae)-like 1	1.385650224
1434369_a_at	Cryab	Crystallin, alpha B	-1.399638118
1455824_x_at	Itm1	Intergral membrane protein 1	-1.466173362
1426021_a_at	Cdc7	Cell division cycle 7 (S. cerevisiae)	1.306432749
1448733_at	Bmi1	B lymphoma Mo-MLV insertion region 1	-1.083333333
1460562_at	Eftud1	Elongation factor Tu GTP binding domain containing 1	-1.169546436
1424544_at	Nrbp2	Nuclear receptor binding protein 2	1.312633833
1425280_at	Leng1	Leukocyte receptor cluster (LRC) member 1	-1.065458207
1434342_at	**S100bp**	**S100 protein, beta polypeptide, neural**	**-1.614798694**
1421096_at	Trpc1	Transient receptor potential cation channel, subfamily C, member 1	-1.074413863
1421252_a_at	Mef2a	Myocyte enhancer factor 2A	-1.200227531
1417101_at	Hspa2	Heat shock protein 2	-1.295047418
1452031_at	**Slc1a3**	**Solute carrier family 1 (glial high affinity glutamate transporter), member 3**	**-1.541755889**
1419114_at	5430428G01Rik	RIKEN cDNA 5430428G01 gene	-1.104568528
1453030_at	Rnf184	Ring finger protein 184	-1.159763314
1426544_a_at	Ttc14	Tetratricopeptide repeat domain 14	1.496462264
1449423_at	Mast1	Microtubule associated serine/threonine kinase 1	1.091571280
1431464_a_at	Pmm2	unnamed protein product; phosphomannomutase 2	-1.462184874
1451004_at	Acvr2a	Activin receptor IIA	1.134570766
1439432_x_at	Morf4l2	Mortality factor 4 like 2	-1.242524917
1451388_a_at	Atp11b	ATPase, Class VI, type 11B	1.457073761
1416886_at		Nuclear DNA binding protein	-1.035425101
1448916_at	Mafg	V-maf musculoaponeurotic fibrosarcoma oncogene family, protein G (avian)	1.184210526
1451132_at	Pbxip1	Pre-B-cell leukemia transcription factor interacting protein 1	1.068852459
1418271_at	Bhlhb5	Basic helix-loop-helix domain containing, class B5	-1.483803553
1434697_at	1110001P04Rik	RKEN cDNA 1110001P04 gene	-1.482479784
1451499_at	Cadps2	Ca2+-dependent activator protein for secretion 2	-1.083249749
1437526_x_at	Hnrpr	Heterogeneous nuclear ribonucleoprotein R mRNA, mRNA sequence.	-1.342741935
1427482_a_at	**Car8**	**Carbonic anhydrase 8**	**-1.522371365**
1416164_at	Fbln5	Fibulin 5	-1.315614618
1419057_at	**Slc5a1**	**Solute carrier family 5 (sodium/glucose cotransporter), member 1**	**-1.882562278**
1424859_at	**Homer3**	**Homer homolog 3 (Drosophila)**	**-1.508792497**
1435327_at	AW112037	Expressed sequence AW112037	-1.405291005
1417456_at	Gnpat	Glyceronephosphate O-acyltransferase	-1.206709957
1449014_at	**Lactb**	**Lactamase, beta**	**-1.549479167**

GENE ID	GENE SYMBOL	GENE TITLE	FOLD CHANGE
1454974_at	Ntn1	Netrin 1	-1.174746336
1435228_at	BC023829	CDNA sequence BC023829	-1.349336057
1439450_x_at	A230046K03Rik	RIKEN cDNA A230046K03 gene	-1.183718372
1448343_a_at	Nbr1	Neighbor of Brca1 gene 1	-1.169133192
1451519_at	Rnf2	Ring finger protein 2	-1.288194444
1418135_at	Aff1	AF4/FMR2 family, member 1	-1.266279070
1427068_x_at	4933439F18Rik	RIKEN cDNA 4933439F18 gene	-1.290456432
1416976_at	Stam2	Signal transducing adaptor molecule (SH3 domain)	-1.289473684
1431765_a_at	Rps2	Ribosomal protein S2	1.229143493
1422824_s_at	Eps8	Epidermal growth factor receptor pathway substrate 8	-1.393640351
1422044_at	Ndst1	N-deacetylase/N-sulfotransferase (heparan glucosaminyl) 1	1.347174164
1451684_a_at	Bicd1	Bicaudal D homolog 1 (Drosophila)	-1.293922652
1416733_at	Msk1	Muskelin 1, intracellular mediator containing kelch motifs	-1.171974522
1427730_a_at	Zfp148	Zinc finger protein 148	-1.280092593
1455214_at	Mitf	Microphthalmia-associated transcription factor	-1.116407982
1425149_a_at	Pdcl	Phosducin-like	-1.408983452
1451089_a_at	**Arcn1**	**Archain 1**	**-1.826985854**
1426047_a_at	**Ptprr**	**Protein tyrosine phosphatase, receptor type, R**	**-1.629200463**
1426952_at	Arhgap18	Rho GTPase activating protein 18	-1.329809725
1426955_at	Col18a1	Procollagen, type XVIII, alpha 1	-1.485714286
1424114_s_at	**Lamb1-1**	**Laminin B1 subunit 1**	**-1.892307692**
1434883_at	Mtdh	Metadherin	-1.041439477
1460004_x_at	Stx6	Syntaxin 6	-1.270299145
1425497_a_at	Prpf4b	PRP4 pre-mRNA processing factor 4 homolog B (yeast)	1.107332625
1454796_at	D5Ertd40e	Expressed sequence AI562086	-1.270132518
1439444_x_at	1110014C03Rik	Similar to Histone deacetylase 1 (HD1)	-1.124724062
1451331_at	**Ppp1r1b**	**Protein phosphatase 1, regulatory (inhibitor) subunit 1B**	**-1.666666667**
1423408_a_at	2500003M10Rik	RIKEN cDNA 2500003M10 gene	-1.224561404
1433906_at	**Abh**	**Aspartate-beta-hydroxylase**	**-1.652654867**
1450632_at	**RasA**	**Ras homolog gene family, member A**	**-1.592517695**
1435725_x_at	Rpl12	Large tumor suppressor 2	1.259171598
1437719_x_at	A230046K03Rik	RIKEN cDNA A230046K03 gene	-1.247925311
1425296_a_at	Rgs3	Regulator of G-protein signaling 3	-1.342792281

TABLE 2 **– Gene list obtained using the GC-RMA algorithm**. A total of 109 genes were obtained after the applying filters in the selection criteria. Yellow denotes genes that have absolute fold changes of 50% or above. Blue represent an unknown gene product also above 50% fold change.

GENE ID	GENE SYMBOL	GENE TITLE	FOLD CHANGE
1448941_at	B4galt2	UDP-Gal:betaGlcNAc beta 1,4- galactosyltransferase, polypeptide 2	1.742566510
1424859_at	Homer3	Homer homolog 3 (Drosophila)	-1.508792497
1427482_a_at	Car8	Carbonic anhydrase 8	-1.522371365
1452031_at	Slc1a3	Solute carrier family 1 (glial high affinity glutamate transporter),	-1.541755889
1449014_at	Lactb	Lactamase, beta	-1.549479167
1450632_at	RasA	Ras homolog gene family, member A	-1.592517695
1434342_at	S100bp	S100 protein, beta polypeptide, neural	-1.614798694
1426047_a_at	Ptprr	Protein tyrosine phosphatase, receptor type	-1.629200463
1416041_at	Sgk	Serum/glucocorticoid regulated kinase	-1.645728643
1433906_at	Abh	Aspartate-beta-hydroxylase	-1.652654867
1451331_at	Ppp1r1b	Protein phatase 1, regulatory (inhibitor) subunit 1B	-1.666666667
1421192_a_at	Itsn1	Intersectin 1 (SH3 domain protein 1A)	-1.690156600
1451089_a_at	Arcn1	Archain 1	-1.826985854
1419057_at	Slc5a1	Solute carrier family 5 (sodium/glucose cotransporter), member 1	-1.882562278
1424114_s_at	Lamb1-1	Laminin B1 subunit 1	-1.892307692

TABLE 3 – 15 selected genes from the GC-RMA algorithm organized by fold change values.

GENE ID	GENE SYMBOL	GENE TITLE	FOLD CHANGE
1417781_at	Lass4	Longevity assurance homolog 4 (S. cerevisiae)	1.3567901
1422697_s_at	Jmd2	Jumonji, AT rich interactive domain 2	-1.2740998
1422824_s_at	Eps8	Epidermal growth factor receptor pathway substrate 8	-1.3936407
1426955_at	Col18a1	Procollagen, type XVIII, alpha 1	-1.4857142
1427482_a_at	Car8	Carbonic anhydrase 8 ***	-1.5223713
1452031_at	Slc1a3	Solute carrier family 1 (glial high affinityg Glutamate transporter), member 3 ***	-1.5417558
1450632_at	RasA	Ras homolog gene family, member A ***	-1.5925176
1426047_a_at	Ptprr	Protein tyrosine phosphatase, receptor type ***	-1.6292004
1416041_at	Sgk	Serum/glucocorticoid regulated kinase ***	-1.6457286
1433906_at	Abh	Aspartate-beta-hydroxylase ***	-1.6526548
1451331_at	Ppp1r1b	Protein phosphatase 1, regulatory (inhibitor) subunit 1B ***	-1.6666666
1421192_a_at	Itsn1	Intersectin 1 (SH3 domain protein 1A) ***	-1.6901566

TABLE 4 – **12 overlapping genes using all three algorithms**. Yellow denotes the genes that are above the absolute 50% fold change which are also part of the 15 genes selected from the GC-RMA algorithm.

We performed a hierarchical cluster heat map to see the relative expression of the 15 selected genes comparing all five chips (Figure 3). The color intensities shown in the figure represent the fold change form each individual genes. The relative change is compared to the wild-type samples which are represented in the two left columns. The more red the blocks are, the more relative overexpression they represent. On the other hand, the other end of the spectrum is a green color which represents an under expressed gene. Yellow is the mean average between red and green and represents an unchanged value. Although some of the samples are represented by yellow when all 5 samples are averaged together the fold change was significant enough to pass the filtering parameters.

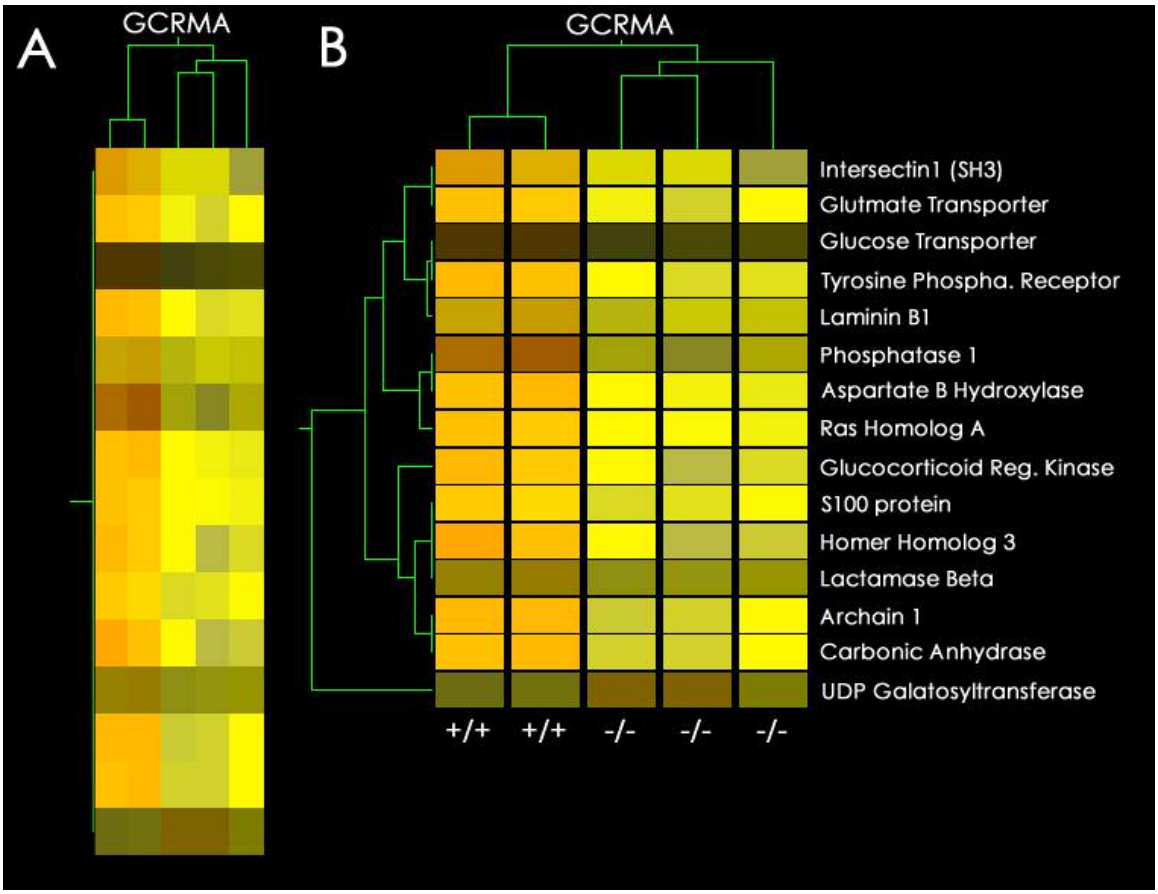

Figure 3 **– Hierarchical clustering heat map of the 15 selected genes by GC-RMA method**. The color intensities represent the fold change of the genes. The reddish colors represent a higher expression. First two columns in A correspond to wild-type samples and other three to NCP1 mutant mice. B is an expansion of A.

We then performed a scatter plot of the 15 genes selected with the GC-RMA method after a 50% fold change filter. This allows us to have a more exact and quantitative measurements. As mentioned above there is only one gene over expressed above 50% (figure 4- point 1) whereas the rest are all under expressed 50%. Note that the closer the spots are to the green lines the less fold change it represents. Point 15 in the figure represents laminin B1 gene which is almost 100% fold change. In this case the scatter plot represents the genes that were up or down regulated an absolute value of 1.5 or 50%.

These results suggest then that lack of NCP1 protein, not only is required for axo-glial junction formation but might have a secondary effect in many cellular processes as demonstrated by the fold change shown by the GeneSpring analysis.

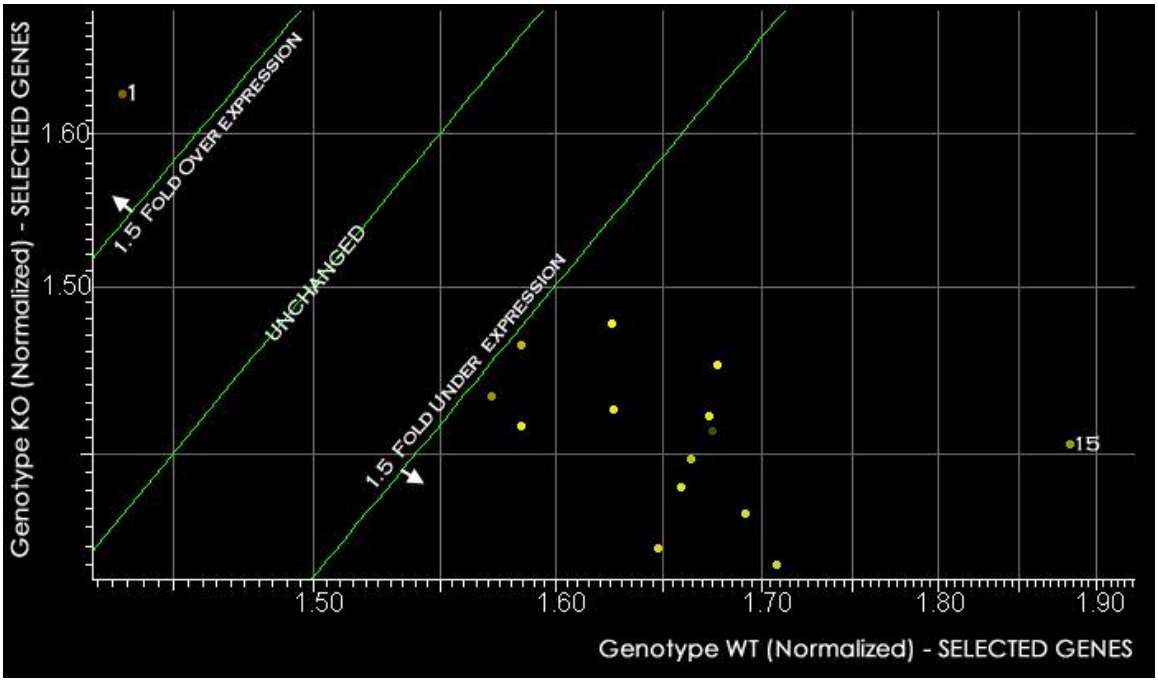

Figure 4 – **Scatter plot of the 15 selected GC-RMA genes**. Points 1 and 15 represent both ends of the scale. Point 1 is the only up regulated gene and point 15 is the gene most down regulated.

DISCUSSION

We describe here a high throughput microarray-based strategy to identify candidate transcripts that are affected by the loss of NCP1 proteins. These genes could serve a potential role in cerebellar function. The approach used takes advantage of the availability of the NCP1 mutant mice, which serves as an excellent model to compare gene expression with wild-type samples. This allowed us to identify 15 potential candidate genes that were for the most part down regulated. Conceptually the same strategy could be applied to other mutant

strains of mutant mice that share a similar phenotype such as *CGT* or *Contactin* mutants (Dupree et al. 1998; Boyle et al. 2001). Both share the similar behavioral as well as structural phenotypes. The contactin mutant has an extended cerebellar phenotype, in which parallel fibers from the granule cell layer are inverted and granule cells have defective claws which ultimately lead to defective synaptic connectivity. This way *Contactin* mutant make an ideal candidate for gene expression profiling experiments that could help identify new candidate genes that affect cerebellar function.

From the 15 genes identified by the Affymetrix chip analysis, it is evident that more than 50% of the proteins are involved directly and/or indirectly in signaling transduction pathways. The rest of the proteins are randomly involved in mechanisms of transport (glutamate transporter, Na/glucose co transporter), structural cell integrity (Laminin β1) and posttranslational modifications (UDP-Gal:betaGlcNAc beta 1,4- galactosyltransferase). All of the genes identified here are known, based on available databases with the exception of one gene (**RIKEN cDNA 6530403A03**), which is underlined in blue on table 2. It would be noteworthy to identify the gene sequence using today's available gene banks since it could represent a potential new gene candidate whose function might be downstream of the axo-glial junctions.

We must keep in mind that only one time point (p10) was selected for the gene expression profile study. We initially rationalized that analyzing mice at an early stage would give us more opportunity to find early development genes that could be regulated by axo-glial junctions. On the other hand, by p10 mutant NCP1 mice as well as wild-type mice do not show significant differences in their development nor their behavior. Additional studies

need to be carried out to address the role of NCP1 and axo-glial junctions in signal transduction pathways or posttranslational modifications.

Despite this fact, we were able to identify two proteins which are interesting and will be pursued for further experiments. These proteins are the solute carrier family 1 glutamate transporter and most importantly intersectin 1. A brief description of their functions, implications and their potential relevance to axo-glial junctions is detailed below.

1 - Carrier family 1 glutamate transporter

L-Glutamate is a major excitatory neurotransmitter in the mammalian central nervous system (CNS) that contribute not only to fast synaptic neurotransmission, but also to complex physiological processes like memory, learning, plasticity, and neuronal cell death (Dingledine et al., 1999; Ozawa et al., 1998). Glutamate activates ionotropic glutamate receptors for fast excitatory neurotransmission and metabotropic receptors for slower modulatory affects on transmission (Balcar, 2002).

The solute carrier family 1 (SLC1) is composed of five high affinity glutamate transporters each of which exhibits distinct functional properties. Glutamate transporters mediate the transport of L-Glu, L-Asp and D-Asp, accompanied by the cotransport of 3 Na+ and 1 H+, and the countertransport of 1 K. One of the main functions of glutamate transporters is protect neurons against glutamate excitotoxicity in the central nervous system (CNS). The regulation and manipulation of their function is a critical issue in the pathogenesis and treatment of CNS disorders involving glutamate excitotoxicity. Loss of function of the glial glutamate transporter GLT1, a transporter mainly expressed in glial

cells, has been implicated in the pathogenesis of amyotrophic lateral sclerosis (ALS), resulting in damage of adjacent motor neurons.

ALS is a progressive neurological disorder characterized by degeneration of upper and lower motor neurons. A decrease in the glutamate transporter activity due to the reduction of GLT1 has been reported in patients with ALS (Rothstein et al., 1994, 1995). This suggests that GLT1 reduction is a direct cause for ALS. Our results are in concordance with the results observed in patients with ALS, which is a reduction of glutamate transporter expression. Based on our Affymetrix data, this protein is reduced over 50% in the mutants. It would then be interesting to see whether NCP1 alone is the major cause for the behavioral phenotypes observed or if the lack of glutamate transporters is an indirect cause that contributes to the phenotypes of the *NCP1* mutant mice. Regardless of the cause, glutamate seems to be an interesting candidate for study in our knock-out mice.

2 - Intersectin 1

Intersectin (ITSN) proteins are present predominantly in the nervous system with lower expression elsewhere (Guipponi et al., 1998; Okamoto et al., 1999; Sengar et al., 1999). It is a multifunctional adaptor protein and has been isolated by a number of groups based on its ability to bind proline-rich peptides (Yamabhai et al., 1998), to form a complex with dynamin (Roos and Kelly, 1998) and SNAP-23/25 (Okamoto et al., 1999).

The domain structure of ITSN suggests that this protein may act as a scaffolding or adaptor protein that regulates various biochemical pathways. It consists of two amino-terminal Eps15 homology domains (EH), a central coiled-coil domain (CC) and five tandem

Src homology 3 domains (SH3). SH3 domains recognize Pro-rich sequences within target proteins and are present in a variety of cytoskeletal and signaling proteins such as NCP1 (Mayer and Eck, 1995, Bhat et al. 2001). It is therefore interesting to test whether NCP1 protein has a direct link between ITSN1 via it SH3 domain. Our laboratory as well as other research groups is interested in identifying an SH3 domain containing protein that could potentially bind to NCP1 and participate in a signaling mechanism. ITSN1 seem to be an ideal candidate for this task. Our Affymetrix data shows that the mRNA is down regulated 70%. One plausible explanation for this could arise from the fact that axo-glial junctions may regulate the expression of ITSN1. Future experiments to address the how the loss of NCP1 affects the expression of ITSN1 are needed in order to better understand the role of axo-glial junctions.

We have not validated the expression of the identified genes, it would now be necessary to carry out further experiments that use quantitative RT-PCR techniques to confirm or validate the results obtained by the GC-RMA microarray analysis. This will then provide us clues about the role of NCP1 or axo-glial junctions in signal transduction pathways.

EXPERIMENTAL PROCEDURES

1 - Brain Tissue Collection and RNA Isolation

P10 wild-type and mutant mice were anesthetized deeply and cerebellums were harvested for analysis. Total RNA extraction was performed using TRIzol Regent according to the

manufacturer's instructions (Invitrogen, CA). Samples were homogenized in TRIzol Reagent for 30 seconds. After mixing with chloroform, samples were centrifuged for 15 minutes at 12.000xg at 4Cº. For RNA precipitation, isopropanol was added to the aqueous phase. This precipitation mix was then centrifuged for 10 minutes at 12.000xg at 4Cº. The RNA pellet was washed once with cold 75% ethanol and air dried for 10 minutes. Total RNA was resuspended in RNase-free water. One cerebellum yielded about 10-20µg RNA, sufficient for 1 array. We used a total of 5 cerebellums. 2 wild-type and 3 mutants.

2 - Microarray hybridization and Analysis

Affymetrix CEL. Files were uploaded to GeneSpring software for analysis by the GCRMA method. The samples were filtered with control gene values less than 53 in 2 out of 5 samples based on the cross gene error model (GEM) estimation. A second filter was applied using genes with an absolute value of 1.2 or 20% fold change when comparing wild-types and knock outs. A Welch t-test was then applied and the value for p-value cutoff was 0.05. A significance analysis of microarray (SAM) was carried following the filters for the two-class unpaired case assuming unequal variances with delta = 0.5, q-value = 0.06. All genes with the fold change greater or less than 1.5 between the wild type and knockout groups in the resulting list by Welch t-test were then selected as well as those by the SAM analysis. Global normalization was applied. Relative change in expression between two samples is given as a fold change value, negative values representing a decrease in expression in the experimental compared to the baseline sample. Candidate genes were retained if they showed at least a 1.5 fold difference in expression levels.

CHAPTER 6

CONCLUSIONS

Myelination, a process carried out by Schwann cells and oligodendrocytes in the PNS and CNS respectively, is an area which remains of great interest. It is a highly regulated process which ensures an efficient and rapid propagation of action potentials. The coordinated differentiation of the axon and its myelinating cell requires a bi-directional axo-glial communication by signaling mechanisms. Signal arising from the axon will then regulate the survival, proliferation and the differentiation of Schwann cells. On the other hand, reciprocal signals from glial cells will affect the cytoskeleton and are required for the axon to survive. As a result the myelinated fibers develop structural features that allow them to maximize the conduction potentials. One such feature is the differentiation of myelinated fibers into distinct molecular functional domains. Of particular interest are the paranodal junctions. In the past few years rapid progress has been made in identifying the molecular constituents of these axo-glial junctions but their functions remain to be characterized.

Novel functions of axo-glial junctions in cellular physiology and diseases are emerging. On this section, a brief discussion is provided on the evolutionary importance of axo-glial junctions, and would like to address the role of paranodal junctions in signaling. Finally, I will highlight the role that paranodal junctions play in neuronal axonopathies and myelinating diseases.

1 - Axo-Glial Junctions: from Flies to Humans

To highlight the importance of paranodal axo-glial junctions it is important to understand its conservation throughout evolution. Recent advances in the composition of axo-glial junctions indicate that insect septate junctions, share several structural and functional components with the vertebrate paranodal junctions. This suggests that both junctions evolved from a common ancestral precursor, and those invertebrate septate junctions were ahead from paranodal junctions in the evolutionary tree (Hortsch and Margolis, 2003).

Two recently published articles provide evidence that the function and its molecular composition are evolutionary conserved when compared to paranodal vertebrate junctions (Genova and Fehon, 2003; Schulte et al., 2003). In these studies they identify new proteins that are required for a functional paracellular barrier in Drosophila. The findings are of great importance since it provides a better understanding of the function and structure of septate junctions as well as leading to a better understanding of axo-glial interactions in the vertebrate system.

Having junctions is crucial throughout the entire organism. Epithelial cells in particular control and maintain distinct extracellular environments. This is mainly achieved by the formation of a paracellular diffusion barrier, which is a tight seal formed between epithelial cells that regulate solute flow between adjacent cells. This seal provides a barrier to help maintain the ionic concentration across the junction and in vertebrates is commonly referred to as tight junction. They are found throughout the organism in many tissues

including intestines, kidneys and the bladder (Firth, 2002). The importance of a paracellular barrier is demonstrated in diseases that involve the blood brain barrier, in which disruption of the barrier is associated with many central nervous system diseases, including Alzheimer's and multiple sclerosis (Huber et al., 2001).

In vertebrate systems the epithelia form tight junctions to provide a barrier between the apical and the basolateral surfaces of the epithelium. Interestingly, invertebrate system achieves this function via its septate junctions, which in the Drosophila nervous system are located between two perineurial glial cells. Ultrastructurally, septate junctions are characterized by regions in the apical-lateral membranes of epithelial cells. These regions contain an electron dense material, or septa that appear in large numbers and are arranged equidistantly giving the junction a ladder like structure.

Genetic analysis of Drosophila proteins has identified several components of the septate junctions. These proteins include adhesive membrane and intracellular linker proteins, similar to those found in vertebrate paranodal junctions, therefore suggesting that they are evolutionary related. Apparently, at some evolutionary time-point after the separation of chordates from the arthropod lineage, claudin based tight junctions replaced septate junctions as the ion seals in vertebrate epithelia and the septate-like junctions became more specialized evolving into what is known today as the paranodal axo-glial junction.

The first two septate junction proteins identified were coracle (COR) and neurexin IV (NRX; Baumgartner et al., 1996; Ward et al., 1998). The coracle gene encodes for a Drosophila homologue of mammalian protein 4.1B, a cytoskeletal protein that links the paranodal junction to the cytoskeleton (chapter 3). NRX is a protein member of the neurexin family and is homologous to the vertebrate NCP1 (figure 1B). NRX binds to COR via its

conserved 4.1 binding domain, the same way NCP1 binds to 4.1b in the vertebrate system. In embryos mutants for either COR or NRX the membranes of adjacent cells maintain their uniform spacing but the septae are lost, and the embryos fail to hatch. Asides from these three proteins, septate junctions have yet two other homologous proteins to paranodal junctions: Drosophila contactin (DCN) and neuroglian (NRG) which are homologous to CN and NF155 respectively (Genova and Fehon, 2003; Faivre-Sarraliah et al., 2004). Just like paranodal junctions in which all three proteins, CN - NCP1 and NF155, form a complex in septate junctions DCN, NRX and NRG do the same (figure 1A). There is one difference and that is that NRG is not exclusively enriched in septate junctions, it is also highly expressed in other areas outside of septate junctions, suggesting that asides from being essential to septate junctions it might also be required to perform other cellular functions. A fourth cell adhesion molecule, fasciclin III (FASIII), has also been found in septate junctions but no homologue has been reported in vertebrate paranodal junctions. Although it is expressed there, it is unclear how FASIII might interact with other septate junction proteins.

Asides from COR there are other cytoskeletal proteins that are involved in the formation of septate junctions. Two of these proteins belong to the PDZ family, namely discs large (DLG) and scribble (SCB). Both these proteins are enriched in septate junctions and are suggested to be linked to the NRX complex via their PDZ domains. Their structure suggests a role as adaptor proteins and perhaps is used to bring together signaling proteins (Tepass et al. 2001; Bilder et al. 2000). There are also two more proteins found to interact in septate

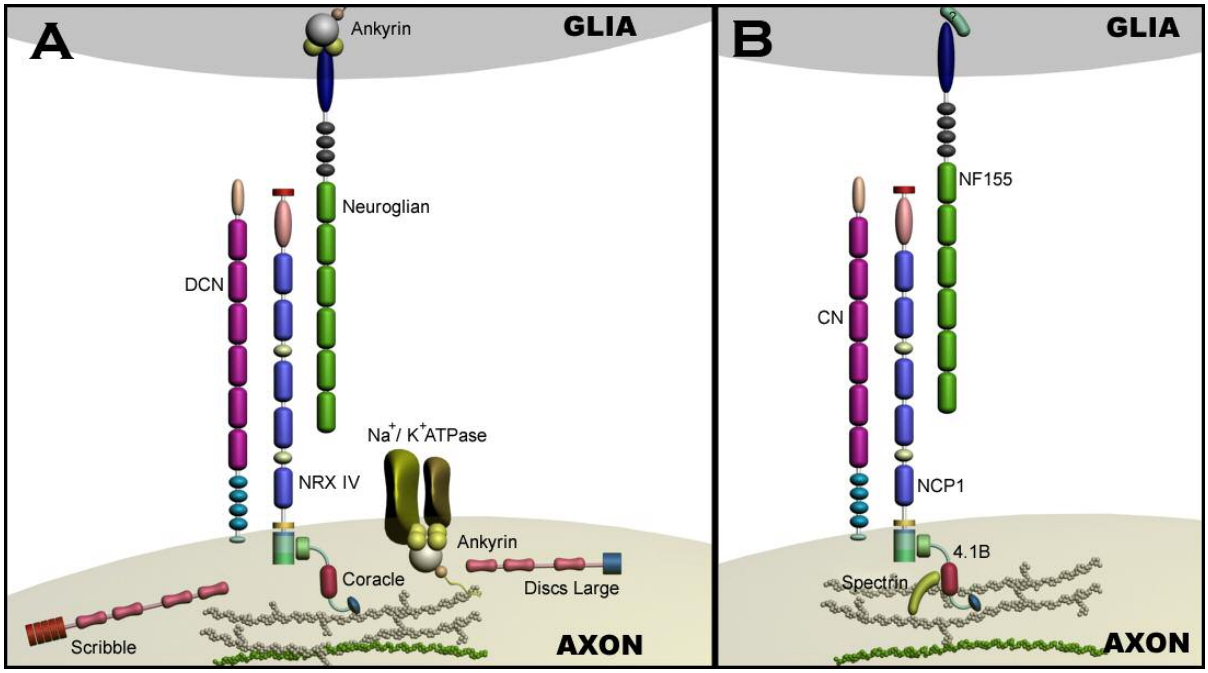

Figure 1 – Comparison between invertebrate and vertebrate axo-glial junctions a conservation throughout evolution. Schematic representation of a *Drosophila* septate junction (A) and a vertebrate paranodal junction (B).

junctions that have been coimmunoprecipitated with NRG, NRX and COR, indicating that they are part of a larger multimolecular protein complex. These proteins are two subunits of the Na^+/K^+ ATPase, the α and the β subunit, which in Drosophila it consist of two genes for the α (atpα and CG17923) and three genes for the β (*nrv1, 2 and 3).* Loss of the α or NRV2, leads to septate junction disruption (Paul et al., 2003).

Although both, the vertebrate and the invertebrate system share slight differences in their protein composition, the bulk of axo-glial junctions have been conserved. We also can't discard the possibility that these differences are only temporary. It might just be a matter of time to find each and every protein that has a role in septate/paranodal junctions.

2 - Axo-Glial Junctions throughout the Nervous System

One interesting question that many research groups focus on is: are axo-glial junctions consistent throughout the nervous system? The first reaction to this question would be yes, in the general scheme of things, axo-glial junctions are highly conserved. They are composed by NCP1 and CN which interact in cis and together with NF155, they form a trans-paranodal complex. This is true for all paranodal axo-glial junctions so far studied, but the question lies deeper, in that: are all paranodal junctions identical? Do CNS and PNS paranodal junctions share the same characteristics or there are differences between them? To answer these questions we must not look at paranodal junctions as a whole but dissect out every player out there that plays a role regulating, maintaining or forming these junctions.

First I want to briefly mention the proteins that make the bulk of axo-glial junctions that thus far have been consistent in every system in the nervous system, whether it is CNS or PNS. As mentioned earlier, NCP1 and CN are the main key players located on the axonal side at paranodal axo-glial junctions; removal of either of these proteins disrupts axo-glial junctions in both CNS and PNS. The third key player is a splice isoform of the neurofascin gene: neurofascin 155 (NF155). Until recently there little evidence of NF155's role in axo-glial junctions, since most the data presented was based on speculations. Dr. Brophy and his team have now generated a neurofascin mutant, in which both splice isoforms namely NF155 (paranodal) and NF186 (nodal) were knocked out (Sherman et al., 2005). The resulting mutant did not form neither paranodal junctions nor nodal complexes. They also transgenically expressed NF155 into the myelinating glia of the knock out mice and they were able to rescue the paranodal axo-glial complex (Sherman et al., 2005). This then corroborates the previous speculations of NF155 and its role in paranodal junctions, leaving

it clear that NF155 is as much needed as is NCP1 and CN proteins for the formation of paranodes.

These three proteins share a common feature, which is they all have an extracellular domain in which they interact with each other. This leaves then the intracellular domain to interact with remaining proteins. CN is a GPI anchor protein with no intracellular domain, thus no partner has been identified at paranodal junctions other than NCP1. Of course one may argue that the lipid microdomains or rafts associated with CN and NCP1 are interacting biological partners, but that is beyond the scope of this discussion. This leaves NCP1 and NF155, both of which contain and intracellular domain, to act as a link between the tripartite complex and the internal structures of the cell. Unfortunately, no interacting partner with NF155 has been found yet; whereas for NCP1 protein 4.1B has been identified as a paranodal cytoskeletal protein that interacts with its intracellular domain in both CNS and PNS.

Based on the data presented in chapter 3, it is evident now that two new members of the paranodal junctions have been identified in sciatic nerve fibers and Purkinje cell axons, namely actin and spectrin. Although not every myelinated tract in the nervous system was tested to see whether all six members of paranodal junctions are present, one can speculate that it would be the case based on the results observed in both CNS and PNS systems. Most differences observed in myelinated fibers whether it is paranodal junctions, nodal domains, signaling mechanisms or protein trafficking, there are usually slight changes when comparing fibers in the PNS or the CNS. Thus when looking at paranodal junctions, having all six proteins expressed in both CNS and PNS, makes it easier to make such assumptions, but remember: it is not absolute!

This brings me then to an earlier question: Are paranodal junctions identical? Take for instance Nogo A. It was recently shown that it is an oligondendroglial component which congregates and interacts with the NCP1/CN complex at paranodal junctions in the CNS and not PNS (Nie et al., 2003). Originally Nogo A together with its receptor Nogo-66 was found to form a complex with P75 neurotrophin receptor which leads to the activation of Rho (Hunt et al., 2003; Yiu and He, 2003). It is clear now that Nogo-A plays differential roles in the nervous system. What is the role of Nogo-A? Nie and others not only shown that NCP1 and Nogo-A interact with each other but they also interact with Kv potassium channels early in paranodal development, before potassium channels are localized to the Juxtaparanodal junctions (Nie et al., 2003). This then suggests that Nogo-A might play a role in modulating the axo-glial junction architecture and possible potassium channel localization.

To determine the importance of Nogo-A at paranodal axo-glial junctions it would be interesting to use Nogo-A knock-out models to see whether these junctions suffer any consequences as it shows when NCP1 is missing. It would also be interesting, and now that the models are available, to determine the Nogo-A expression in NCP1, CN and NF155 mutants. Nogo-A could potentially be a binding partner for NF155 on the glial side as is CN with NCP1.

CD9, a member of the tetraspanin family, has been shown to be at paranodal junctions (Ishibashi, et al., 2004). CD9 is concentrated in the paranode as myelination proceeds, but CD9 clusters become diffuse, associated with disruption of the paranode, in cerebroside sulfotransferase-deficient mice (CST). They also show that ablation of CD9 in mutant mice disrupt junctional attachment at the paranode and alter the paranodal components NCP1 and NF155. This then suggested that CD9 is a myelin protein important

for the formation of paranodal junctions and that plays a role in the formation of compact myelin in the PNS. In contrary to Nogo-A where it is expressed in CNS paranodal junctions, CD9 is present only in PNS nerve fibers, which then highlights once again the diversity of paranodal junctions throughout the nervous system.

Myelin and lymphocyte protein (MAL) is yet another protein that serves as an example to further stress out the fact that paranodal junctions are not one hundred percent consistent throughout the nervous system. In this case the protein is not directly involved with the paranodal junction machinery; instead it affects paranodal junctions indirectly. MAL is a tetraspan raft-associated proteolipid protein that is mainly expressed in oligodendrocytes and Schwann cells.

It was recently shown that genetic ablation of the *mal* gene resulted in paranodal abnormalities similar to those observed in CN, NCP1 and CGT mutants (Schaeren-Wiemers et al., 2004). This suggested that MAL is required for the maintenance of axon-glial interactions in the CNS and not PNS, likely by controlling the trafficking and/or sorting of NF155 and other membrane components in oligodendrocytes. This could be due to compensatory mechanisms of another yet unknown raft-associated proteolipid protein, which might replace the functional role of MAL, or known basic structural differences between myelinated PNS and CNS nerve fibers (Salzer, 2003). Regardless of the cause MAL is only required in the CNS. This example again supports the idea that microenvironments whether it is the paranodal junction itself or its surrounding areas can have a differential effect in distinct areas of the nervous system in this particular case MAL is a protein expressed in CNS (not PNS) glial cells and has a role in the maintenance of axo-glial junctions.

As a final example, paranodal junctions not only are distinct in their structural components as clearly stated with the Nogo-A protein but there could be also differences in their functions throughout the nervous system. Take for example a well studied system that is the clustering of voltage gated sodium channels. During development, Nav1.2 first appears in the predicted nodes during myelination, and Nav1.6 replaces it in the mature nodes. This switch seems to have a physiological relevance to action potential conduction in myelinated nerves. Suzuki and others examined the influence of the paranodal junction on switching of sodium channel subunits using the sulfatide-deficient mouse (Suzuki et al., 2004). CGT mutants displayed disruption of paranodal axo-glial junctions and altered nodal lengths and channel distributions. The initial switching of Nav1.2 to Nav1.6 occurred in the mutant optic nerves. However, such subtype abnormality was not observed in the sciatic nerve, where paranodal disruption was observed. Thus, the paranodal junction significantly influences the retention of Nav1.6 in the node, which is followed by disorganization of nodal structures. However, its importance may differ between the central and peripheral nervous system.

Taken all together all, it is now evident that there are subtle changes caused by critical players that have a role in establishing, maintaining and regulating axo-glial paranodal junctions. This answers our question regarding the consistency of paranodal axo-glial junctions throughout the nervous system. There are differences amongst axo-glial junctions that make them variable through out the nervous system. Perhaps one way that myelinated fibers cope with this, is through compensatory mechanisms that involve proteins yet to be discovered. It is in our major interest to find these members in order to have a better understanding of the molecular machinery that underlies axo-glial junctions.

3 - Axo-Glial Junctions and Signaling

During myelination, a myelinating cell wraps around an axon to elaborate a myelin sheath, therefore allowing the establishment of a rapid, saltatory conduction of action potentials along the axon. In PNS, myelination is achieved by Schwann cells whereas oligodendrocytes are the myelinating cells in the central nervous system (CNS). There is an active zone of communication between the myelinating glia with the underlying axon. This tight interaction implies reciprocal signaling between the oligodendrocytes (or the Schwann cells) and the axons to be myelinated.

Throughout the myelinated fiber there are distinct domains where axo-glial communication is established. These include the internode, the juxtaparanode, the paranode and the node of Ranvier. As stated in chapter I there are clear molecular complexes that are clustered in these specific regions and are in active communication with the overlying glial cell. Take for instance the internodal region. This region has no direct contact with the overlying glial cell. The space between glia and neuron is much greater than that observed at paranodes. Nevertheless, there is a very active communication between both cells, and one of these signaling cascades is responsible for the regulation of the axonal caliber of the neuron axon.

This cascade of events involves myelin associated glycoprotein (MAG). It was found to be implicated in an "outside-in" signaling cascade that mediates radial growth Garcia et al., 2003). During myelination MAG is redistributed to membrane domains juxtaposed to axonal regions timing that is consistent with the initial wave of radial growth (Trapp et al., 1989). P^{75} was recently identified as a probable receptor for MAG (Wang et al., 2002;

Yamashita et al., 2002) which occurs in association with neuronal gangliosides GT1b and GD1a (Vyas et al., 2002). Activation of the P^{75} receptor causes three type II MAGE family members to be activated which interact with p^{75}: NRAGE, necdin and MAGE-H1 (Tcherpakov et al. 2002; Salehi et al., 2000). The recruitment of the three proteins together with the P^{75} receptor forms a cytoplasmic surface that recruits signal transduction molecules including ERK1/2 which phosphorylates NF-M.

As mentioned in chapter III, neurofilaments are the major cause for establishing axonal diameter. Several lines of evidence suggest that neurofilament phosphorylation is essential for proper axonal diameter and that phosphorylation is regulated by myelinating glial cells (Yin et al., 1998). Loss of functional P^{75} receptor either through antibody inhibition or through gene deletion inhibits the accumulation of MAG and the formation of mature myelin internodes, and reduces the number of myelinated axons in adult nerves (Cosgaya et al. 2002). Here we depict a clear example of a signaling cascade that regulates a myelinating event and is a result of an interaction between the neurons and their ensheathing glial cells.

Keeping this model in mind one can look for similar models throughout the myelinated fiber. One such popular candidate, the paranodal junction, has been thought to be involved in signaling for almost a decade now. Although such signaling cascades have not been established, our group as well as others have been looking for a putative intracellular partner of NCP1.

As mentioned earlier (chapters I and V), NCP1 bears an SH3 binding domain on its cytoplasmic tail. SH3 domains have long been implicated in binding proteins that participate in signaling cascades. One such group of proteins is the Src family proteins (Pawson 1995)

which include Fyn and Lyn kinases. These two kinases have been shown to interact with contactin and have been isolated from lipid rafts (Olive et al., 1995; Umemori et al., 1999). They have also been implicated in signaling cascades involving myelin associated glycoprotein (MAG) at internodal regions (Garcia et al. 2003). It is therefore not hard to place NCP1 as a strong candidate for a signaling cascade complex.

Another interesting way to look at signaling complexes is through microdomains, that is domains within domains. We all understand that the paranodal junction is considered a domain of a myelinated fiber. But within the paranodal junctions there are microdomains, which generally involve lipid rafts, characterized by their high density of glycosphingolipids and cholesterol. The preponderance of saturated hydrocarbon chains in cell sphingolipids allows for cholesterol to be tightly intercalated giving the lipid raft a more compact characteristic as compared to the phospholipids in their surroundings which give the membrane a more liquid like property (Brown and London, 1998b). This then gives the lipid rafts a unique property that distinguishes them from the rest of the membrane components, not only for their lipid/cholesterol contents but also by their protein contents. This then generates a microenvironment within the paranodal environ with unique properties so that it constitutes its own domain.

A number of proteins have been reported to be enriched in lipid rafts, most of which are modified postranslationally at the Golgi level, where the lipid rafts assemble. These modifications which some of them include, glycosylphosphatidylinositol (GPI) anchor, palmitolation and acylation are in some cases essential and provides the protein the ability to be tightly packed into an ordered lipid environment (Brown and London, 1998a; Arni, et al. 1998; zhang, et al. 1998; Melkonian, et al. 1999; Moffett, et al. 2000).

Lipid Rafts seem to have two main functions. First they seem to act as protein carriers to target them to their proper locations and second they play a very important role in signal transduction. One way of doing this is by concentrating proteins that participate in signaling events in the lipid microenvironment. This allows them to interact with specific proteins within the lipid raft and excludes them from proteins and lipids in their surroundings (Brown and London, 1998a).

The importance of rafts for the assembly of signaling platforms during oligodendrocytes differentiation has been also demonstrated previously for the interaction of integrins with the PDGFa receptor, the activation of fyn kinase by interaction with N-CAM120 and CN and the segregation of NgR (Baron et al., 2003; Kramer et al., 1999; Vyas et al. 2001; Yu et al., 2004),

Except for Nogo-A, and perhaps contactin, paranodal proteins have not been involved in signaling cascades. Despite this, they have been implicated in lipid raft assemblies, including NF155, CN, and NCP1 (Maier, et al. 2005; Popko, 2000; Olive, et al. 1995; Simons, et al. 1997; Schaeren-Wiemers, et al. 2004; Schafer, et al. 2004; Kramer, et al. 1999). Maier, et al. has recently shown that the association of NF155 to lipid rafts is required for its proper partitioning in the formation of paranodal junctions (Maier, et al. 2005)**.** To confirm this even further, NF155 is absent from paranodal loops, and fail to fractionate in lipid fractions CGT -/- mice indicating that indeed raft assembly might be essential for NF155 to localize properly at paranodal junctions (Menon, et al. 2003; Schafer, et al. 2004). It is tempting to speculate that NF155 becomes part of such signaling platforms during oligodendrocyte development. Thus, raft association of NF155 may be important for its interaction with other proteins. On the same line of experiments, NCP1, Contactin (CN), and

Ncam 120, were also isolated in low density fractions as well (Kramer, et al. 1997; Schaeren-Wiemers, et al. 2004).

Taken together the information presented here, NCP1 protein and perhaps also NF155, seem to be two key candidates able to participate either directly or indirectly in signaling mechanisms.

4 – Axo-glial Junctions and Neuropathies

There is increasing evidence suggesting that disturbances of the axonal domain organization and function are an important source of neurological disorders (see Poliak and Peles, 2003 for review). Disorders can arise from mislocalized channels, improper domain formation, defects of the axonal cytoarchitecture or from a miscommunication between the axon and the overlaying glial cell (Bhat et al., 2001; Boyle et al., 2001; Boiko et al., 2001; Boiko et al., 2003; Tait et al., 2000; Rasband et al., 1999a-b; Rasband et al., 2003; Lambert et al., 1997; Ishibashi et al., 2002; Ishibashi et al., 2003; Dupree et al., 1998, Dupree et al., 1999; Poliak et al., 2001; Poliak et al., 2003; Rosenbluth et al., 2003; Traka et al., 2002; Gollan et al., 2002; Rios et al., 2003; Honke et al., 2003; Mathis et al., 2001; Vabnick and Shrager 1998). Although communication between neuron and glial cells is essential, loss of myelin does not have an immediate detrimental effect as observed in some demyelinating diseases (Mathis et al, 2001; Vabnick and Shrager 1998). Several mutant mice form normal myelin during development, as time goes by, axo-glial communication is truncated resulting in the death of the axon. Some of these mutants include MAG, PLP, CGT, and NCP1 (Yin et al., 1998; Griffiths et al. 1998; Dupree et al., 1998; Garcia-Fresco et al., 2005).

Amongst the most common axonopathies is multiple sclerosis (MS). It was discovered over one hundred years ago (1868) by Dr. Charcot. Although considered an autoimmune disease, MS is now beginning to fall into the field of axo-glial neuropathies (Arroyo et al., 2002; Mathis et al., 2001; Wolswijk and Balesar 2003). Evidence for this came from studies of MS patient's myelinated fibers. MS axons have aberrant Na^+ channel isoform switching as seen in *NCP1* mutant mice and paranodal markers are lost earlier than nodal markers following demyelination (Rios et al., 2003; Kearney et al., 2002; Arroyo et al., 2002; Mathis et al., 2001; Wolswijk and Balesar 2003). These results suggest that paranodes can be a potential target for pathogenic mechanisms that lead to dispersion of the node and paranodal markers.

Another feature of MS nerve fibers is the abnormalities observed in the phosphorylation of neurofilaments (Trapp et al., 1998). Neurofilaments, the intermediate filaments of axons, are a major component of the axonal cytoskeleton. One of the main functions of neurofilaments is to control axonal caliber, which is crucial since the speed of conductivity of an impulse down the axon is proportional to the axonal caliber. Tampering with the neurofilament network has been shown to cause deficits in axonal transport and caliber of myelinated fibers, leading to axonal accumulations (axonal swellings) and degeneration (Griffiths et al., 1998; Popko 2003). Axonal swellings have been shown in a number of myelin deficient mice such as *CGT*, *CST*, *CN*, *Jimpy*, and *PLP* (Jenkins et al., 2002; Griffiths et al., 1998; Boyle et al., 2001; Dupree et al., 1998; Honke et al., 2002).

The precise mechanism of how neurofilaments accumulate is not known, one possibility arises from the work on NCP1 mutant mice (chapter III) which suggest that a disrupted axonal cytoskeleton affects the axonal transport leading to neurofilament

accumulation. Interestingly a disruption of axonal neurofilaments is an early pathological feature seen in many diseases including amyotropic lateral sclerosis, multiple sclerosis, Charcot Marie tooth disease, and Parkinson's disease. This then suggest that neurofilaments are an important requirement of the neuronal cytoskeleton, since they interact with other elements in their surroundings that are involved in transport and cytoarchitecture integrity.

Remyelination is a potential treatment for demyelinating diseases such as MS. This process requires new axo-glial interactions to be formed by differentiating oligodendrocytic cell (Maier et al., 2005). NF155, a glial paranodal marker, is important for the establishment of paranodal junctions. It has been previously shown that NF155 is recruited to paranodal junctions via lipid rafts (Schafer et al.. 2004; Maier et al., 2005), which are required for glial cell development and hence myelination. This was corroborated in CGT mutant mice where action potentials along the axon as well as paranodal junctions are perturbed (Dupree et al., 1998; Ishibashi et al., 2002). Intriguingly, NF155, which is normally highly enriched in paranodal myelin fractions, is completely absent from paranodes of CGT mutant mice, indicating that raft assembly might be critical for its accumulation in paranodes (Menon et al., 2003).

NF155 could then play a potential role in myelination. Using a mouse model for MS, namely the experimental allergic encephalomyelinitis (EAE) mice, Maier and others showed that although the expression of NF155 was not altered, it was greatly enhanced in lesion sites. The results suggest that the association of NF155 to microdomains in the oligodendrocyte membrane is required for its participation in intermolecular interactions, which are important for myelination and/or myelin integrity.

This then concludes my four years of work as a graduate student. Hopefully I have clearly emphasized the importance of axo-glial interactions and how their integrity is dependent on the survival of neuronal cells. These junctions are critical and having deficiencies leads to several well known axonal neuropathies. If we look back in the last five years, a tremendous effort has been made to advance the field of paranodal/septate junctions. I am confident that our knowledge and understanding of the mechanisms involved in axo-glial junctions will continue to grow and will hopefully will help us develop better methods for treating diseases such as MS, CMT or ALS.

REFERENCES

Adlkofer K., Martini R., Aguzzi A., Zielasek J., Toyka K., Suter U. 1995. Hypermyelination and demyelinating peripheral neuropathy in Pmp22-deficient mice. *Nature Genetics.* **11:** 274-280.

Alberts B., Bray D., Lewis J., Raff M., Roberts K., and Watson J. (1994). "Molecular Biology of the Cell". Garland Publishing, New York and London.

Altevogt, B., Kleopa, K., Postma, F., Scherer, S., and Paiul, D. (2002). Connexin29 is uniquely distributed within myelinated glial cells of the central and peripheral nervous systems. *J. of Neuroscience.* **22:** 6458- 6470.

Altman, J., and Bayer, S. A. (1997). Development of the Cerebellar System: in relation to its evolution, structure and functions (CRC Press, Inc.).

Andres, K, (1965). Über die Feinstruktur besonderer Einrichtungen in markhaltigen Nervenfasern des Kleinhirns der Ratte. *Z. Zellforsch. Mikrosk. Anat.* **65**: 701–712.

Arbuthnott E., Boyd I., and Kalu K. 1980. Ultrastructural dimensions of myelinated peripheral nerve fibers in the cat and their relation to conduction velocity. *Journal of Physiology***. 308:** 125-157.

Arni, S., Keilbaugh, S., Ostermeyer, A., and Brown, D. (1998). Association of GAP-43 with detergent-resistant membranes requires two palmitolated cysteine residues. *J. of Biological Chemistry.* **273:** 28478-28495.

Arroyo, E., Xu, Y., Zhou, L., Messing, A., Peles, E., Chiu, S., and Scherer, S. (1999). Myelinating Schwann cells determine the internodal localization of Kv1.1, Kv1.2, Kvbeta2, and Caspr. *J. of Neurocytology.* **28:**333- 347.

Arroyo, E., Xu, T., Grinspan, J. Lambert, S. Levinson, S. Brophy, P., Peles, E. and Scherer, S. (2002). Genetic dysmyelination alters the molecular architecture of the nodal region. *J. of Neuroscience*. **22:** 1726-1737**.**

Baba, H., Akita, H., Ishibashi, T., Inoue, Y., Nakahira, K., and Ikenaka, K. (1999). Completion of myelin compaction, but not the attachment of oligodendroglial processes triggers K(+) channel clustering. *J. of Neuroscience Research.* **58:** 752-764.

Balcar V. (2002). Molecular pharmacology of the Na+-dependent transport of acidic amino acids in the mammalian central nervous system. *Biological Pharmaceutical Bulletin*. **25**: 291–301.

Baumgartner, S., Littleton, J., Broadie, K., Bhat, M., Harbecke, R., Lengyel, J., Chiquet-Ehrismann, R., Prokop, A. and Bellen, H., (1996). A Drosophila neurexin is required for septate junction and blood-nerve barrier formation and function. *Cell* **87**: 1059–1068.

Bellen, H., Lu, Y., Beckstead, R. and Bhat, M., (1998). Neurexin IV, caspr and paranodin—novel members of the neurexin family: encounters of axons and glia. *Trends Neuroscience.* **21**: 444–449.

Bennett, V. and Lambert, S., (1999). Physiological roles of axonal ankyrins in survival of premyelinated axons and localization of voltage-gated sodium channels. *J. Neurocytol.* **28**: 303–318.

Berghs, S., Ferracci, F., Maksimove, E., Gleason, S., Butler, M., De Camilli, P., and Solimena, M. (2000). BetaIV spectrin, a new spectrin localized at the axon initial segments and nodes of Ranvier in the central and peripheral system. *J. of Cell Biology.* **151:** 985-1002.

Berglund, E., Murai, K., Fredette, B., Sekerkova, G., Marturano, B., Weber, L., Mugnaini, E. and Ranscht, B., (1999). Ataxia and abnormal cerebellar microorganization in mice with ablated contactin gene expression. *Neuron* **24**: 739–750.

Bergmann, W. and Lindner, E., (1964). Über den Feinbau des Nebennierenmarkes des Igels (*Erinaceus europaeus L*). *Z. Zellforsch. Mikrosk. Anat.* **64**: 868–912.

Bhat, M., Philp, A., Glover, D. and Bellen, H., (1996). Chromatid segregation at anaphase requires the *barren* product, a novel chromosome-associated protein that interacts with topoisomerase II. *Cell* **87**: 1103–1114.

Bhat, M. A. (2003a). Molecular organization of axo-glial junctions. *Current Opinion in Neurobiology*. **13**: 552-559.

Bhat, M. A. (2003b). Myelin Biology and Disorders. In, R. A. Lazzarini, ed. (Elsevier Academic Press).

Bhat, M., Izaddoost, S., Lu, Y., Cho, K., Choi, K. and Bellen, H., (1999). Discs Lost, a novel multi-PDZ domain protein, establishes and maintains epithelial polarity. *Cell* **96**: 833–845.

Bhat, M., Rios, J., Lu, Y., Garcia-Fresco, G., Ching, W., St Martin, M., Li, J., Einheber, S., Chesler, M., Rosenbluth, J., Salzer, J., and Bellen, H. (2001). Axon-glia interactions and the domain organization of myelinated axons requires neurexin IV/Caspr/Paranodin. *Neuron.* **30:** 369-383.

Bjartmar, C., Karlsson, B., and Hildebrand, C. (1994). Cellular and extracellular components at nodes of Ranvier in rat white matter. *Brain Research.* **667:** 111-114.

Bjartmar, C., Wujek, J., and Trapp, B. (2003). Axonal loss in the pathology of MS consequences for understanding the progressive phase of the disease. *Journal of Neuroscience*. **206**: 165-171.

Black, J., and Waxman, S. (1988). The perinodal astrocyte. *Glia.* **1:** 169-183.

Blakemore W. (1969). Schmidt-Lantermann incisures in the central nervous system. *Journal of Ultrastructure Research.* **29:**496 -498.

Boiko, T., Rasband, M., Levinson, S., Caldwell, J., Mandel, G., Trimmer, J., and Mathews, G. (2001). Compact myelin dictates the differential targeting of two sodium channel isoforms in the same axon. *Neuron.* **30:**91 -104.

Boiko, T., Van Wart, A., Caldwell, J., Levinson, S., Trimmer, J., and Matthews, G. (2003). Functional specialization of the axon initial segment by isoform-specific sodium channel targeting. *J of Neuroscience.* **23:**2306- 2313.

Bosio, A., Binczek, E. and Stoffel, W. (1996). Functional breakdown of the lipid bilayer of the myelin membrane in central and peripheral nervous system by disrupted galactocerebrosides synthesis. *Proc. Natural Academy of Science.* **93:** 13280-13285.

Bosio, A., Bussow, H., Adam, J. and Stoffel, W., (1998). Galactosphingolipids and axon-glial interaction in myelin of the central nervous system. *Cell Tissue Res.* **292**: 199–210.

Boyle, M., Berglund, E., Murai, K., Weber, L., Peles, E., and Ranscht, B. (2001). Contactin orchestrates assembly of the septate-like junctions at the paranode in myelinated peripheral nerve. (2001). *Neuron*. **30:** 385-397.

Bretscher, A., Edwards, K., and Fehon, R. (2002). ERM proteins and merlin: integrators at the cell cortex. *Nature Review of Molecular Cell Biology.* **3:** 586-599.

Brown, D., and London, E. (1998). Functions of lipid rafts in biological membranes. *Annual Review of Cell and Developmental Biology.* **14:** 111-136.

Brown, D., and London, E. (1998). Structure and origin of ordered lipid domains in biological membranes. *J. of Membrane Biology.* **164:** 103-114.

Brownlees, J., Ackerley, S., Grierson, A., Jacobsen, N., Shea, K., Anderton, B., Leigh, P., Shaw, C., and Miller, C. (2002). Charcot-Marie-Tooth disease neurofilament mutations disrupt neurofilament assembly and axonal transport. *Human Molecular Genetics*. **11**: 2837-2844.

Bunge, M.; Bunge R. and Pappas, G. (1962). Electron microscopic demonstration of connections between glia and myelin sheaths in the developing mammalian nervous system.. *Journal of Cell Biology.* **12:**448 -453.

Bunge, R., Bunge, M. and Bates, M., (1989). Movements of the Schwann cell nucleus implicate progression of the inner (axon-related) Schwann cell process during myelination. *J. Cell Biol.* **109**: 273–284.

Butt, A., Kiff, J., Hubbard, P., and Berry, M. 2002. Synantocytes: new functions for novel NG2 expressing glia. *J. Neurocytology.* **31:** 551-565.

Cajal, R. y (1888a). Nota sobre la estructura de los tubos nerviosos del lobulo cerebral electrico del torpedo. *Revista Trimestral de Histologia Normal y Patologia*. **1:** 49-55.

Cajal, R. y (1888b). Estructura de los centros nerviosos de las aves. *Revista Trimestral de Histologia Normal y Patologia*. **1:** 1-10.

Cajal, R. y (1889a). Contribucion al studio de la estructura de la medulla espinal. *Revista Trimestral de Histologia Normal y Patologia*. **1:** 1-79.

Cajal, R. y (1889b). Sobre las fibras nerviosas de la capa granulose del cerebelo. *Revista Trimestral de Histologia Normal y Patologia*. **1:** 107-118.

Cajal, R. y (1920a). Algunas consideraciones sobre la *mesoglia* de Robertson y Rio Hortega. *Trabajo de Laboratori de Investigacion Biologica.* **18:** 109-127.

Cajal, R. y (1920b). Una modificacion del metodo de Bielschowsky para la impregnacion de la neuroglia comun y mesoglia y algunos consejos acerca de la tecnica del oro-sublimado. *Trabajo de Laboratori de Investigacion Biologica.* **18:** 129-141.

Caldwell, J., Schaller, K., Lasher, R., Peles, E., and Levinson, S. (2000). Sodium channel Nav1.6 is localized at nodes of Ranvier, dendrites, and synapses. *Proc. Natural Academy of Sciences.* **97:** 5616-5620.

Carey D., Eldridge C., Cornbrooks C., Timpl R., and Bunge R. 1983. Biosynthesis of type IV collagen by cultured rat Schwann cells. *Journal of Cell Biology.* **97:** 473-479.

Catterall, W. (2000). From ionic currents to molecular mechanisms: the structure and function of voltage gated sodium channels. *Neuron.* **26:** 13-25.

Charles, P., Tait, S., Faivre-Sarrailh, C., Barbin, G., Gunn-Moore, F., Denisenko- Nehrbass, N., Guennoc, A., Girault, J., Brophy, P., and Lubetzki, C. (2002). Neurofascin is a glial receptor for the paranodin/Caspr-contactin axonal complex at the axoglial junction. *Current Biology.* **12:**217- 220.

Ching, W., Zanazzi, G., Levinson, S., and Salzer, J. (1999). Clustering of neuronal sodium channels requires contact with myelinating Schwann cells. *J. of Neurocytology.* **28:** 295-301.

Cleveland, D. (1996). Neuronal growth and death: order and disorder in the axoplasm. *Cell* **84**: 663-666.

Coetzee, T., Dupree, J., and Popko, B. (1998). Demyelination and alteredexpression of myelin-associated glycoprotein isoforms in the central nervous system of galactolipid-deficient mice. *J. of Neuroscience.* **54:** 613-622.

Coetzee, T., Fujita, N., Dupree, J., Shi, R., Blight, A., Suzuki, K., Suzuki, K., and Popko, B. (1996). Myelination in the absence of galactocerebroside and sulfatide: normal structure with abnormal function and regional instability. *Cel.l* ***86*****:** 209-219.

Collard, J., Cote, F., and Julien, J. (1995). Defective axonal transport in a transgenic mouse model of amyotrophic lateral sclerosis. *Nature.* **375**: 61-64.

Collinson, J., Marshall, D., Gillespie, C. and Brophy, P., (1998). Transient expression of neurofascin by oligodendrocytes at the onset of myelinogenesis: implications for mechanisms of axon-glial interaction. *Glia* **23**: 11–23.

Cosgaya J., Chan J., and Shooter E. (2002). The neurotrophin receptor p75NTR as a positive modulator of myelination. *Science.* **298:** 1245-1248.

Davis, J.Q., Lambert, S. and Bennett, V., (1996). Molecular composition of the node of Ranvier: identification of ankyrin-binding cell adhesion molecules neurofascin (mucin+/third FNIII domain-) and NrCAM at nodal axon segments. *J. Cell Biol.* **135**: 1355–1367.

Denisenko-Nehrbass, N., Oguieveskaia, K., Goutebroze, L., Galvez, T., Yamakawa, H., Ohara, O., Carnaud, M., and Girault, J. (2003). Protein 4.1B associates with both caspr/paranodin and caspr2 at paranodes and juxtaparanodes of myelinated fibers. *European J. of Neuroscience.* **17:** 411-416.

de Waegh S., Lee V., and Brady ST. 1992. Local modulation of neurofilament phosphorylation, axonal caliber, and slow axonal transport by myelinating Schwann cells. *Cell*. **68:** 451-463.

Devaux, J., Kleopa, K., Cooper, E., Bennett, V., and Scherer, S. (2003). Anatomical and physiological evidence of KNCQ2 subunits at PNS and CNS nodes. *Neuroscience.* **28:** 368.

Devaux, J., Alcaraz, G., Grinspan, J., Bennett, V., Joho, R., Crest, M., and Scherer, S. (2003). Kv1.3b is a novel component of CNS nodes. *J. of Neuroscience.* **23:** 4509-4518.

Dieters, O. (1865). "Unterschungen Uber Gehirn und Ruckenmark des Menschen und der Saugethiere". (M. Schultze, ed.) Vieweg, Braunschweig, pp. 318.

Dingledine R., Borges K., Bowie D., and Traynelis S. (1999). The glutamate receptor ion channels. *Pharmacological Reviews.* **51:**7 – 61.

Duncan I., Hammang J., and Trapp B. 1987. Abnormal compact myelin in the myelin-deficient rat: absence of proteolipid protein correlates with a defect in the intraperiod line. *Procedures Nat. Academy of Sciences.* **84:** 6287-6291.

Dupree, J., Coetzee, T., Blight, A., Suzuki, K., and Popko, B. (1998). Myelin galactolipids are essential for proper node of Ranvier formation in the CNS. *J. of Neuroscience.* **18:** 1642-1649.

Dupree, J., Coetzee, T., Suzuki, K., and Popko, B. (1998). Myelin abnormalities in mice deficient in galactocerebroside and sulfatide. *Journal of Neurocytology*. **27**: 649-659.

Dupree, J., Girault, J., and Popko, B. (1999). Axo-glial interactions regulate the localization of axonal paranodal proteins. *J. Cell Biology.* **147:** 1145-1152.

Dupree, J. and Popko, B., (1999). Genetic dissection of myelin galactolipid function. *J. Neurocytol.* **28**: 271–279.

Einheber, S., Zanazzi, G., Ching, W., Scherer, S., Milner, T., Peles, E., and Salzer, J. (1997). The axonal membrane protein Caspr, a homologue of neurexin IV, is a component of the septate-like paranodal junctions that assemble during myelination. *J. Cell Biology.* **139:** 1495-1506.

Elder G., Friedrich V Jr., Bosco P., Kang C., Gourov A., Tu P., Lee V., and Lazzarini R. (1998). Absence of the mid-sized neurofilament subunit decreases axonal calibers, levels of light neurofilament (NF-L), and neurofilament content. *Journal of Cell Biology.* **141:** 727-739.

Elder G., Friedrich V Jr, Chu K., and Lazzarini R. 2001. Schwann cells and oligodendrocytes read distinct signals in establishing myelin sheath thickness. *Journal of Neuroscience Research.* **65:**493 -499.

Faivre-Sarrailh, C. and Rougon, G., (1997). Axonal molecules of the immunoglobulin superfamily bearing a GPI anchor: their role in controlling neurite outgrowth. *Mol. Cell. Neurosci.* **9**: 109–115.

Faivre-Sarrailh, C., Gauthier, F., Denisenko-Nehrbass, N., Le Bivic, A., Rougon, G., and Girault, J. (2000). The glycosylphosphatidyl inositol-anchored adhesion molecule F3/contactin is required for surface transport of paranodin/contactin-associated protein (caspr). *J. of Cell Biology.* **149:** 491-502.

Faivre-Sarrailh, C., Banerjee, S., Li, J., Hortsch, M., Laval, M., and Bhat, M. (2004). Drosophila contactin, a homolog of vertebrate contactin, is required for septate junction organization and paracellular barrier function. *Development.* **131**: 4931-4942.

Fanarraga M., Griffiths I., Zhao M., and Duncan I. 1998. Oligodendrocytes are not inherently programmed to myelinate a specific size of axon. *Journal of Comparative Neurology.* **399:** 94-100.

Ferreirinha, F., Quattrini, A., Pirozzi, M., Valsecchi, V., Dina, G., Broccoli, V., Auricchio, A., Piemonte, F., Tozzi, G., Gaeta, L., (2004). Axonal degeneration in paraplegin-deficient

mice is associated with abnormal mitochondria and impairment of axonal transport. *Journal of Clinical Investigations*. **113**: 231-242.

Fjell, J., Hjelmstrom, P., Hormuzdiar, W., Melenkovic, M., Agleico, F., Tyrell, L., Waxman, S., and Black, J. (2000). Localization of the tetrodotoxin-resistant sodium channel NaN in nocireceptors. *Neuroreports.* **11:**199- 202.

Garcia, M., Lobsiger, C., Shah,, S., Deerinck, T., Crum, J., Young, D., Ward, C., Crawford, T., Gotow, T., Uchiyama, Y., Ellisman, M., Clcutt, N., and Cleveland, D. (2003). NF-M is an essential target for the myelin-directed "outside-in" signaling cascade that mediates radial axonal growth. *J. Cell Biology.* **163:** 1011-1020.

Garcia-Fresco, G., Sousa, A., Pillai, A., Moy, S., Crawley, J., Tessarollo, L., Dupree, J., and Bhat, M. 2005. Disruption of axo-glial junctions causes cytoskeletal disorganization and degeneration of Purkinje neuron axons. *PNAS.* Submitted December 2005.

Garver, T., Ren, Q., Tuvia, S. and Bennett, V. (1997). Tyrosine phosphorylation at a site highly conserved in the L1 family of cell adhesion molecules abolishes ankryn binding and increases lateral mobility of neurofascin. *J. Cell Biology.* **137:** 703-714.

Gatto, C., Walker, B., and Lambert, S. (2003). Local ERM activation and dynamic growth cones at Schwann cell tips implicated in efficient formation of nodes of Ranvier. *J. Cell Biology.* **162:** 489-498.

Gennarelli, T., Tipperman, R., Maxwell, W., Graham, D., Adams, J., and Irvine, A. (1993). Traumatic damage to the nodal axolemma: an early, secondary injury. *Acta Neurochir. Suppl*. (Wien). **57**: 49-52.

Genova, J., Fehon, G. 2003. Neuroglian, Gliotactin, and the Na+/K+ ATPase are essential for septate junction function in Drosophila. *Journal of Cell Biology.* **161:** 979-989.

Giese K. Martini R. Lemke G. Soriano P. and Schachner M. 1992. Mouse P0 gene disruption leads to hypomyelination, abnormal expression of recognition molecules, and degeneration of myelin and axons. *Cell*. **61:**565 -576.

Guipponi M., Scott S., Hattori M., Ishii K., Sakaki Y., and Antonarakis S. (1998). Genomic structure, sequence, and refined mapping of the human intersectin gene (ITSN), which encompasses 250 kb on chromosome 21q22.1-->q22.2. *Cytogenet Cell Genetics*. **83:** 218-20

Geren, B. (1954). The formation from the Schwann cell surface of myelin in the peripheral nerves of chick embryos. *Expreimental Cell Research.* **7:** 558-562.

Goldin, A., Barchi, R., Caldwell, J., Hofmann, F., Howe, J., Hunter, J., Kallen, R., Mandel, G., Meisler, M., Netter, Y., Noda, M., Tankun, M., Waxman, S., Wood, J., and Catterall, W. (2000). Nomenclature of voltage gated sodium channels. *Neuron.* **28:**365- 368.

Goldin, A. (2001). Resurgence of sodium channel research. *Annual Review of Physiology.* **63:**871 -894.

Gollan, L., Sabanay, H., Poliak, S., Berglund, E., Ranscht, B., and Peles, E. (2002). Retention of a cell adhesion complex at the paranodal junction requires the cytoplasmic region of Caspr. *J. Cell Biology.* **157:** 1247-1256.

Gollan, L., Salomon, D., Salzer, J., and Peles, E. (2003). Caspr regulates the processing of contactin and inhibits its binding to neurofascin. *Journal of Cell Biology.* **163:** 1213-1218.

Greenberg S. (2001). DNA microarray gene expression analysis technology and its application to neurological disorders. *Neurology.* **57**:755–761.

Greenfield S., Brostoff S., Eylar E., and Morell P. (1973). Protein composition of myelin of the peripheral nervous system. *Journal of Neurochemistry.* **20:** 1207-1216.

Griffiths I,, Klugmann M,, Anderson T,, Yool D,, Thomson C,, Schwab M,, Schneider A,, Zimmermann F,, McCulloch M,, Nadon N,, and Nave K. (1998). Axonal swellings and degeneration in mice lacking the major proteolipid of myelin. *Science*. **280:** 1610-1613.

Hirokawa, N., Cheney, R., and Willard, M. (1983). Location of a protein of the fodrinspectrin-TW260/240 family in the mouse intestinal brush border. *Cell.* **32**: 953-965.

Hsieh S., Kidd G., Crawford T., Xu Z., Lin W., Trapp B., Cleveland D., and Griffin J. (1994). Regional modulation of neurofilament organization by myelination in normal axons. *Journal of Neuroscience*. **14:**6392 -6401.

Hoffman P., Cleveland D., Griffin J., Landes P., Cowan N., and Price D. (1987). Neurofilament gene expression: a major determinant of axonal caliber. *Pocedures Natl Academy of Sciences.* **84:** 3472-3476.

Honke, K., Hirahara, Y., Dupree, J., Suzuki, K., Popko, B., Fukushima, K., Fukushima, J., Nagasawa, T., Yoshida, N., Wada, Y., and Taniguchi, N. (2002). Paranodal junction formation and spermatogenesis require sulfoglycolipids. *Proc. Natural Acedemy of Sciences.* **99:**4227 -4232.

Hunt D., Coffin R., and Anderson P. (2003). The Nogo receptor, its ligands and axonal regeneration in the spinal cord; a review. *Journal of Neurocytology*. **31:** 93–120.

Ichimura, T. and Ellisman, M. (1991). Three-dimensional fine structure of cytoskeletal-membrane interactions at nodes of Ranvier. *Journal of Neurocytology.* **20:** 667-681.

Ishibashi T., Dupree, J., Ikenaka, K., Hirahara, Y., Honke, K., Peles, E., Popko, B., Suzuki, K., Nishino, H., and Baba, H. (2002). A myelin galactolipid, sulfatide, is essential for maintenance of ion channels on myelinated axon but not essential for initial cluster formation. *J. of Neuroscience.* **22:** 6507-6514.

Ishibashi, T., Ikenaka, K., Shimizu, T., Kagawa, T., and Baba, H. (2003). Initiation of sodium channel clustering at the node of Ranvier in the mouse optic nerve. *Neurochemical Research.* **28:**117 -125.

Ishibashi T., Ding L., Ikenaka K., Inoue Y., Miyado K., Mekada E., Baba H. (2004). Tetraspanin protein CD9 is a novel paranodal component regulating paranodal junctional formation. *Journal of Neuroscience*. **24:** 96-102.

Ito M. (1984). The Cerebellum and Neural Control, Raven Press, New York, 1984, 580

Ito M. (1987). Signal processing in cerebellar Purkinje cells, Physiol. Bohemoslov. **36**: 203–216.

Jacomy H., Zhu Q., Couillard-Despres S., Beaulieu J., and Julien J. (1999). Disruption of type IV intermediate filament network in mice lacking the neurofilament medium and heavy subunits. *Journal of Neurochemistry.* **73:** 972-984.

Kaplan, M., Cho, M., Ullian, E., Isom, L., Levinson, S., and Barres, B. (2001). Differential control of clustering of the sodium channels Na(v) 1.2 and Na(v) 1.6 at developing CNS nodes of Ranvier. *Neuron*. **30:**105 -119.

Jenkins, S., and Bennett, V. (2002). Developing nodes of Ranvier are defined by ankryn-G clustering and are independent of paranodal axoglial adhesions. *Prec. Natural Academy of Science.* **99:** 2303-2308.

Jin K., Mao X., Eshoo M., Nagayama T., Minami M., Simon R., and Greenberg D. (2001). Microarray analysis of hippocampal gene expression in global cerebral ischemia. *Annals of Neurology.* **50**:93–103.

Kazarinova-Noyes, K., Malhotra, J., McEdwen, D., Mattei, L., Berglund, E., Ranscht, B., Levinson, S., Schachner, M., Shrager, P., and Xiao, Z. (2001). Contactin associates with Na+ channels and increases their functional expression. *J. of Neuroscience.* **21:** 7517-7525.

Kearney, J., Buchner, D., De Haan, G., Adamska, M., Levin, S., Furay, A., Albin, R., Jones, J., Montal, M., and Stevens, M. (2002). Molecular and pathological effects of a modifier gene on deficiency of the sodium channel Scn8a (Na9V)1.6). *Human Molecular Genetics.* **11:**2765 -2775.

Kelm, S., Pelz, A., Schauer, R., Filbin, M., Tang, S., de Bellard, M., Schnaar, R., Mahoney, J., Hartnell, A., Bradfield, P., and Crocker, P. (1994). Sialoadhesin, myelin-associated glycoprotein and CD22 define a new family of sialic acid-dependent adhesion molecules of the immunoglobulin superfamily. *Current Biology.* **4:** 965-972.

Klugmann, M., Schwab, M., Puhlhofer, A., Schneider, A., Zimmermann, F., Griffiths, I. R., and Nave, K. A. (1997). Assembly of CNS myelin in the absence of proteolipid

protein. *Neuron*. **18**: 59-70.

Koch, T., Brugger, T., Bach, A., Gennarini, G. and Trotter, J., (1997). Expression of the immunoglobulin superfamily cell adhesion molecule F3 by oligodendrocyte-lineage cells. *Glia* **19**: 199–212.

Kordeli, E., Lambert, S., and Bennett, V. (1995). AnkrynG. A new ankyrin gene with neural-specific isoforms localized at the axonal initial segment and node of Ranvier. *J. of Biological Chemistry.* **270:** 2352-2359.

Kramer E., Klein C., Koch T., Boytinck M., and Trotter J. (1999). Compartmentation of Fyn kinase with glycosylphosphatidylinositol-anchored molecules in oligodendrocytes facilitates kinase activation during myelination. *Journal of Biological Chemistry*. **274:** 29042-29049.

Lambert, S., Davis, J., Bennett, V. (1997). Morphogenesis of the node of Ranvier; co-clusters of ankyrin and ankyrin-binding internal proteins define early developmental intermediates. *J. of Neuroscience.* **17:** 7025-7036.

Landis S. (1975). Histochemical demonstration of mitochondrial dehydrogenases in developing normal and nervous mutant mouse Purkinje cells. *Journal Histochemistry Cytochemistry.* **23**: 136– 143.

Lappe-Siefke, C., Goebbels, S., Gravel, M., Nicksch, E., Lee, J., Braun, P., Griffiths, I., and Nave, K. (2003). Disruption of Cnp1 uncouples oligodendroglial functions in axonal support and myelination. *Nature Genetics*. **33:** 366-374.

Lazzarini R., Griffin J., Lassman H., Nave K., Miller R., and Trapp B. (2004). "Myelin Biology and Disorders". Elsevier Academic Press.

Lees M. and Brostoff S. 1984. Proteins of myelin. *In* "Myelin", pp 197-224. Plenum Press, New York.

Lemaillet, G., Walker, B., and Lambert, S. (2003). Identification of a conserved ankyrin-bindin motif in the family of sodium channels α-subunits. *J. of Biological Chemistry.* **278:** 27333-27339.

Li, X., Lynn, B., Olson, C., Meier, C., Davidson, K., Yasumura, T., Rash, J., and Nagy, J. (2002). Connexin29 expression, immunocytochemistry and freeze-fracture replica immunogold labelling (FRIL) in sciatic nerve. *Euripean J. of Neuroscience.* **16:** 795-806.

Lu A., Tang Y., Ran R., Clark J., Aronow B., and Sharp F. (2003). Genomics of the periinfarction cortex after focal cerebral ischemia. *Journal of Cerebral Blood Flow Metabolism.* **23**:786–810.

Maier, O., van der Heide, T., van Dam, A., Baron, W., de Vries, H., and Hoekstra, D. (2005). Alteration of the extracellular matrix interferes with raft association of neurofascin in

oligodendrocytes. Potential significance for multiple sclerosis? *Molecular Cell Neuroscience.* **28:**390 -401.

Malhotra, J., Kazen-Gillepsie, K., Hortsch, M., and Isom, L. (2000). Sodium channel β subunits mediate homophilic cell adhesion and recruit ankyrin to points of cell-cell contact. *J. of Biological Chemistry.* **275:** 11383-11388.

Malhotra, J., Koopmann, M., Kazen-Gillespie, K., Fettman, N., Hortsch, M., and Isom, L. (2002). Structural requirements for interaction of sodium channel beta 1 subunits with ankyrin. *J. of Biological Chemistry.* **277:** 26681-26688.

Marcus, J., Dupree, J., and Popko, B. (2002). Myelin associated glycoprotein and myelin galactolipids stsbilize developing axoglial interactions. *J. Cell Biology.* **156:** 567-577.

Mariani J., Crepel F., Mikoshiba K., Changeux J., and Sotelo C. (1977). Anatomical, physiological and biochemical studies of the cerebellum from Reeler mutant mouse, *Philos. Trans. R. Soc. Lond., B Biol. Sci.* **281**: 1 – 28.

Marszalek J., Williamson T., Lee M., Xu Z., Hoffman P., Becher M., Crawford T., and Cleveland D. (1996). Neurofilament subunit NF-H modulates axonal diameter by selectively slowing neurofilament transport. *Journal of Cell Biology.* **135:** 711-724.

Martin, S., Levine, A., Chen, Z., Ughrin, Y., and Levine, J. (2001). Deposition of the NG2 proteoglycan at nodes of Ranvier in the peripheral nervous system. *J. of Neuroscience.* **21:** 8119-8128.

Martini, R. (2001). The effect of myelinating Schwann cells on axons. *Muscle Nerve.* **24:** 456-466.

Martini, R., Schachner, M., and Faissner, A. (1990). Enhanced expression of the extracellular matrix molecule J1/tenascin in the regenerating adult mouse sciatic nerve. *J. Neurocytology.* **19:**601 -616.

Mathis, C., Denisenko-Nehrbass, N., Girault, J., and Borelli, E. (2001). Essential role of oligodendrocytes in the formation and maintenance of central nervous system nodal regions. *Development.* **128:** 4881-4890.

Maxwell, W., Watt, C., Graham, D., and Gennarelli, T. (1993). Ultrastructural evidence of axonal shearing as a result of lateral acceleration of the head in non-human primates. *Acta Neuropathol. (Berl).* **86**: 136-144.

Mayer J., Eck M. (1999). SH3 domains. Minding your p's and q's. *Current Biology*. **1**:364-7.

Melendez-Vasquez, C., Rios, J., Zanazzi, G., Lambert, S., Bretscher, A., and Salzer, J. (2001). Nodes of Ranvier form in association with ezrin-radixin-moesin (ERM)-positive Schwann cell processes. *Proc. Natural Academy of Sciences.* **98:**1235 -1240.

Melkonian, K., Ostermeyer, A., Chen, J., Roth, M., and Brown, D. (1999). Role of lipid modifications in targeting proteins to detergent-resistant membrane rafts. Many raft proteins are acylated, while few are prenylated. *J. of Biological Chemistry.* **274:** 3910-1917.

Menegoz, M., Gaspar, P., Le Bert, M., Galvez, T., Burgaya, F., Palfrey, C., Ezan, P., Arnos, F., and Girault, J. (1997). Paranodin, a glycoprotein of neuronal paranodal membranes. *Neuron*. **19:**319- 331.

Menon, K., Rasband, M,, Taylor, C., Brophy, P., Bansal, R., and Pfeiffer, S. (2003). The myelin-axolemmal complex: biochemical dissection and the role of galactosphingolipids. *J. of Neurochemistry.* **87:**995 -1009

Miller, R, and da Silva P. (1977) Particle rosettes in the periaxiaxonal Schwann cell membrane and particle clusters in the axolema of rat sciatic nerve. *Brain Research*. **130:** 135-141.

Missler, M. and Südhof, T., (1998). Neurexins: three genes and 1001 products. *Trends Genet.* **14**: 20–26.

Moffett, S., Brown, D., and Linder, M. (2000). Lipid-dependent targeting of G proteins into rafts. *J. of Biological Chemistry.* **275:** 2191-2198.

Montag D, Giese KP, Bartsch U, Martini R, Lang Y, Bluthmann H, Karthigasan J, Kirschner DA, Wintergerst ES, Nave KA, Zielasek J., Toyka K., Lipp, H., and Schachner M. 1994. Mice deficient for the myelin-associated glycoprotein show subtle abnormalities in myelin. *Neuron.* **13:**229- 246.

Mugnaini E., and Floris A. (1994). The unipolar brush cell: a neglected neuron of the mammalian cerebellar cortex. *Journal of Comparative Neurology*. **339**: 174– 180.

Mullen R., Eicher E., and Sidman R. (1976). Purkinje cell degeneration, a new neurological mutation in the mouse. *Proceedures of the Natural Academy of Science.* **73**: 208– 212.

Nakagawa T., Chen J., Zhang Z., Kanai Y., and Hirokawa N. (1995). Two distinct functions of the carboxyl-terminal tail domain of NF-M upon neurofilament assembly: cross-bridge formation and longitudinal elongation of filaments. *Journal of Cell Biology.* **129:** 411-429.

Nie D., Zhou Z., Ang B., Teng F., Xu G., Xiang T., Wang C., Zeng L., Takeda Y., Xu T., Ng Y., Faivre-Sarrailh C., Popko B., Ling E., Schachner M., Watanabe K., Pallen C., Tang B., and Xiao Z. (2003). Nogo-A at CNS paranodes is a ligand of Caspr: possible regulation of K+ channel localization. *EMBO Journal*. **22:** 5666–5678.

Nordquist D., Kozak C., and Orr H. (1988). cDNA cloning and characterization of three genes uniquely expressed in cerebellum by Purkinje neurons. *Journal of Neuroscience*. **8:** 4780–4789.

Norton W., and Poduslo S. 1973. Myelination in rat brain: method of myelin isolation. *Journal of Neurochemistry.* **21:**749 -757.

Oberdick J., Levinthal E., and Levinthal C. (1988). A Purkinje cell differentiation marker shows a partial DNA sequence homology to the cellular sis/PDGF2 gene. *Neuron*. **1**: 367–376.

Ohara, R., Yamakawa, H., Nakayama, M., and Ohara, O. (2000). Type II brain 4.1 (4.1B/KIAA0987), a member of the protein 4.1 family, is localized to neuronal paranodes. *Molecular Brain Research.* **85:**41 -52.

Okamoto M., Schoch S., Sudhof, T. (1999). EHSH1/intersectin, a protein that contains EH and SH3 domains and binds to dynamin and SNAP-25. A protein connection between exocytosis and endocytosis? *Journal of Biological Chemistry*. **274**:18446-54.

Olive, S., Dubois, C., Schachner, M., and Rougon, G. (1995). The F3 neuronal glycosylphosphatidylinositol-linked molecule is localized to glycolipid-enriched membrane subdomains and interacts with L1 and fyn kinase in cerebellum. *J. Neurochemistry.* **65:** 2307-2317.

Oohashi, T., Hirakawa, S., Bekku, Y., Rauch, U., Zimmermann, D., Su, W., Ohtsuka, A., Murakami, T., and Ninomiya, Y. (2002). Bral1, a brain-specific link protein, colocalizing with the versican V2 isoform at the nodes of Ranvier in developing and adult mouse central nervous systems. *Molecular Cell, Neuroscience.* **19:** 43-57.

Ozawa S., Kamiya H., and Tsuzuki T. (1998). Glutamate receptors in the mammalian central nervous system. *Progress in Neurobiol*ogy. **54**: 581– 618.

Palay, S., and Chan-Palay, V. (1974). Cerebellar Cortex (New York, Springer-Verlag). Pedraza, L., Huang, J., and Colman, D. R. (2001). Organizing principles of the axoglial apparatus. *Neuron.* **30**: 335-344.

Parra, M., Gascard, P., Walensky, L., Gimm, J., Blackshaw, S., Chan, N., Takakuwa, Y., Berger, T., Lee, G., Chasis, J., Snyder, S., Mohandas, N., and Conboy, J. (2000). Molecular and functional characterization of protein 4.1B, a novel member of the protein 4.1 family with high level, focal expression in brain. *J. of Biological Chemistry.* **275:** 3247-3255.

Pawson, T. (1995). Protein modules and signaling networks. *Nature.* **373:** 573-580

Pedraza L., Huang J., and Colman D. (2001). Organizing principles of the axoglial apparatus. *Neuron*. **30:**335- 344.

Peles, E., Nativ, M., Lustig, M., Grumet, M., Schilling, J., Martinez, R., Plowman, G., and Schlessinger, J. (1997). Identification of a novel contactin-associated transmembrane

receptor with multiple domains implicated in protein-protein interactions. *EMBO J.* **16:** 978-988.

Peles, E., and Salzer, J. (2000). Molecular domains of myelinated axons. *Current Opinion of Neurobiology.* **10:**558- 565.

Pellegrino, L., and Altman, J. (1979). Effects of differential interference with postnatal cerebellar neurogenesis on motor performance, activity level, and maze learning of rats: developmental study. *Journal of Comparative Physiological Psychol*ogy. **93**: 1-33.

Poliak, S., Gollan, L., Martinez, R., Custer, A., Einheber, S., Salzer, J., Trimmer, J., Shrager, P., and Peles, E. (1999). Caspr2, a new member of the neuraxin superfamily, is localized at the juxtaparanodes of myelinated axons and associates with K+ channels. *Neuron.* **24:**1037 - 1047.

Poliak, S., Gollan, L., Salomon, D., Berglund, E., Ohara, R., Ranscht, B., and Peles, E. (2001). Localization of Caspr2 in myelinated nerves depends on axon-glia interactions and the generation of barriers along the axon. *J. of Neuroscience.* **21:** 7568-7575.

Poliak, S., Salomon, D., Elhanany, H., Sabanay, H., Kiernan, B., Pevny, L., Stewart, C., Xu, X., Chiu, S., Shrager, P., Furley, A., Peles, E. (2003). Juxtaparanodal clustering of Shaker-like K+ channels in myelinated axons depends on Caspr2 and TAG-1. *J. of Cell Biology.* **162:** 1149-1160.

Poliak, S., and Peles, E. (2003). The local differentiation of myelinated axons at nodes of Ranvier. Nature Reviews Neuroscience. **4**: 968-980.

Popko, B. (2003). Myelin: not just a conduit for conduction. *Nature Genetics*. **33:**327 -328.

Privat A., Jacque C., Bourre J., Dupouey P., and Baumann N. 1979. Absence of the major dense line in myelin of the mutant mouse "shiverer". *Neuroscience Letters.* **12:** 107-112.

Quackenbush J. (2001). Computational analysis of microarray data. *Nature Reviews Genetics*. **2:** 418– 427.

Raghavendra Rao V., Bowen K., Dhodda V., Song G., Franklin J., Gavva N., and Dempsey R. (2002). Gene expression analysis of spontaneously hypertensive rat cerebral cortex following transient focal cerebral ischemia. *Journal of Neurochemistry.* **83**:1072–1086.

Rao M., Houseweart M., Williamson T., Crawford T., Folmer J., and Cleveland D. (1998). Neurofilament-dependent radial growth of motor axons and axonal organization of neurofilaments does not require the neurofilament heavy subunit (NF-H) or its phosphorylation. *Journal of Cell Biology.* **143:**171-181.

Rasband, M., Trimmer, J., Schwarz, T., Levinson, S., Ellisman, M., Schachner, M., Shrager, P. (1998). Potassium channel distribution, clustering, and function in remyelinating rat axons. *J. of Neuroscience.* **18:** 36-47.

Rasband, M., Peles, E., Trimmer, J., Levinson, S., Lux, S., Shrager, P. (1999). Dependence of nodal sodium channel clustering on paranodal axoglial contact in the developing CNS. *J. of Neuroscience.* **19:**7516 -7528.

Rasband, M. Trimmer, J., Peles, E., Levinson, S., and Shrager, P. (1999). K+ channel distribution and clustering in developing and hypomyelinatied axons of the optic nerve. *J. of Neurocytology.* **28:**319- 331.

Rasband, M, Kagawa, T., Park, E., Ikenaka, K., and Trimmer, J. (2003). Dysregulation of axonal sodium channel isoforms after adult-onset chronic demyelination. *J. of Neuroscience Research.* **73:**465 -470.

Rasband, M., Taylor, C., and Bensal, R. (2003). Paranodal transverse bands are required for maintenance but not initiation of the Nav1.6 sodium channel clustering in CNS optic nerve axons. *Glia*. **44:**173- 182.

Rasband, M., Park, E., Zhen, D., Arbuckle, M., Poliak, S., Peles, E., Grant, S., and Trimmer, J. (2002). Clustering of neuronal potassium channels is independent of their interaction with PSD-95. *J. of Cell Biology.* **159:** 663-672.

Ratcliffe, C., Qu, Y., McCormick, K., Tibbs, V., Dixon, J., Scheuer, T., and Catterall, W. (2000). A sodium channel signaling complex modulation by associated receptor protein tyrosine phosphatase β. *Nature Neuroscience.* **3:** 437-444.

Ratcliffe, C., Wetenbroek, R., Curtis, R., and Catterall, W. (2001). Sodium channel beta1 and beta3 subunits associate with neurofascin through their extracellular immunoglobulin domain. *J. of Cell Biology.* **154:** 427-434.

Rhodes, K., Strassle, B., Monaghan, M., Bekele-Arcuri, Z., Matos, M., and Trimmer, J. (1997). Association and colocalization of the Kvbeta1 and Kvbeta2 beta-subunits with Kv1 alpha-subunits in mammalian brain K+ channel complexes. *J. of Neuroscience.***17:** 8246-8258.

Rhyu, I., Abbott, L., Walker, D., and Sotelo, C. (1999). An ultrastructural study of granule cell/Purkinje cell synapses in tottering (tg/tg), leaner (tg(la)/tg(la)) and compound heterozygous tottering/leaner (tg/tg(la)) mice. *Neuroscience.* **90**: 717-728.

Rieger, F., Daniloff, J., Pincon-Raymond, M., Crossin, K., Grumet, M., and Edelman, G. (1986). Neuronal cell adhesion molecules and cytotactin are colocalized at the node of Ranvier. *J. of Cell Biology.* **103:** 379-391.

Rios, J., Melendez-Vasquez, C., Einheber, S., Lustig, M., Grumet, M., Peles, E., and Salzer, J. (2000). Contactin associated protein (caspr) and contactin form a complex that is targeted to the paranodal junctions during myelination. *Journal of Neuroscience.***20:** 8354-8364.

Rio Hortega, P. del (1921). La glia de escasas radiaciones (oligodendroglia). *Boletin R. Soc. Esp. Hist. Nat.* **21:**63- 92.

Rio Hortega, P. del (1928). Tercera aportacion al conocimiento morfologico e interpretacion functional de la oligodendroglia. *Mem. R. Soc. Esp. Hist. Nat.* **14:** 5-122.

Rios, J., Melendez-Vasquez, C., Einheber, S., Lustig, M., Grumet, M., Hemperly, J., Peles, E., and Salzer, J. (2000). Contactin-associated protein (Caspr) and contactin form a complex that is targeted to the paranodal junctions during myelination. *Journal of Neuroscience*. **20**: 8354-8364.

Rios, J., Rubin, M., St Martin, M., Downey, R., Einheber, S., Rosenbluth, J., Levinson, R., Bhat, M., and Salzer, J. (2003). Paranodal interactions regulate expression of sodium channel subtypes and provide a diffusion barrier for the node of Ranvier. *J. of Neuroscience.* **23:**7001 -7011.

Robertson, J., (1957). The ultrastructure of nodes of Ranvier in frog nerve fibers. *J. Physiol.* **137**: 8–9.

Roos J., and Kelly R. (1998). Dap160, a neural-specific Eps15 homology and multiple SH3 domain containing protein that interacts with Drosophila dynamin. Journal of Biological Chemistry. **273:** 19108-19119.

Rosenbluth, J. (1976). Intramembranous particle distribution at the node of Ranvier and adjacent axolema in myelinated axons of the frog brain. *J. Neurocytology.* **5:** 731-745.

Rosenbluth, J. (1981). Axoglial junctions in the mouse mutant Shiverer. *Brain Research*. **208**: 283-297.

Rosenbluth, J. (1987). Abnormal axoglial junctions in the myelin-deficient rat mutant. *J. of Neurocytology.* **16:**497- 509.

Rosenbluth, J., (1995). Glial membranes and axoglial junctions. In: Kettenmann, H. and Ransom, B.R., Editors, 1995. *Neuroglia*, Oxford University Press, New York 613–633.pp

Rosenbluth, J., Dupree, J., and Popko, B. (2003). Nodal sodium channel domainintegrity depends on the presence of transverse bands. *Glia*. **41:** 318-325.

Rosenfeld, J., and Freidrich, V., Jr. (1983). Axonal swellings in jimpy mice: does lack of myelin cause neuronal abnormalities? *Neuroscience.* **10**: 959-966.

Rothstein D., Martin L., Levey I., Dykes-Hoberg M., Jin L., Wu D., Nash N., Kuncl W. (1994). Localization of neuronal and glial glutamate transporters. *Neuron*. **13**: 713– 725.

Rothstein D., Van Kammen M., Levey I., Martin J., and Kuncl W. (1995). Selective loss of glial glutamate transporter GLT-1 in amyotrophic lateral sclerosis. *Ann. Neurol*. **38**: 73–84.

Rudenko, G., Nguyen, T., Chelliah, Y., Sudhof, T. and Deisenhofer, J., (1999). The structure of the ligand-binding domain of neurexin Ibeta: regulation of LNS domain function by alternative splicing. *Cell* **99**: 93–10.

Saito, F., Masaki, T., Kamakura, K., Anderson, L., Fujita, S., Fukuta-Ohi, H., Sunada, Y., Shimizu, T., and Matsumura, K. (1999). Characterization of the transmembrane molecular architecture of the dystroglycan complex in schwann cells. *J. of Biological Chemistry.* **274:** 8240-8246.

Salehi A., Roux P., Kubu C., Zeindler C., Bhakar A., Tannis L., Verdi J., and Barker P. (2000). NRAGE, a novel MAGE protein, interacts with the p75 neurotrophin receptor and facilitates nerve growth factor-dependent apoptosis. *Neuron.* **27:** 279-288.

Salzer J., Holmes W., and Colman D. 1987. The amino acid sequences of the myelin-associated glycoproteins: homology to the immunoglobulin gene superfamily. *Journal of Cell Biology.* **104:** 957-965.

Salzer, J. L. (2003). Polarized domains of myelinated axons. *Neuron*. **40*:*** 297-318.
Sanchez I., Hassinger L., Paskevich P., Shine H., and Nixon R. 1996. Oligodendroglia regulate the regional expansion of axon caliber and local accumulation of neurofilaments during development independently of myelin formation. *Journal of Neuroscience.* **16:** 5095-5105.

Schaeren-Wiemers N., Bonnet A., Erb M., Erne B., Bartsch U., Kern F., Mantei N., Sherman D., and Suter U. (2004). The raft-associated protein MAL is required for maintenance of proper axon--glia interactions in the central nervous system. *Journal of Cell Biology*. **166:** 731-42.

Schafer, D., Bansal, R., Hedstrom, K., Pfeiffer, S., and Rasband, M. (2004). Does paranode formation and maintenance require partitioning of neurofascin 155 into lipid rafts? *J. of Neuroscience.* **24:** 3176-3185.

Scherer, S., Xu, T., Crino, P., Arroyo, E., and Guttmann, D. (2001). Ezrin, radixin, and moesin are components of Schwann cell microvilli. *J. of Neuroscience Research.* **65:** 150-164.

Sengar S.,Wang W., Bishay J., Cohen S., and Egan E. (1999). The EH and SH3 domain Ese proteins regulate endocytosis by linking to dynamin and Eps15. *EMBO Journal.* **18**: 1159-1171.

Sheikh K., Sun J., Liu Y., Kawai H., Crawford T., Proia R., Griffin J., and Schnaar R. 1999. Mice lacking complex gangliosides develop Wallerian degeneration and myelination defects. *Procedures Nat. Academy of Sciences.* **96:** 7532-7537.

Sherman D., Tait S., Melrose S., Johnson R., Zonta B., Court F., Macklin W., Meek S, Smith A., Cottrell D., and Brophy P. (2005). Neurofascins are required to establish axonal domains for saltatory conduction. *Neuron*. **48**:737-42.

Sidman R., Lane P., and Dickie M. (1962). Staggerer, a new mutation in the mouse affecting the cerebellum. *Science*. **137:** 610– 612.

Sidman R., and Green M. (1970). Nervous a mutant mouse with cerebellar disease, in: M. Sabourdy (Ed.), Les Mutants Pathologiques Chez L'Animal, Edition du Centre National de la Recherche Scientique, Orleans-la-Source, France, 1970, 69–79 pp.

Sidman R. (1983). Experimental neurogenetics, Res. Publ.-Assoc. Res. *Nervous Mental Disorders*. **63:**19–46.

Simons, M, and Ikonen, I. (1997). Functional rafts in cell membranes. *Nature***. 387:** 569-572.

Snipes G., Suter U., Welcher A., and Shooter E. 1992. Characterization of a novel peripheral nervous system myelin protein (PMP-22/SR13). *Journal of Cell Biology.* **117:** 225-238.

Soriano M., Tessier M., Certa U., and Gill R. (2000). Parallel gene expression monitoring using oligonucleotide probe arrays of multiple transcripts with an animal model of focal ischemia. *Journal of Cerebral Blood Flow Metabolism.* **20**:1045–1055.

Spiegel, I., Salomon, D., Erne, B., Sxhaeren-Wiemers, N., and Peles, E. (2002). Caspr3 and Caspr4, two novel members of the caspr family are expressed in the nervous system and interact with PDZ domains. *Molecular Cell Neuroscience.* **20:** 283-297.

Sotelo C. (2004). Cellular and genetic regulation of the development of the cerebellar system. *Progress in Neurobiology.* **72:**295 – 339.

Stoffel W., Boison D., and Bussow H. 1997. Functional analysis in vivo of the double mutant mouse deficient in both proteolipid protein (PLP) and myelin basic protein (MBP) in the central nervous system. *Cell Tissue Research.* **289:** 195-206.

Stokin, G., Lillo, C., Falzone, T., Brusch, R., Rockenstein, E., Mount, S., Raman, R., Davies, P., Masliah, E., Williams, D., and Goldstein, L. (2005). Axonopathy and transport deficits early in the pathogenesis of Alzheimer's disease. *Science.* **307**: 1282-1288.

Stolinski, C., Breathnach, A., Thomas, P., Gabriel, G., and King, R. (1985). Distribution of particle aggregates in the internodal axolema and adaxonal Schwann cell membrane of reedent peripheral nerve. *J. of Neurological Sciences.* **67:** 213-222.

Suzuki A., Hoshi T., Ishibashi T., Hayashi A., Yamaguchi Y., and Baba H. (2004). Paranodal axoglial junction is required for the maintenance of the Nav1.6-type sodium channel in the node of Ranvier in the optic nerves but not in peripheral nerve fibers in the sulfatide-deficient mice.*Glia*. **46:**274- 83.

Svitkina, T., Verkhovsky, A., and Borisy, G. (1996). Plectin sidearms mediate interaction of intermediate filaments with microtubules and other components of the cytoskeleton. *Journal of Cell Biology*. **135**: 991-1007.

Tait, S., Gunn-Moore, F., Collinson, J., Huang, J., Lubetzki, C., Pedraza, L., Sherman, D., Colman, D., and Brophy, P. (2000). An oligodendrocyte cell adhesion molecule at the site of assembly of the paranodal axo-glial junction. *J. of Cell Biology.* **150:** 657-666.

Talts, J., Andac, Z., Gohring, W., Brancaccio, A. and Timpl, R., (1999). Binding of the G domains of laminin alpha1 and alpha2 chains and perlecan to heparin, sulfatides, alpha-dystroglycan and several extracellular matrix proteins. *EMBO J.* **18**: 863–870.

Tang Y., Lu A., Aronow B., Wagner K., and Sharp F. (2002). Genomic responses of the brain to ischemic stroke, intracerebral haemorrhage, kainate seizures, hypoglycemia, and hypoxia. *European Journal of Neuroscience.* **15**:1937–1952.

Tao-Cheng, J., and Rosenbluth, J. (1983). Axolemal differentiation in myelinated fibers of rat peripheral nerves. *Brain Research*. **285:** 251-263.

Tcherpakov M., Bronfman F., Conticello S., Vaskovsky A., Levy Z., Niinobe M., Yoshikawa K., Arenas E., and Fainzilber M. (2002). The p75 neurotrophin receptor interacts with multiple MAGE proteins. *Journal of Biological Chemistry.* **277:** 49101-49104.

Thullier, F., Lalonde, R. and Lestienne, F., (1999). Effects of dopaminergic agents and of an NMDA receptor antagonist on motor coordination in Lurcher mutant mice. *Pharm. Biochem. Behav.* **63**: 213–219.

Traka, M, Dupree, J., Popko, B., and Karagogeos, D. (2002). The neuronal adhesion protein TAG-1 is expressed by Schwann cells and oligodendrocytes and is localized to the juxtaparanodal region of myelinated fibers. *J. of Neurosciences.* **22:** 3016-3024.

Traka, M., Goutebroze, L., Denisenko, N., Bessa, M., Nifli, A., Havaki, S., Iwakura, Y., Fukamauchi, F., Watanabe, K., Soliven, B., Girault, J., and Karagogeos, D. (2003). Association of TAG-1 with Caspr2 is essential for the molecular organization of juxtaparanodal regions of myelinated fibers. *J. of Cell Biology.* **162:** 1161-1172.

Trapp, B. (1990). The myelin associated glycoprotein: location and potential functions. In myelination and Dysmyelination, D. Colman, I. Duncan, and R. Skoff, eds. (New York: The New York Academy of Sciences), pp. 29-43.

Trapp B. (1988). Distribution of the myelin-associated glycoprotein and P0 protein during myelin compaction in quaking mouse peripheral nerve. *Journal of Cell Biology.* **107:** 675-685.

Trapp, B. D., Andrews, S. B., Cootauco, C., and Quarles, R. (1989). The myelinassociated glycoprotein is enriched in multivesicular bodies and periaxonal membranes of actively myelinating oligodendrocytes. *Journal of Cell Biology*. **109**: 2417-2426.

Umemori, H., Kadowaki, Y., Hirosawa, K., Yoshida, Y., Hironaka, K., Okano, H., and Yamamoto, T. (1999). Stimulation of myelin basic protein gene transcription by Fyn tyrosine kinase for myelination. *J. of Neuroscience.* **19:** 1393-1397.

Uschkureit T., Sporkel O., Stracke J., Bussow H., and Stoffel W. (2000). Early onset of axonal degeneration in double (plp-/-mag-/-) and hypomyelinosis in triple (plp-/-mbp-/-mag-/-) mutant mice. *Journal of Neuroscience.* **20:** 5225-5233.

Vabnick, I., Novakovic, S., Levinson, S., Schachner, M., and Shrager, P. (1996). The clustering of axonal sodium channels during development if the peripheral nervous system. *Journal of Neuroscience.* **16:**49140 -4922.

Vabnick, I., and Shrager, P. (1998). Ion channel redistribution and functioning during development of the myelinated axon. *J. of Neurobiology.* **37:** 80-96.

Vabnick, I., Trimmer, J., Schwarz, T., Levinson, S., Risal, D., and Shrager, P. (1999). Dynamic potassium channel distributions during axonal development prevent aberrant firing patterns. *J. of Neuroscience.* **19:** 747-758.

Valentine, W., Amarnath, V., Graham, D., Morgan, D., and Sills, R. (1997). CS2-mediated cross-linking of erythrocyte spectrin and neurofilament protein: dose response and temporal relationship to the formation of axonal swellings. *Toxicol. Appl. Pharmacol.* **142**: 95-105.

Vyas K., Patel H., Vyas A., and Schnaar R. (2001). Segregation of gangliosides GM1 and GD3 on cell membranes, isolated membrane rafts, and defined supported lipid monolayers. *Biological Chemistry.* **382:** 241-250.

Vyas A., Patel H., Fromholt S., Heffer-Lauc M., Vyas K., Dang J., Schachner M., and Schnaar R. (2002). Gangliosides are functional nerve cell ligands for myelin-associated glycoprotein (MAG), an inhibitor of nerve regeneration. *Procedures NAtl Academy of Sciences.* **99:** 8412-8417.

Wang, H., Kunkel, D., Martin, T., Schwartzkroin, P, and Tempel, B. (1993). Heteromultimeric K+ channels in terminal and juxtaparanodal regions of neurons. *Nature.* **365:** 75-79**.**

Wang K., Kim J., Sivasankaran R., Segal R., and He Z. (2002). P75 interacts with the Nogo receptor as a co-receptor for Nogo, MAG and OMgp. *Nature.* **420:** 74-78.

Ward, R., Lamb, R. and Fehon, R., (1998). A conserved functional domain of Drosophila coracle is required for localization at the septate junction and has membrane-organizing activity. *J. Cell Biol.* **140**: 1463–1473.

Waxman, S. (1980). Determinants of conduction velocity in myelinated and nerve fibers. *Muscle Nerve.* **3:** 141-150.

Weber, P., Bartsch, U., Rasband, M., Lang, Y., Bluethmann, H., Margolis, R., Levinson, S., Shrager, P., Montag, D., and Schachner, M. (1999). Mice deficient for tensacin-R display alterations of the extracellular matrix and decreased axonal conduction velocities in the CNS. *J. of Neuroscience.* **19:** 4245-4262.

Windebank A., Wood P., Bunge R., and Dyck P. 1985. Myelination determines the caliber of dorsal root ganglion neurons in culture. *Journal of Neuroscience.* **6:** 1563-1569.

Wolswijk, G. and Balesar, R. (2003). Changes in the expression and localization of the paranodal protein caspr on axons in chronic multiple sclerosis. *Brain.* **126:** 1638-1649.

Wong P., Marszalek J., Crawford T., Xu Z., Hsieh S., Griffin J., and Cleveland D. (1995). Increasing neurofilament subunit NF-M expression reduces axonal NF-H, inhibits radial growth, and results in neurofilamentous accumulation in motor neurons. *Journal of Cell Biology.* **130:** 1413-1422.

Workman, R., and Low, P. (1998). Biochemical analysis of potential sites for protein 4.1-mediated anchoring of the spectrin-actin skeleton to the erythrocyte membrane. *Journal of Biochemistry*. **273**: 6171-6176.

Xu Z., Marszalek J., Lee M., Wong P., Folmer J., Crawford T., Hsieh S., Griffin J., and Cleveland D. (1996). Subunit composition of neurofilaments specifies axonal diameter. *Journal of Cell Biology.* **133:** 1061-1069.

Yamabhai M., Hoffman N., Hardison N., McPherson P., Castagnoli L., Cesareni G., and Kay B. (1998). Intersectin, a novel adaptor protein with two Eps15 homology and five Src homology 3 domains. *Journal Biological Chemistry*. 20: 31401-31407.

Yamashita T., Higuchi H., and Tohyama M. (2002). The p75 receptor transduces the signal from myelin-associated glycoprotein to Rho. *Journal of Cell Biology.* **157:** 565-570.

Yang, Y., Dowling, J., Yu, Q., Kouklis, P., Cleveland, D., and Fuchs, E. (1996). An essential cytoskeletal linker protein connecting actin microfilaments to intermediate filaments. *Cell.* **86:** 655-665.

Yin X., Crawford T., Griffin J., Tu P., Lee V., Li C., Roder J., and Trapp B. 1998. Myelin-associated glycoprotein is a myelin signal that modulates the caliber of myelinated axons. *Journal of Neuroscience*. **18:**1953 -1962.

Yiu G. and He Z. (2003). Signaling mechanisms of the myelin inhibitors of axon regeneration. *Current Opinion of Neurobiology*. **13:** 545–551.

Yu W., Guo W., and Feng L. (2004). Segregation of Nogo66 receptors into lipid rafts in rat brain and inhibition of Nogo66 signaling by cholesterol depletion. *FEBS Letters*. **577:** 87-92.

Zagon, I., Higbee, R., Riederer, B., and Goodman, S. (1986). Spectrin subtypes in mammalian brain: an immunoelectron microscopic study. *Journal of Neuroscience.* ***6*:** 2977-2986.

Zhang, X., Davis, J., Carpenter, S., and Bennett, V. (1998). Structural requirements for association of neurofascin with ankyrin. *J. of Biological Chemistry.* **273:** 30785-30794.

Zhu Q., Couillard-Despres S., and Julien J. (1997). Delayed maturation of regenerating myelinated axons in mice lacking neurofilaments. *Experimental Neurology.* **148:** 299-316.

Zhou, L. Messing, A., and Chiu, S. (1999). Determinants of excitability at transition zones in Kv1.1-deficient myelinated nerves. *J. of Neuroscience.* **19:** 5768-5781.

Ziai M., Sangameswaran L., Hempstead J., Danho W., and Morgan J. (1988). An immunochemical analysis of the distribution of a brainspecific polypeptide, PEP-19, *Journal of. Neurochemistry.* **51:**1771 – 1776.

Zoghbi, H., and Orr, H. (2004). Molecular and Metabolic Bases of the Inherited Disease, McGraw Hill).